Journal of Paleontology, 89(5), 2015, p. 695–729

0022-3360/16/0088-0906
doi: 10.1017/jpa.2015.56

Journal of PALEONTOLOGY
A JOURNAL OF THE PALEONTOLOGICAL SOCIETY

A new approach to ancient microorganisms: taxonomy, paleoecology, and biostratigraphy of the Lower Cambrian Berkuta and Chulaktau microbiotas of South Kazakhstan

J. William Schopf,[1] Vladimir N. Sergeev,[2] and Anatoliy B. Kudryavtsev[3]

[1]Department of Earth, Planetary, and Space Sciences, Center for the Study of Evolution and the Origin of Life, and Molecular Biology Institute, University of California, Los Angeles 90095 USA; PennState Astrobiology Research Center, Deike Building, University Park, PA 16802 USA; and University of Wisconsin Astrobiology Research Consortium, Madison, WI 53706, USA; ⟨schopf@ess.ucla.edu⟩
[2]Geological Institute, Russian Academy of Sciences, Pyzhevskii per., 7, Moscow, 119017, Russia, ⟨sergeev-micro@rambler.ru⟩
[3]Center for the Study of Evolution and the Origin of Life, University of California, Los Angeles 90095 USA; PennState Astrobiology Research Center, Deike Building, University Park, PA 16802 USA; and University of Wisconsin Astrobiology Research Consortium, Madison, WI 53706, USA; ⟨kudryavtsev@ess.ucla.edu⟩

Abstract.—Peritidal cherts and silicified phosphorites of the Early Cambrian Kyrshabakta (Berkuta Member) and Chulaktau formations of South Kazakhstan contain diverse assemblages of cellularly permineralized microorganisms that like other microbiotas of similar age and setting are dominated by cyanobacteria, both filamentous (oscillatoriacean trichomes and empty sheaths) and coccoidal (chroococcaceans). Although these near-shore assemblages contain sphaeromorph acritarchs, they differ from Neoproterozoic and Early Cambrian microbiotas of more open-marine environments by lacking morphologically complex planktonic eukaryotes such as the acanthomorphic acritarchs that are abundant in the Chulaktau-overlying Shabakta Formation. In general composition, the Berkuta and Chulaktau assemblages are similar both to microfossil assemblages of the pre-trilobite Rovno and Lontova Regional Stages of the East European Platform and to Early Cambrian microbiotas known from chert-phosphorite deposits worldwide.

The studies reported here are based on use of optical microscopy combined with techniques recently introduced to paleobiology: confocal laser scanning microscopy, and Raman and fluorescence spectroscopy and imagery. Taken together, these provide information in situ, in three dimensions and at high spatial resolution, about the organismal morphology; cellular anatomy; chemical composition; and mode, fidelity, and environment of preservation of the permineralized microfossils. Data are presented suggesting that the substitution of samarium for calcium in fossil-preserving apatite may provide evidence of its oxic or anoxic paleoenvironment of formation.

We interpret the Berkuta and Chulaktau assemblages to be composed of 27 taxa assigned to 17 genera of microscopic prokaryotes and eukaryotes that include one new genus and species, *Berkutaphycus elongatus*.

Introduction

Lowest Cambrian rocks are distinguished by the presence of the earliest-known diverse assemblages of shelly fossils. This benchmark, the global appearance of metazoans having robust carapaces and "hard parts," is perhaps the sharpest and arguably one of the most important biostratigraphic boundaries in Earth history. Phytoplankton also exhibit major changes across the Precambrian-Phanerozoic boundary that are evidenced in Ediacaran-Cambrian successions worldwide (e.g., Australia, China, India, the East-European Platform, India, North America, and Siberia). Of these, one of the most notable is that of the Neoproterozoic to Early Paleozoic succession of the Maly Karatau Range of South Kazakhstan and its stratigraphic equivalents in the Tian-Shan mountains of Kirghizia and China. In these regions, the upper parts of this succession contain abundant shelly fossils that evidence its Cambrian age. The units of the Maly Karatau Range studied here not only preserve such shelly fossils, but, also, diverse assemblages of chert- and phosphate-permineralized Early Cambrian microorganisms—the focus of our report.

In previous studies we described the chert-permineralized microbiota of the Cryogenian (Neoproterozoic, Upper Riphean) Maly Karatau Range Chichkan Formation (Schopf et al., 2010a; Sergeev and Schopf, 2010). We here extend our investigations of the microfossil assemblages of this region by describing the permineralized microbiotas of the Early Cambrian Kyrshabakta (Berkuta Member) and Chulaktau formations, microbial assemblages that are appreciably less diverse than that permineralized in the underlying Chichkan cherts. The results reported document the use of standard optical microscopy combined with those obtained by confocal laser scanning microscopy (Schopf et al., 2006) and Raman and fluorescence spectroscopy and imagery (Schopf and Kudryavtsev, 2010; Schopf et al., 2002, 2005), techniques that permit analyses of the submicron-scale morphology and carbonaceous composition of

the permineralized microbes, the composition of the fossil-permineralizing, -infilling, and -encrusting minerals and enclosing matrix, and that suggest a new way to infer the oxic/anoxic nature of the fossil-preserving environment.

Geology of the Maly Karatau Range (South Kazakhstan)

Geographic and stratigraphic setting.—The Maly Karatau Range (Fig. 1.1) is located within the Karatau-Talass folded zone of the Ulutau-Sinian structural belt that extends southeastward from the Ulutau Mountains of central Kazakhstan into northern China. The basinal sediments that comprise this monocline (Fig. 1.2), deposited during the Caledonian tectonic cycle, span an interval that extends from the Neoproterozoic to the mid-Paleozoic. The Neoproterozoic (Upper Riphean) to Lower Cambrian part of this succession includes six stratigraphic groups, defined and discussed in detail in numerous publications (Bezrukov, 1941; Ankinovich, 1961; Korolev, 1961, 1971; Keller et al., 1965; Krylov, 1967; Eganov and Sovietov, 1979; Korolev and Ogurtsova, 1981, 1982; Missarzhevskii and Mambetov, 1981; Ogurtsova, 1985; Eganov et al., 1986; Ogurtsova and Sergeev, 1987, 1989; Missarzhevskii, 1989; Sergeev, 1989, 1992, 2006; Sergeev and Ogurtsova, 1989; Mambetov, 1993; Popov et al., 2009; Meert et al., 2011). The source of the Lower Cambrian Kyrshabakta and Chulaktau microbiotas studied here is the uppermost of the six stratigraphic units, the Ediacaran through Ordovician Tamda Group.

The Tamda Group is composed of three formations: the lowermost terrigenous-carbonate 6- to 300-m thick Kyrshabakta Formation, characterized by basal diamictites (the "Aktas tillites"; Meert et al., 2011) and an overlying carbonate unit containing interbedded microfossiliferous chert lenses that has been referred to as the "Lower Dolomite" or "Berkuta Formation" (Korolev, 1971) or the "Berkuta Member" (Missarzhevskii and Mambetov, 1981); the mid-Tamda Group siliceous-phosphate Chulaktau Formation, up to a few tens of meters in thickness; and the >3000-m-thick uppermost carbonate Shabakta Formation. For clarity, we refer to the post-glacial carbonate unit of the lowermost Tamda Group Kyrshabakta Formation, the source of one of the two fossil assemblages described here, as the "Berkuta Member."

As discussed by Meert et al. (2011), deposition of the lowermost, pre-Berkuta part of the Kyrshabakta Formation commenced with sedimentation of the ~30-m thick Aktas tillites, a unit that was then overlain by a massive widespread cap-dolomite that ranges from 1–3 to 10–12 m thick (Eganov and Sovietov, 1979; Eganov et al., 1986). Separated by a hiatus from the cap-dolomite, deposition continued by sedimentation of a fine-grained dolomite that, in turn, was overlain by a mixed terrigenous and brownish carbonate succession documented only along the Kyrshabakata River (viz., at outcrop K-28 of the present paper). In most of the stratigraphic sections studied here—viz., the Koksu (outcrop K-27), Berkuta (K-29), Au-Sakan (K-30), Zhaanaryk (K-32), Aktogai (K-33), and Kurtlybulak (K-40) sections (Fig. 2)—the lower (pre-Berkuta) part of formation is represented either by interbedded siltstones and argillites or is missing from the succession with a 6–8 m thick part of the Berkuta sediments directly overlying tuffs of the immediately underlying Neoproterozoic Kurgan Formation of the Maly Karoy Group.

The Berkuta Member of the Kyrshabakta Formation—strata assigned by Eganov and Sovietov (1979) to the overlying Chulaktau Formation—is composed predominately of dolostone augmented by microfossil-bearing nodules of phosphorite and chert, and contains problematic stromatolites, thrombolites, and metazoan burrows. Following the suggestion of Missarzhevskii and Mambetov (1981) and Missarzhevskii (1989), we regard this microfossiliferous unit—which unconformably overlies older rocks, primarily those of the Maly Karoy Group—as the terminal member of the Kyrshabakta Formation. Sequence stratigraphy indicates that the Berkuta Member and overlying strata of the formation represent a transgressive sequence that decreases in thickness toward the Besh Tash stratigraphic section along the Tian Shan Mountains (outcrop #9 in Missarzhevskii and Mambetov, 1981) to the southeast of the sections sampled here (Fig. 1).

The Lower Cambrian Chulaktau Formation conformably overlies the Kyrshabakta Formation and the slightly eroded surface of its uppermost Berkuta Member. Silicified phosphorites of the Chulaktau occur as reentrants infilling cracks and erosional features at the top of the Berkuta Member and as phosphatic breccias and interclastic grainstones (flat-pebble conglomerates).

Traditionally, the Chulaktau Formation has been divided into three subunits, in ascending order the Aksai, Karatau, and Ushbass Members (Missarzhevskii and Mambetov, 1981; Mambetov, 1993; Popov et al., 2009). The Aksai (known also as the "Cherty Member"), a few centimeters to a few meters in thickness, is composed of silicified and non-silicified oolitic phosphorites interbedded with dolomites, shales and bedded cherts and contains abundant thrombolites, in some areas forming reef- or bioherm-like bodies. As documented here, silicified rocks of this unit are richly microfossiliferous.

The middle, Karatau Member of the formation—up to tens of meters thick and composed mainly of nonsilicified or partially silicified (and sporadically microfossiliferous) phosphorites interbedded with shales, cherts, and dolomites—is the principal phosphate-producing unit of the succession. Because of its economic importance, the predominantly oolitic and coarse-grained phosphorites of this unit have been described in numerous publications (e.g., Eganov and Sovietov, 1979; Baturin, 1978; Kholodov and Paul, 1993a, 1993b, 1994).

In the traditional stratigraphic scheme, the immediately overlying iron and manganese oxide-rich limestones and limy dolostones of the Ushbass Member—having a maximum thickness of ~3 m and present sporadically throughout the Maly Karatau Range—have been regarded to comprise the uppermost unit of the Chulaktau Formation. Ushbass strata are overlain disconformably by cherty dolomites of the >3000-m thick Early Cambrian (Atdabanian Stage) through the Ordovician Shabakta Formation.

Opinions vary regarding the stratigraphic boundary between the Shabakta and Chulaktau formations (e.g., Eganov and Sovietov, 1979; Eganov, 1988; Meert et al., 2011). Here, we follow Missarzhevskii and Mambetov (1981), who assign the Ushbass Member to the Shabakta Formation rather than the

https://doi.org/10.1017/jpa.2015.56 Published online by Cambridge University Press

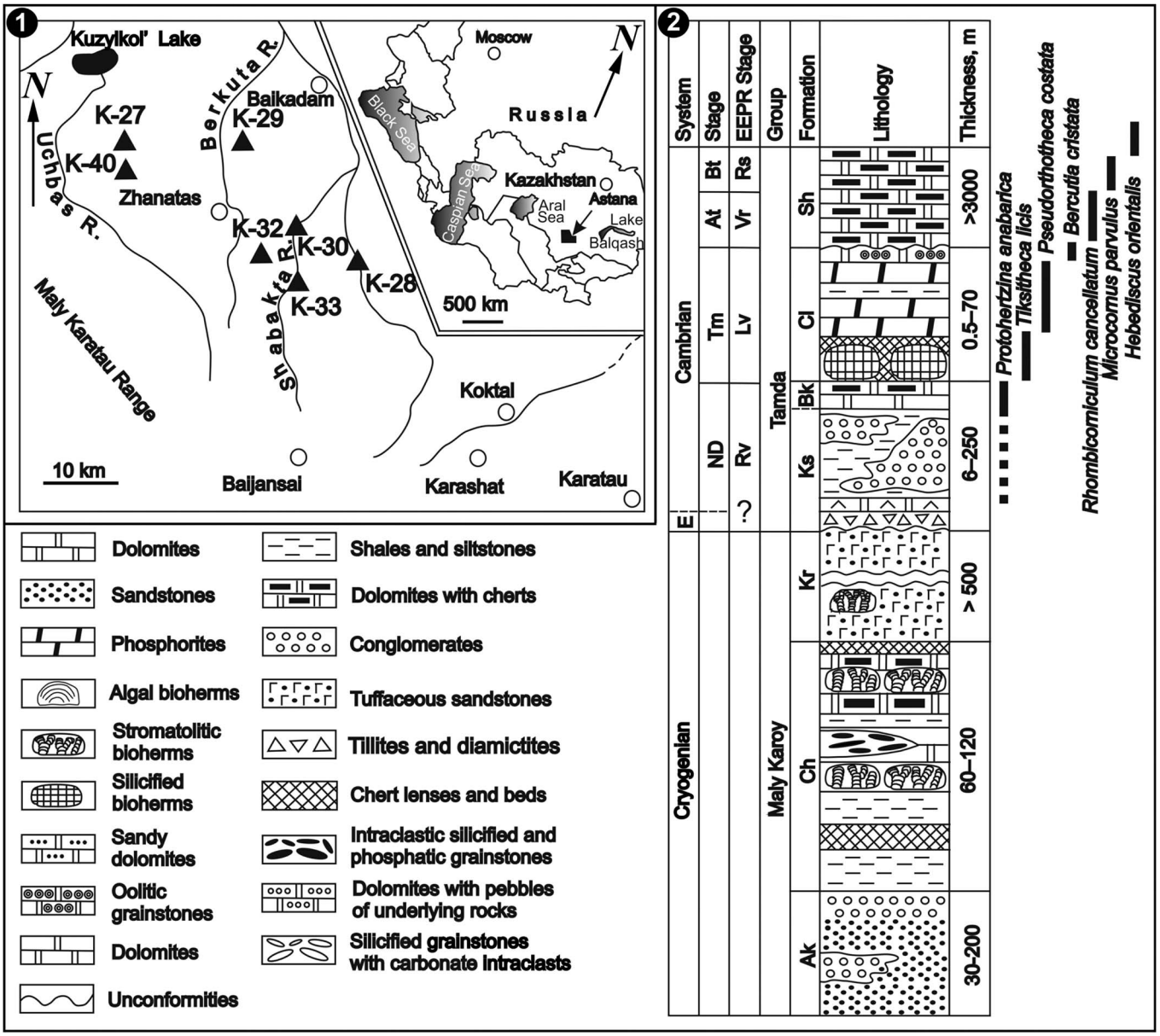

Figure 1. (1) Map of the Maly Karatau Range showing the locations of the fossiliferous Kyrshabakta (Berkuta Member) and Chulaktau Formation cherts collected from outcrop at stratigraphic sections K-27, K-28, K-29, K-30, K-32, K-33 and K-40 shown in Fig. 2; the inset map at the upper right indicates the location of the region studied in South Kazakhstan (southwest of Astana, the filled region denoted by the arrow between the Aral Sea and Lake Balqash). (**2**) Generalized stratigraphic column (at right) and lithologies (at lower left) of the Neoproterozoic (Cryogenian through Ediacaran) and Cambrian deposits of the Maly Karatau Range. Abbreviations for formations: Ak = Aktogai, Ch = Chichkan, Kr = Kurgan, Ks = Kyrshabakta; Bk = Berkuta (known also as the "Lower Dolomite" and here regarded as the Berkuta Member of the Kyrshabakta Formation); Cl = Chulaktau, Sh = Shabakta. Abbreviations for Stages: ND = Nemakit-Daldynian, Tm = Tommotian, At = Atdabanian, Bt = Botomian; and, for East European Platform Regional (EEPR) Stages: Rv = Rovno, Lv = Lontova, Vr = Vergale, Rs = Rausve; E = Ediacaran system. Biostratigraphic zones of Lower Cambrian small shelly fossils and trilobites are shown at the upper right.

Chulaktau, an interpretation supported by biostratigraphic data both for small shelly fossils (Missarzhevskii and Mambetov, 1981; Missarzhevskii, 1989) and microfossils (Korolev and Ogurtsova, 1981, 1982; Ogurtsova, 1985; Sergeev, 1989, 1992).

Chronostratigraphic nomenclature adopted here.—Internationally accepted stratigraphic nomenclature for Upper Proterozoic-Lower Cambrian successions is in a state of flux. In addition to terms preferred by the International Union of Geological Sciences (IUGS), workers in Russia and central Asia commonly subdivide the lowest Cambrian into the Nemakit-Daldynian, Tommotian and Atdabanian Stages, with those in China including the widely known Meishucuanian Stage. Given this lack of uniformity and the long-established use in Kazakhstan of the Russian stratigraphic system, we use this system for the Lower Cambrian deposits of the Maly Karatau Range. For the Precambrian part of the Maly Karatau succession, we use IUGS nomenclature. We therefore place the Proterozoic-Cambrian boundary as defined by the latest Ediacaran *Trichophycus pedum* biostratigraphic zone, approximately correlative with the Early Cambrian–defining presence of small shelly fossils of the *Protohertzina anabarica* zone, and

https://doi.org/10.1017/jpa.2015.56 Published online by Cambridge University Press

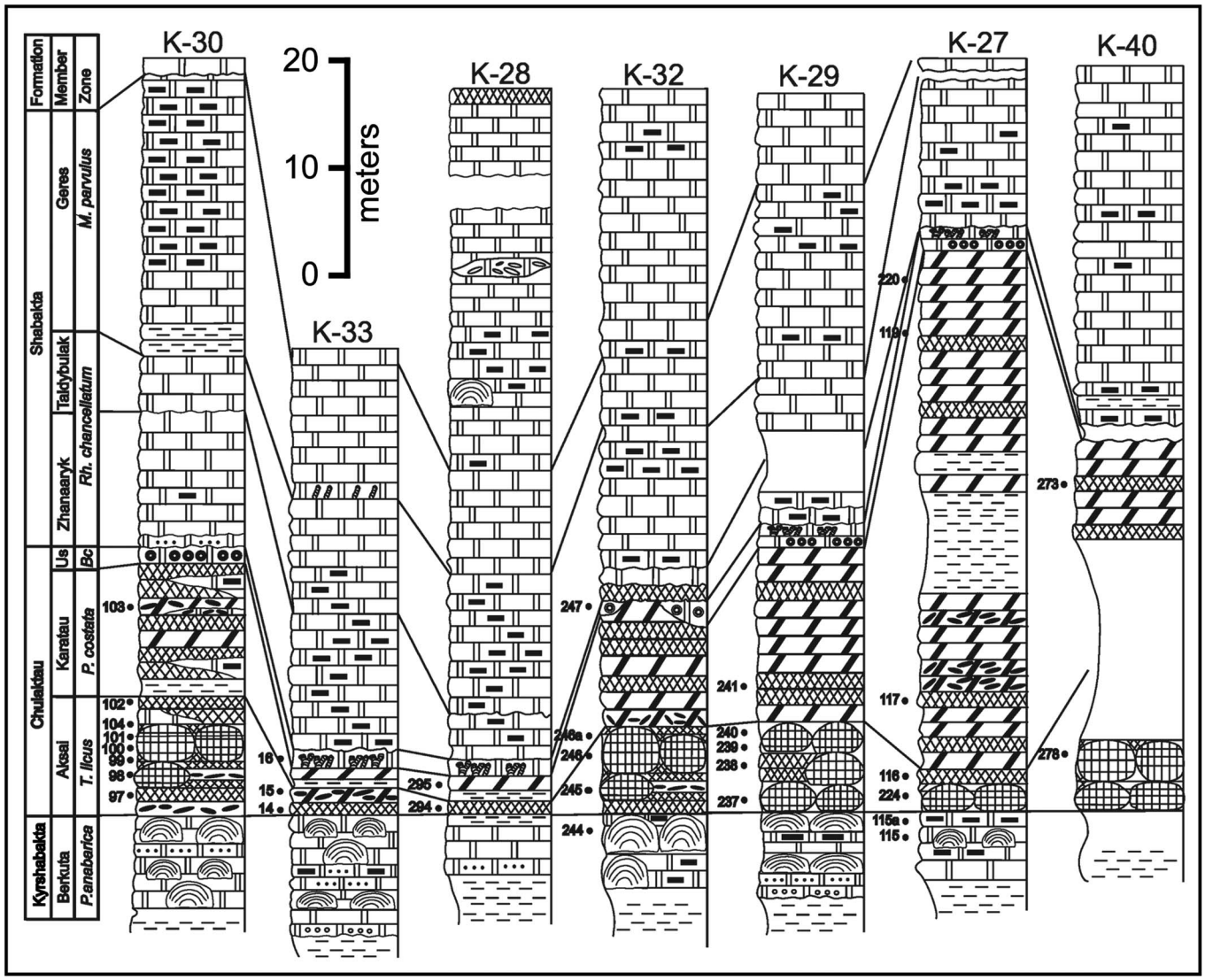

Figure 2. Stratigraphic correlation of sampled microfossiliferous cherts of the Berkuta Member of the Kyrshabakta Formation and the Chulaktau Formation at stratigraphic sections K-27, K-28, K-29, K-30, K-32, K-33, and K-40 (the geographic locations of which are specified in the text) in the part of the Maly Karatau Range shown in Fig. 1. Sample numbers with adjacent filled circles indicate the stratigraphic levels of the fossiliferous cherts studied here; symbols denoting rock types are shown in Fig. 1; Us = the Ushbass Member of the Chulaktau Formation; Bc = the *B. cristata* biostratigraphic zone.

in Fig. 1.2 indicate the approximate stratigraphic relationships between such zones and the Russian and East European Platform Regional Stages.

Age of the microfossiliferous Tamda Group.—A pre-Cambrian, pre-Ediacaran, late Neoproterozoic, and evidently Cryogenian, 800- to 750-Ma age of the Maly Karoy Group that underlies the microfossiliferous Tamda Group strata studied here is supported by radiometric and biostratigraphic data. U-Pb dates on zircons in tuffs of the uppermost Maly Karoy Group Kurgan Formation have yielded ages of 779 ± 17 Ma (Sovietov, 2008) and 766 ±7 Ma (Levashova et al., 2011). Similarly, the composition of the chert-permineralized microbiota of the Chichkan Formation, immediately underlying the uppermost Maly Karoy Group Kurgan Formation, provides strong evidence of its late Neoproterozoic (Cryogenian) age. This assemblage contains numerous taxa typical of pre-Ediacaran Neoproterozoic deposits including vase-shaped microfossils (e.g., *Melanocyrillium*); morphologically complex and acanthomorphic acritarchs (e.g., *Cerebrosphaera*, *Stictosphaeridium*, *Trachyhystrichosphaera*, and *Vandalosphaeridium*); and the spiral-filamentous cyanobacterium *Obruchevella exilis* (Schopf et al., 2010a; Sergeev and Schopf, 2010).

The Neoproterozoic to Cambrian organic-walled microfossils and the biozones of earliest Cambrian small shelly fossils present in Tamda Group strata, the source of the two microfossil assemblages studied here, establish its Early Cambrian age.

The lowermost strata of the Tamda Group Kyrshabakta Formation, immediately overlying those of the Maly Karoy Group, have been reported to contain terminal Neoproterozoic acritarchs of the so-called "valdaian-type" (e.g., *Leiosphaeridia*, *Origmatosphaeridium* and *Protosphaeridium*; Ogurtsova, 1985). The age of these strata, the Aktas tillites, is uncertain: they may be correlatives of the Marinoan, Gaskiers or Baykonurian glacial episodes. Meert et al. (2011) tentatively assigned these tillites to the Marinoan glacial event that marks

https://doi.org/10.1017/jpa.2015.56 Published online by Cambridge University Press

the end of the immediately pre-Ediacaran (pre-Vendian) Cryogenian. This interpretation was based primarily on the presence in Kyrshabakta Formation carbonates of a large negative shift in $\delta^{13}C$ values (up to −9‰) that may correspond to the Shuram/Wonoka carbon isotope anomaly of approximately the same age. In contrast, Chumakov (2009, 2010, 2011) correlates the Aktas tillites and similarly aged glacial sequences of Kazakhstan and Kirghizia to Late Ediacaran (Vendian)-Nemakit-Daldyn Baykonurian glacial deposits and, thus, with tillites of the Luoquan Formation (North China), Hankalchough Formation (Tarim, northwestern China), Zabit Formation (East Sayan, northwestern Mongolia-southern Siberia) and the Pourpree de l'Ahnet Group (West African Craton, Algeria). Similarly, rather than correlating the negative carbon isotope excursion in the Kyrshabakta carbonates with the Shuram/Wonoka $\delta^{13}C$ anomaly, Chumakov (personal communication to V.N.S.) correlates this shift to the negative $\delta^{13}C$ Dounce anomaly of South China (Zhou et al., 2004) and assigns an age to this glaciation of 550–540 Ma.

Although Chumakov's interpretation is consistent with the reported occurrence of lowermost Cambrian-defining small shelly fossils of the *Protohertzina anabarica* biozone in the cap dolomite immediately overlying the Aktas tillites (Mambetov, 1993), subsequent searches of these strata by Missarzhevskii (personal communication to V.N.S.) were unable to confirm this finding. Eganov and Sovietov (1979) also recorded the presence of small shelly fossils in this cap dolomite—for which, however, they did not provide taxonomic descriptions. At present, therefore, the oldest confirmed and appropriately documented occurrence of *Protohertzina anabarica* biozone fossils in the succession here studied is that in the Berkuta Member of the Kyrshabakta Formation (Missarzhevskii and Mambetov, 1981).

Fossils typical of Early Cambrian Tommotian Stage faunas occur in phosphorites of the Kyrshabakta-overlying Chulaktau Formation (Missarzhevskii and Mambetov, 1981). The two lower members of the formation, the Aksai and Karatau, correspond, respectively, to the *Tiksitheca licis* and *Pseudorthotheca costata* Tommotian faunal zones, and the uppermost Ushbass Member to the *Berkutia cristata* zone (which has been suggested, however, to occur in the Atdabanian Stage; Cook and Shergold, 2005, p. 318).

Lower units of the Chulaktau-overlying Shabakta Formation contain Late Atdabanian faunas of the *Rhombocorniculum cancellatum* zone (Missarzhevskii and Mambetov, 1981; Missarzhevskii, 1989; Mambetov, 1993; Popov et al., 2009) whereas the upper strata of the formation contain *Microcornus parvulus* zone small shelly fossils and, higher in the succession, trilobites of the *Hebediscus orientalis*, *Ushbaspis limbata* and *Redlichia chinensis-Kootenia gimmelfarbi* faunal zones of the Lower Cambrian Botomian and Toyonian Stages (Ergaliev and Pokrovskaya, 1977; Mambetov, 1993; Popov et al., 2009).

Such fauna-based biostratigraphic data for the Early Cambrian age of the Tamda Group strata are supported by organic-walled microfossils of the Chulaktau and overlying Shabakta Formation. The Chulaktau shales contain microfossil assemblages that include such time-diagnostic acritarch taxa as *Granomarginata prima*, *G. squamacea*, and *Leiomarginata simplex*, indicating their temporal correlation to the Early Cambrian Lontova Regional Stage (Horizon) of the East European Platform (Korolev and Ogurtsova, 1981, 1982; Ogurtsova, 1985; Sergeev, 1989, 1992). Similarly, and although none of the chert- and phosphate-permineralized Chulaktau microfossils reported here are time-diagnostic, this microbiota is dominated by the distinctive helically coiled cyanobacterium *Obruchevella* typical of Early Cambrian phosphorite-bearing deposits worldwide (Sergeev, 1989, 1992; Sergeev and Ogurtsova, 1989). Furthermore, acanthomorphic acritarch taxa present in the Chulaktau-overlying Shabakta Formation correspond well to those of the late Early Cambrian Vergale Regional Stage of the East European Platform.

In sum, the Early Cambrian age of Berkuta and Chulaktau microfossil assemblages described here seem firmly established by radiometric analyses of underlying deposits and by biostratigraphic data, both faunal- and microfossil-based, and from both underlying and overlying strata.

New analytical techniques and preservation of the microbiotas

Permineralized ("petrified") fossils, studied typically in petrographic thin sections, are among the best preserved and, thus, the biologically and taphonomically most informative. Nevertheless, until recently it had not been possible to document accurately, in situ and at high spatial resolution, the organismal form and cellular anatomy of such three-dimensional fossils, a deficiency particularly detrimental to studies of the morphology and cellular structure of microscopic fossilized microorganisms. Similarly, there had been no means by which to analyze in situ the molecular-structural composition and geochemical maturity of the coal-like carbonaceous organic matter (kerogen) that comprises permineralized fossils, factors crucial to assessment of their fidelity of preservation, nor had there been means—suggested here for the first time—to assess the oxic or anoxic nature of the fossil-permineralizing environment. The studies reported here of the Berkuta and Chulaktau microbiotas document use of three analytical techniques recently introduced to paleobiology that together meet these needs: confocal laser scanning microscopy (CLSM; Schopf et al., 2006), and Raman (Schopf et al., 2002, 2005) and fluorescence (Schopf and Kudryavtsev, 2010) spectroscopy and imagery.

Applicable to permineralized organic-walled fossils of all major biologic groups (animals, plants, fungi, protists, and microbes), whether preserved in quartz, apatite, calcite or gypsum, the four principal matrices in which permineralization occurs, CLSM, and Raman and fluorescence spectroscopy and imagery—used in tandem to study individual specimens—can provide data by which to characterize, in three dimensions and at submicron spatial resolution, a one-to-one match of cellular form and carbonaceous (kerogenous) composition as well as the spatial distribution of permineralizing minerals (Schopf and Kudryavtsev, 2010; Schopf et al., 2010b, 2012). Moreover, their use can elucidate the preservational history (e.g., apatite-permineralization of the soft tissues of a metazoan embryo followed by calcite-infilling of interstices and fluid-filled cavities; Chen et al., 2007) and the fidelity of their geochemical preservation (measured by the Raman index of preservation [RIP], a metric that documents the geochemical maturity of their

https://doi.org/10.1017/jpa.2015.56 Published online by Cambridge University Press

kerogenous components; Schopf et al., 2005). All three techniques are nonintrusive and nondestructive—factors that permit their application to specimens archived in museum collections—and unlike optical photomicrographs, the three-dimensional digitized images provided by CLSM and three-dimensional spectroscopic imagery can be rotated and examined from multiple perspectives, a major advance over standard optical microscopy of particular relevance to studies of the taxonomy and taphonomy of minute fossil organisms.

Confocal laser scanning microscopy.—The history of the development of CLSM, and its principles and technical details are summarized in Claxton et al. (2005). By suppressing the image-blurring input of out-of-focus planes above and below the focal plane analyzed, CLSM provides a crisp image of a thin in-focus plane that cannot be provided by standard optical microscopy. The laser of such systems excites fluorescence in the material analyzed, for organic-walled kerogenous fossils emitted from the interlinked polycyclic aromatic hydrocarbons, "PAHs," of which they are primarily composed (Schopf et al., 2005). This kerogen-derived fluorescence is then collected by the detector of the system in a wide spectral range at precisely defined depths of a rock-embedded fossil to produce its three-dimensional image at submicron lateral spatial resolution.

Raman spectroscopy.—Raman spectroscopy is an analytical technique used widely in geochemistry for the identification and molecular-structural characterization of minerals (e.g., McMillan and Hofmeister, 1988; Williams et al., 1997) including graphite, the end-point of the geochemical alteration of kerogenous organics (e.g., Pasteris and Wopenka, 1991; Wopenka and Pasteris, 1993; Jehlička et al., 2003). Raman can also be used to document the carbonaceous composition of geochemically less altered organic-walled fossils and the mineralogy of their enclosing matrices (Schopf et al., 2002, 2005, 2012; Schopf and Kudryavtsev, 2005, 2012; Chen et al., 2007).

In analyses of permineralized carbonaceous matter, CLSM and Raman are complementary, both being used to measure signals derived from properties of the kerogenous materials analyzed—for CLSM, laser-induced fluorescence derived chiefly from the electronic transitions of the interlinked PAHs that predominate in kerogen (Schopf et al, 2006); for Raman, vibrational transitions of such PAHs and their associated functional groups (Schopf et al., 2005)—with both being applicable to specimens analyzed at depths of up to 150μm within a fossil-containing thin section. Like CLSM, Raman is capable of providing both two- and three-dimensional images of the specimens analyzed (e.g., Schopf and Kudryavtsev, 2005, 2010, 2012; Schopf et al., 2002, 2005). Unlike CLSM, however, Raman provides definitive molecular-structural data about the materials analyzed and for permineralized kerogen-walled fossils and associated carbonaceous matter provides a reliable index, the RIP, of its geochemical maturity (Schopf et al., 2005).

Fluorescence spectroscopy.—Unlike CLSM, which also relies on the fluorescence of the material analyzed, fluorescence spectroscopy analyzes narrow spectral ranges specific to particular luminophores. Prior to the current study, this technique had been applied to only one other fossiliferous deposit (Schopf and Kudryavtsev, 2010; Cohen et al., 2011), primarily because fluorescing minerals are rarely associated with permineralized fossils. Apatite, however, prevalent in the Chulaktau cherts studied here, is an exception. Generally assumed to be nonfluorescing, apatite can be rendered laser-excitably fluorescent by the presence of the rare earth element samarium^{+3} substituting for calcium in the Ca I and II sites of the apatite lattice (Gaft et al., 2005, p. 142, 143, 148). Such Sm^{+3}-replacement at the highly symmetric Ca I site has been shown to occur under vacuum whereas that at the low-symmetry Ca II site occurs in the presence of air (Gaft et al., 1997a, 1997b), observations that applied to fossil-associated apatite may provide evidence of its environment of formation.

Although additional studies are needed to confirm the usefulness of such substitution to establish paleoenvironmental settings, it is likely that the cause of this effect is the presence or absence of oxygen. Air is 78% nitrogen, 21% oxygen, and <1% Ar, CO_2, and other gases. The dominant component, triple-bonded N_2, has a bond-energy of 226 kcal/mol, among the highest in nature. N_2 is therefore essentially inert and was therefore originally named "azote" (meaning "without life") by the French chemist Antoine Lavoisier, a property that explains its absence from common rock-forming minerals and its resulting accumulation in Earth's atmosphere. In contrast, oxygen, the other principal component, is highly reactive and is soluble in apatite-depositing waters where it is present in variable concentrations that, as discussed below, are consistent with oxygen-related patterns of samarium-substitution.

Morphology, geochemistry, and permineralization of the Berkuta and Chulaktau microbiotas.—As is shown in Figure 3 for five organic-walled fossils permineralized in the Chulaktau cherts, optical microscopy, confocal laser scanning microscopy, and Raman and fluorescent spectroscopic imagery can be used to analyze the same individual specimen. Because of its confocal capability and high resolution—having a lateral spatial resolution of ~0.2 μm, some 50% greater than optical microscopy—CLSM is particularly useful for documenting the morphology and fine structure of three-dimensionally sinuous fossil filaments such as the specimen of *Obruchevella parva* shown in Figure 3.1 through 3.5. Similarly, the capability of such CLSM images to be rotated enables them to be studied from perspectives not permitted by optical microscopy, as shown in Figure 4.3 and 4.7 for cask-like to spheroidal vesicles of *Berkutaphycus elongatus* new gen. and sp. permineralized in cherts of the Berkuta Member of the Kyrshabakta Formation.

As is typical of permineralized organic-walled fossils (e.g., Schopf and Kudryavtsev, 2010; Schopf et al., 2010a, 2010b, 2012), comparison of the CLSM (black and white) and Raman-kerogen images (blue) in Figures 3 and 4 shows that much of the CLSM-detected fluorescence of the Chulaktau and Berkuta specimens is derived from the PAHs of their kerogenous cell walls and associated carbonaceous components. In addition, however, Raman imagery shows that apatite has permineralized the walls of various of the Chulaktau fossils and infilled their interiors, not only of the kerogen-walled trichomes of helically coiled *Obruchevella parva* (Fig. 3.4) and the cellular lumina of *O*. cf. *meishucunensis* (Fig. 3.9), but also of coccoidal sheath-enclosed cells of the colonial

https://doi.org/10.1017/jpa.2015.56 Published online by Cambridge University Press

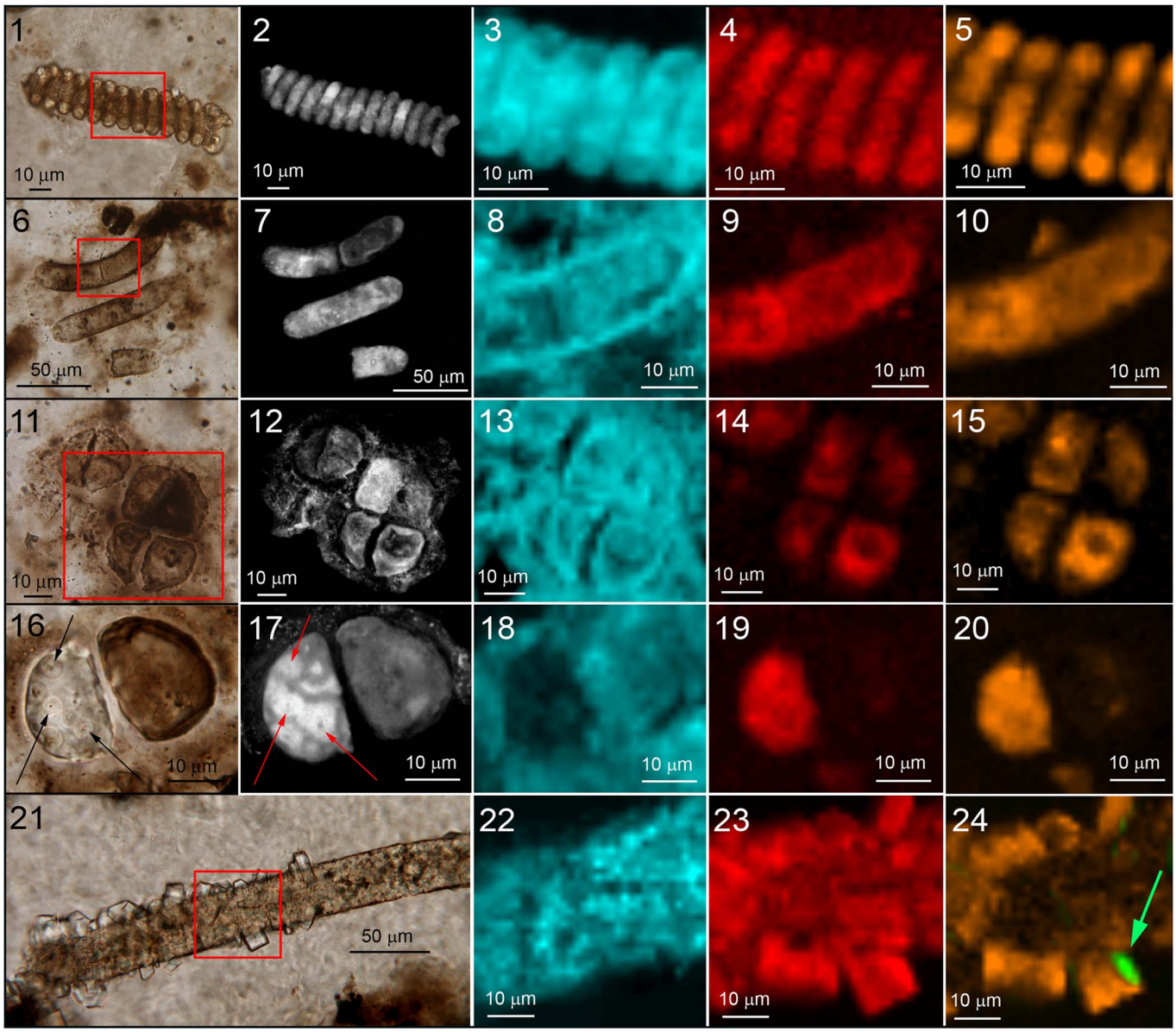

Figure 3. Quartz- and apatite-permineralized organic-walled microfossils from the Chulaktau Formation shown in optical photomicrographs (**1**, **6**, **11**, **16**, **21**); confocal laser scanning micrographs (**2**, **7**, **12**, **17**); two-dimensional Raman images documenting the spatial distribution of kerogen (**3**, **8**, **13**, **18**, **22**; blue, acquired at its ~1605 cm^{-1} major Raman band); and apatite (**4**, **9**, **14**, **19**, **23**; red, acquired at its ~965 cm^{-1} major Raman band); and two-dimensional spectroscopic fluorescence images showing the spatial distribution of fossil-permineralizing apatite (**5**, **10**, **15**, **20**; orange, acquired in the spectral range centered at ~603 nm that includes its major fluorescence bands)—fluorescent because of the presence of Sm^{+3} replacing both Ca I and Ca II sites—and of later-emplaced fossil-encrusting apatite in which Sm^{+3}-replaced Ca I sites (**24**; orange, acquired at ~597 nm) and Ca II sites (*24*; green, acquired at ~605 nm) are spatially distinct. The red rectangle in (**1**) denotes the part of the specimen shown in (**3–5**); that in (**6**), in (**8–10**); that in (**11**), in (**13–15**); and that (**21**), in (**22–24**); (**16**) shows the same area as that in (**17–20**); the arrows in (**16**) and (**17**) indicate sites of apatite nucleation. (**1-5**) *Obruchevella parva* Reitlinger, 1959, 4681-391 (102) specimen location point (p.) **11**, England Finder Slide (EFS) G32[1], GINPC 202. (**6–10**) *O*. cf. *meishucunensis* Song, 1984, 4681-391 (102), p. 17, EFS K41[4], GINPC 197. (**11–20**) *Tetraphycus acutus* Sergeev, 1989: (**11-15**) 4681-391 (102), p. 29, EFS R29[0], GINPC 210; (**16–20**) 4681-399 (103), p. 26b, EFS P31[0], GINPC 1269. (**21–24**) *Siphonophycus solidum* Golub, 1979, 4681-1026 (273), p. 81, EFS W23[1], GINPC 1270.

cyanobacterium *Tetraphycus acutus* (Fig. 3.14 and 3.19) in which sites of apatite-nucleation are discernible both in optical (Fig. 3.16) and CLSM images (Fig. 3.17).

Raman spectra (Fig. 5.1) document the kerogenous composition of the cell walls and associated organic matter of the Berkuta and Chulaktau fossils. Analyses of these spectra to determine their Raman Index of Preservation (RIP) value—an easily calculated metric that ranges from 1 to 10 used to compare the molecular-structural composition and fidelity of preservation of kerogenous permineralized fossils in permineralized fossil assemblages (Schopf et al., 2005)—shows them to have an RIP of ~7.5. This value indicates that the kerogen comprising the Berkuta and Chulaktau fossils is appreciably less geochemically altered ("better preserved") than that of the carbonaceous components of numerous Proterozoic and Archean microbiotas but is more altered than that of the especially well-preserved ~800-Ma-old Bitter Springs Formation (RIP = 9.0), the ~1900-Ma Gunflint Formation (RIP = 8.8), and the ~750-Ma-old Berkuta- and Chulaktau-underlying Chichkan Formation (RIP = 8.6; Schopf et al., 2005, 2010a).

https://doi.org/10.1017/jpa.2015.56 Published online by Cambridge University Press

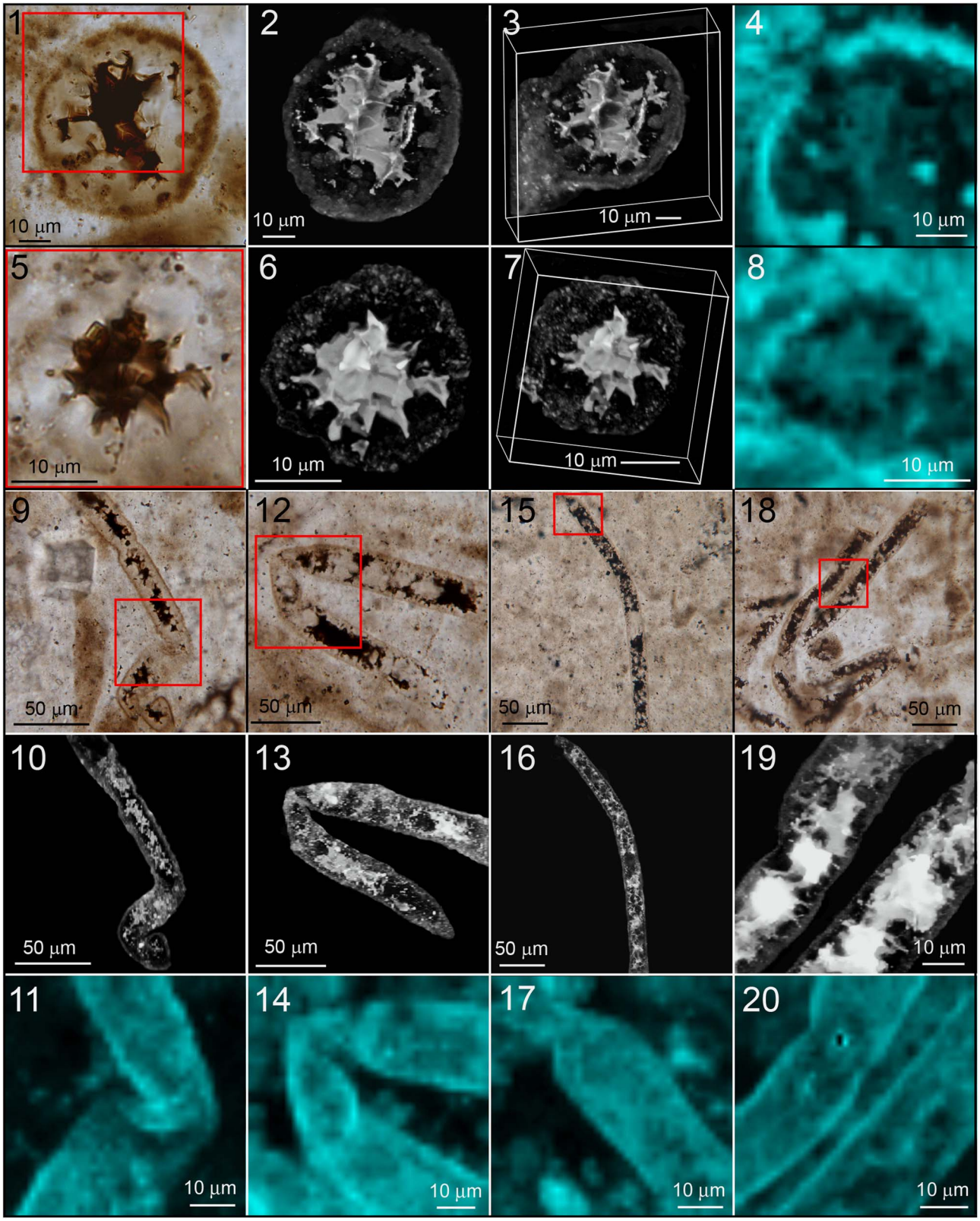

Figure 4. Optical photomicrographs (**1**, **5**, **9**, **12**, **15**, **18**), confocal laser scanning micrographs (**2**, **3**, **6**, **7**, **10**, **13**, **16**, **19**), and two-dimensional Raman images showing the spatial distribution of kerogen (**4**, **8**, **11**, **14**, **17**, **20**; blue, acquired at its ~1605 cm^{-1} major band) of quartz-permineralized organic-walled microfossils from the Berkuta Member of the Kyrshabakta Formation. The red rectangle in (**1**) denotes the part of the specimen shown in (**4**); that in (**5**), in (**8**); that in (**9**), in (**11**); that in (**12**), in (**14**); that in (**15**), in (**17**); and that in (**18**), in (**20**). *Berkutaphycus elongatus* new genus and new species, (**1–4**) 4681-372 (115a), location point (p.) 22, England Finder Slide (EFS) N35[2], GINPC 1276; (**5–8**) 4681-372 (115a), p. 31, EFS P39[1], GINPC 1277; (**9-11**) 4681-372 (115a), p. 26, EFS R41[0], GINPC 1278; (**12–14**) 4681-373 (115a), p. 7, EFS K44[3], GINPC 1279; (**15–17**) 4681-373 (115a), p. 10, EFS M38[0], GINPC 1280; (**18-20**) 4681-382 (115a), p. 13, EFS T46[3], GINPC 1281.

https://doi.org/10.1017/jpa.2015.56 Published online by Cambridge University Press

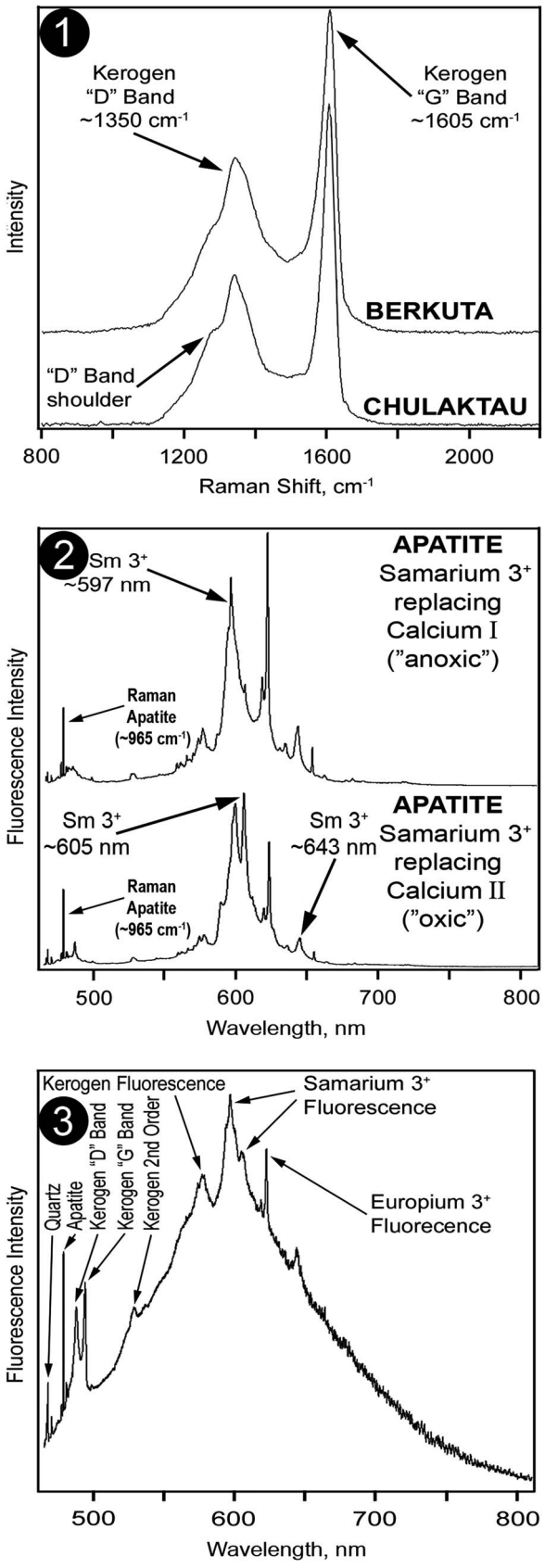

Like Raman spectra, fluorescence spectra (Fig. 5.2, 5.3) document the composition of the Chulaktau fossils and their associated matrix. The fluorescence spectra show also that the fossil-permineralizing and -infilling apatite of the deposit contains a mixture of Sm^{+3}-replaced Ca I and Ca II lattice sites. Although the analytical uncertainty in measurement of the position of fluorescence bands is typically ≤2 nm, spectral differences between these two varieties of apatite are firmly evidenced by the position and intensity of their fluorescence bands: (1) the upper spectrum in Figure 5.2 exhibits a prominent Sm^{+3} fluorescence band at ~597 nm, corresponding to the ~598 nm band (Gaft et al., 2005) and ~599 nm bands (Reisfeld et al., 1996; Gaft et al., 1997a) reported for Sm^{+3} replacing the Ca I site of apatite under vacuum conditions; (2) the lower spectrum includes a prominent Sm^{+3} fluorescence band at ~605 nm that corresponds to the ~607 nm band reported for Sm^{+3}-replacement of the Ca-II site of apatite exposed to air (Reisfeld et al., 1996; Gaft et al., 1997a; Gaft et al., 2005), a band in such fossil-associated apatite that is virtually imperceptible in the upper spectrum; and (3) the assignment of these bands to Sm^{+3} is supported by the presence of a band at ~643 nm (Fig. 5.2) that corresponds in position and relative intensity to a secondary Sm^{+3} fluorescence band reported to be situated at ~645 nm (Reisfeld et al., 1996; Gaft et al., 1997a; Gaft et al., 2005).

Much of the Chulaktau fossil-associated apatite (e.g., that permineralizing and infilling the fossils shown in fluorescence images in Fig. 3.5, 3.10, 3.15, and 3.20) exhibits a mixture of Sm^{+3}-replaced Ca I and Ca II sites. Unmixed varieties of Sm^{+3}-replaced apatite also occur. In contrast with the fossil-permineralizing and -infilling apatite (Fig. 3.1–3.20), crystals of fossil-encrusting apatite (Fig. 3.21–3.24) are mostly composed entirely of Ca I site-substituted apatite with some exhibiting peripheral zones of Ca II site-substitution (Figs. 3.24, 5.2), their euhedral form indicating that these apatite crystals were precipitated before consolidation of the surrounding sediment. Both the mode of occurrence of these encrusting apatite crystals and their unmixed rather than intermixed pattern of Sm^{+3}-substitution indicate that they represent a generation of apatite-formation different from that permineralizing and infilling the fossils.

Coupled with the paleoenvironmental setting of the Chulaktau fossil-bearing cherts—and assuming that local oxygen concentrations were determinant in Sm^{+3}-replacement of the calcium sites of apatite, as discussed above—the spectroscopic fluorescence data seem readily explicable. Initially, before microbial decay and disintegration of the fossils, permineralizing and infilling apatite was emplaced in the low-oxygen (dysoxic)

Figure 5. Raman (**1**) and fluorescence spectra (**2, 3**) of quartz- and apatite-permineralized organic-walled Early Cambrian Maly Karatau Range microfossils. (**1**) Raman spectra of kerogen comprising permineralized fossils of the Kyrshabakta (Berkuta Member) and Chulaktau formations, in both units having an RIP value of ~7.5 (see text). The relatively prominent D band shoulder of the Chulaktau kerogen, derived largely from hydrogen situated on the periphery of the platy polycyclic aromatic hydrocarbons (PAHS) of which it is dominantly composed, indicates that that it has a somewhat higher H:C composition than the Berkuta kerogen (Schopf et al., 2005). (**2**) Fluorescence spectra acquired from differing areas of the *Siphonophycus solidum*-encrusting apatite crystal denoted by the green arrow in Fig. 3.24 in which Sm^{+3} replaced Ca II and Ca I sites are spatially distinct. (**3**) Complete fluorescence spectrum of this apatite-encrusted Chulaktau specimen of *S. solidum*.

https://doi.org/10.1017/jpa.2015.56 Published online by Cambridge University Press

environment of basinal waters at and near the sediment-water interface (resulting in Sm^{+3}-replacement of a mixture of the Ca I and Ca II lattice sites). After burial in unconsolidated anoxic mud, permeating waters carried in phosphate that emplaced fossil-encrusting apatite crystals (and Sm^{+3}-replacement of their Ca I lattice site). At some later time, presumably by an influx of oxygen-containing waters, the peripheries of some encrusting crystals became oxidized (resulting in replacement at the Ca II lattice site).

This scenario is consistent with what is now is known regarding both samarium-replacement of calcium in apatite and the paleoecology of the Chulaktau basin. Nevertheless, the use of such substitution in apatite-permineralized fossils to establish the relative oxygen-concentrations of their preservational history is a concept new to paleobiology. Confirmation of this novel interpretation will depend on additional investigations.

In summary, as with virtually all comparable permineralized microbiotas, the Early Cambrian Berkuta and Chulaktau assemblages inhabited a carbonate-precipitating shallow photic-zone environment. The localized relatively low pH produced by microbial metabolism in these benthic communities resulted in dissolution of associated carbonate and its replacement by colloidal silica that infused microbial cell walls and mucilaginous envelopes and sheaths prior to their decay and disintegration. Upwelling of phosphate-laden deep marine waters into the restricted Chulaktau basin resulted in the deposition of phosphorites and, in the benthic dysoxic parts of near-shore facies, the infusion of phosphate into partially silicified microbes and its intracellular precipitation to infill cells. After near-surface burial but before consolidation of the anoxic microbe-enclosing mud, extracellular precipitation of a later insurge of phosphate produced swaths of microbe-encrusting euhedral apatite crystals, the surfaces of some of which were subsequently oxidized by interaction with oxygen-bearing percolating waters.

It has been suggested that microbial physiology may have played an active role in the concentration and precipitation of phosphate in apatite-mineralized fossil microbes (e.g., Gerasimenko et al., 1996, 1999; Zhegallo et al., 2000). Although it is plausible that an influx of dissolved phosphate into the Chulaktau basin may have promoted the proliferation of cyanobacteria, as it does in similarly shallow water settings today, the evidence presented here indicates that the infusion of silica and phosphate into the microbes that resulted in their quartz- and apatite-permineralization and -infilling were post-mortem, not under biological control. An analogous occurrence of apatite-permineralization, of essentially the same age as the Chulaktau fossils and also studied by CLSM and Raman, has been documented for a ctenophore ("comb jelly") embryo from the ~540 million-year-old Kuanchuanpu phosphorite of China (Chen et al., 2007).

Materials and methods

Fossiliferous localities.—As shown in Figures 1 and 2, the Berkuta and Chulaktau microfossils studied here occur in chert samples from the Maly Karatau Range of South Kazakhstan collected from stratigraphic sections at seven outcrops: K-27, K-28, K-29, K-30, K-32, K-33 (designations used also in Sergeev, 1992), and K-40. Listed below are the geographic localities of these outcrops of Early Cambrian fossiliferous chert (which for outcrops K-27, K-30, and K-33 differ slightly from those previously noted for microfossiliferous strata of the underling Neoproterozoic Chichkan Formation; Sergeev and Schopf, 2010).

Outcrop K-27: to the northwest of Zhanatass town in the basin of Koksu River (Google Map Coordinates, decimal degrees latitude and longitude, 43.6208 N lat., 69.6094 E long., samples 4681/115-119, 220).

Outcrop K-28: along the middle reaches of the Kyrshabakta River, north of Baikadam (43.5859N, 69.9642E, samples 4681/294, 295).

Outcrop K-29: to the southeast of Zhanatass town in the basin of Berkuta River about 1 km east from the Berkuta settlement (43.5941N lat., 69.7365E long., samples 4681/237-241).

Outcrop K-30: north of outcrop K-33, in the Au-Sakan region where the Shabakta River valley widens (43.5226N lat., 69.8739E long., samples 4681/97-104).

Outcrop K-32: near the Zhanaaryk settlement along the Zhanaaryk Creek valley and adjacent to the road between Karatau and Zhanatass towns (43.5146N lat., 69.79072E long., samples 4681/244-247).

Outcrop K-33: along the lower reaches of the Shabakta River near the Aktogai settlement, north of Baijansai (43.4744N, 69.8610E, samples 4681/14-16).

Outcrop K-40: near and south of outcrop K-27 in the basin of Koksu River along the Kurtlybulak Creek valley (decimal degree coordinates not available, samples 4681/273, 278).

The best preserved and most fossilferrous samples studied are from the cherty-phosphorite Aksai Member of the Chulaktau Formation. Abundant though less well-preserved microfossils are also here reported from the Berkuta Member of the underlying Kyrshabakta Formation (outcrops K-27 and K-32).

Repository of illustrated specimens.—The specimens illustrated here are reposited in the Paleontological Collection of the Geological Institute (GIN), Russian Academy of Sciences, Moscow.

Location of specimens within thin sections.—All illustrated fossils are from cherts of GIN field collection 4681. The figure caption for each illustrated specimen indicates its catalogue number in the GIN paleontological collection (GINPC); the field collection number of the fossil-bearing rock; the Kyrshabakta Formation (Berkuta Member) or Chulaktau Formation horizon from which the studied rock sample was obtained; the identifying number of the specimen containing petrographic thin section; and the location of the specimen within the fossiliferous thin section (indicated both by its England Finder Slide coordinates and by a "p", the point within the section where the specimen occurs and a number indicating the position of this point in an overlay map attached to the section).

Optical microscopy.—At UCLA, photomicrographs were obtained by use of Leitz Orthoplan 2 (#0026635) and Orthoplan (#654016659) microscopes (Leitz, Wetzlar, Germany) equipped, respectively, with a Nikon Digital Sight DS-Fi1 Camera System

https://doi.org/10.1017/jpa.2015.56 Published online by Cambridge University Press

(Nikon, Melville, NY) and an Olympus DP12 Microscope Digital Camera (Olympus, Melville, NY). At GIN, transmitted-light optical photomicrographs were acquired by use of an RME 5 microscope (Mikroskop Technik, Rathenow, Germany) equipped with a Cannon EOS 300D digital camera (Canon, Tokyo, Japan) and a Zeiss Axio Imager A1 microscope (#3517002390) equipped with an AxioCam MRc 5 digital camera (Carl Zeiss, Jena, Germany).

Confocal laser scanning microscopy.—CLSM images were obtained with an Olympus Fluoview 300 confocal laser scanning biological microscope system equipped with two Melles Griot lasers, a 488 nm, 20 mW output argon ion laser and a 633 nm, 10 mW output helium-neon laser (Melles Griot, Carlsbad, CA). The images were acquired using a 60× oil-immersion objective (numerical aperture 1.4) and fluorescence-free microscopy immersion oil (Cargille Laboratories, Cedar Grove, NJ) with the use of filters in the light-path, to remove wavelengths <510 nm (for 488 nm laser excitation) and <660 nm (for 633 nm laser excitation) from the laser-induced fluorescence emitted by the specimen, and of the Olympus Protocol Processor, to maximize useful data throughout the specimen. To provide maximum spatial information, most images were deconvoluted by use of the computer program Huygens Essential v3.2 (Scientific Volume Imaging, the Netherlands) and were subsequently processed by use of the VolView v2.0 three-dimensional-rendering computer program (Kitware, Clifton Park, NY) that permits their vertical and horizontal manipulation.

Raman and fluorescence spectroscopy.—Analyses of the fossils and associated minerals were carried out at UCLA by use of a T64000 (JY Horiba, Edison, NJ) triple-stage laser-Raman system that has macro-Raman and confocal micro-Raman and fluorescence spectroscopic capabilities. This system permitted acquisition of point spectra and of Raman and fluorescence images that display the two-dimensional spatial distribution of molecular-structural components of the specimens and their associated matrix, with the varying intensities in such images corresponding to the relative concentrations of the molecular structures detected. Due to the confocal capability of this system, use of a 50× objective (having an extended working distance of 10.6 mm and a numerical aperture of 0.5) provided a horizontal resolution of ~1.5 μm and a vertical resolution of 2–3 μm, with use of a 100× objective (working distance: 3.4 mm; numerical aperture: 0.8) providing a horizontal resolution of <1 μm and a vertical resolution of ~1 μm. For thin sections overlain by a glass cover slip, a 40× objective having a cover slip correction-collar was used (working distance: 4.2 mm; numerical aperture: 0.6) that provided horizontal and vertical resolution similar to that noted above. A Coherent Innova (Santa Clara, CA) argon ion laser provided excitation at 457.9 nm permitting Raman data to be obtained over a range from ~300 to ~3000 cm^{-1} by use of a single spectral window centered at 1800 cm^{-1}. Fluorescence spectra were acquired over the wavelength range extending from <465 to ~900 nm.

For Raman and fluorescence imaging, specimen-containing thin sections lacking an overlying cover slip were veneered by a thin layer of the fluorescence-free microscopy immersion oil noted above, the presence of which has been shown to have no discernable effect on the Raman and fluorescence spectra acquired (Schopf and Kudryavtsev, 2010; Schopf et al., 2005), and the fossil was centered in the path of the laser beam projected through the microscope of the system. The laser power used for Raman imaging was ~1–8 mW over an ~1 μm spot, an instrumental configuration well below the threshold resulting in radiation damage to such specimens (Schopf et al., 2005). Two-dimensional spectroscopic fluorescence images that show the spatial distribution of fossil-permineralizing and -infilling apatite, rendered fluorescent by the presence of samarium^{+3} replacing both its calcium I and Ca II sites, were acquired in a narrow, ~20-nm broad spectral window centered at ~603 nm to include both the ~597 nm and 605 nm bands. For euhedral crystals of fossil-encrusting apatite that exhibit spatially distinct regions of Sm^{+3}-substituted Ca I and Ca II sites, images were acquired in 4- to 6-nm broad spectral windows centered at ~597 nm, for Ca I-replaced sites, and at ~605 nm, for Ca II-replaced sites.

Measurement of specimens and notations used in taxonomic descriptions.—At GIN, the specimen and cell sizes reported here were measured by use of Zeiss Axio Imager A1 software (Carl Zeiss, Jena, Germany). Where appropriate, the taxonomic descriptions indicate the mean cell size of the population measured (μ), standard deviation of the population(σ), the relative standard deviation of the population (RSD, where RSD = [σ/μ] × [100%]), and the number of measured specimens (n). For many of the spheroidal morphotypes, the taxonomic description indicates the divisional dispersion index (DDI), a metric designed to interrelate the endpoints of a population size range defined as "the least number of sequential vegetative divisions required to mathematically 'reduce' the largest cell of a population to the smallest cell of that population" and a genetically determined trait shown for 473 species and varieties of modern coccoidal prokaryotes and eukaryotes to cluster in the range from 2 to 4 with the great majority (~94%) having DDIs of 6 or less (Schopf 1976; 1992a, p. 1159).

Terminology.—We here use the term 'cell' to refer to spheroidal or ellipsoidal bodies defined by distinct carbonaceous walls that we interpret to be the originally cytoplasm-containing vegetative units of unicellular or colonial chroococcacean cyanobacteria and/or eukaryotic microalgae, or the similarly distinct spheroidal to box-like segments that comprise the trichomes of filamentous cyanobacteria. In general, this terminology is the same as that in our earlier papers on the Tamda Group-underlying Chichkan microbiota (Schopf et al., 2010a; Sergeev and Schopf, 2010).

Biological composition of the Berkuta and Chulaktau microbiotas

The taxonomic composition of the Berkuta and Chulaktau microfossil assemblages is summarized in Fig. 6. The 27 distinct entities recognized (illustrated in Figs. 3–14) are grouped into four morphological categories: (1) mat-forming filamentous cyanobacteria, (2) colonial and single-celled chroococcacean

https://doi.org/10.1017/jpa.2015.56 Published online by Cambridge University Press

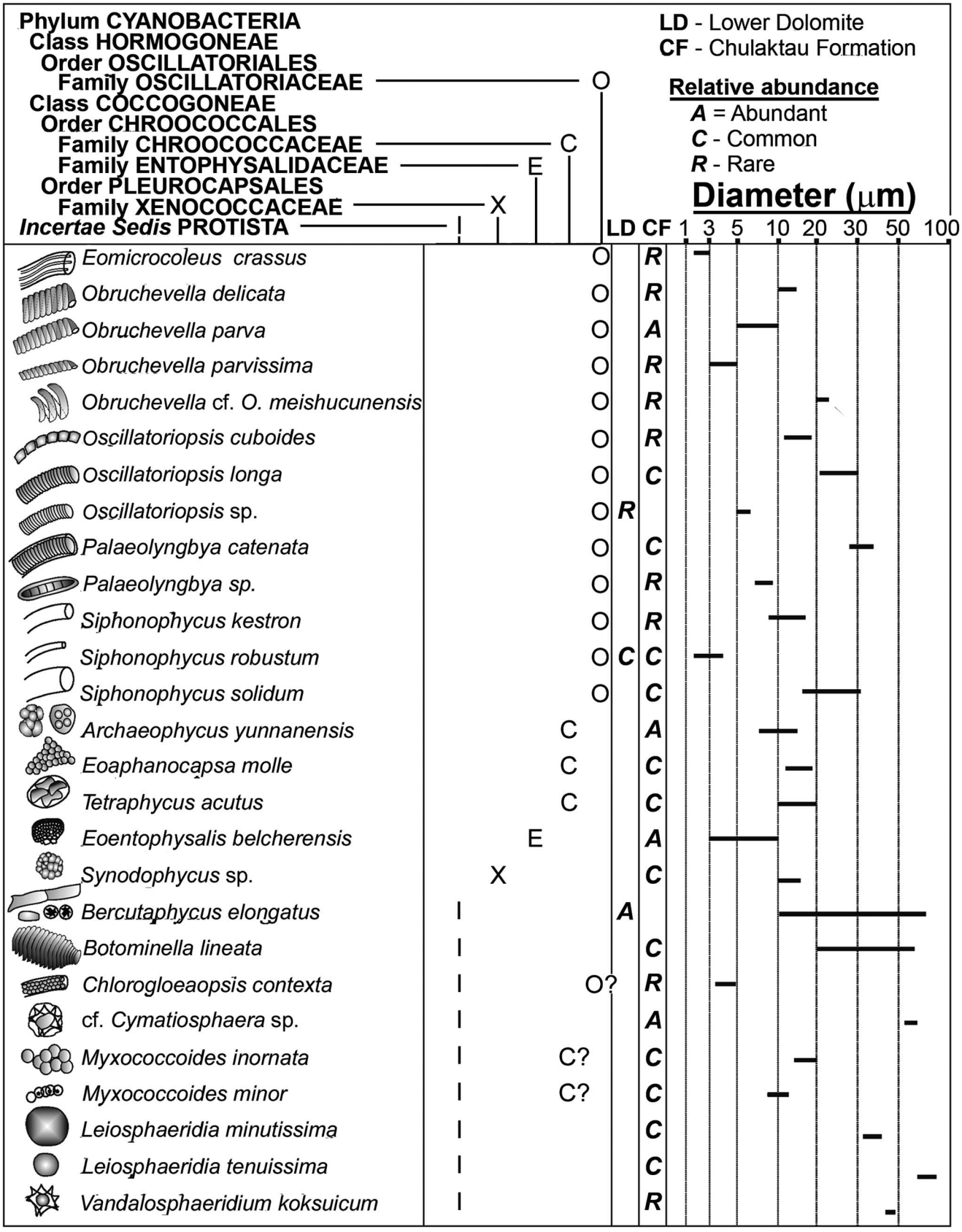

Figure 6. Synoptic listing of the microfossil taxa reported here from the Berkuta Member of the Kyrshabakta Formation and the Chulaktau Formation, indicating their inferred affinities, relative abundance in the microbiotas, and their size ranges displayed on a logarithmic scale.

https://doi.org/10.1017/jpa.2015.56 Published online by Cambridge University Press

cyanobacteria, (3) planktonic acritarchs and other unicells, and (4) filamentous microfossils of uncertain affinities. Many of these Early Cambrian morphotypes have long time ranges, including virtually all of the cyanobacteria and such sphaeromorph acritarchs as *Leiosphaeridia* spp., known also from the Meso- and Neoproterozoic.

Throughout the Chulaktau strata studied, the most abundant fossils are helical filaments of *Obruchevella* and empty sheaths, trichomes, and colonial unicells of other cyanobacteria. Assured acanthomorphic acritarchs, abundant in other Early Cambrian units, were not detected and have not been reported from strata either of the Kyrshabakta or Chulaktau formations. The relative abundance of the morphotypes dectected in the Berkuta and Chulaktau microbiotas varies greatly among the samples here investigated. In our taxonomy of the cyanobacterial morphotypes of these units, we follow the classifications of Butterfield et al. (1994) and Sergeev et al. (2012).

Mat-forming filamentous cyanobacteria.—In the Chulaktau assemblage, well-preserved spiral filaments of *Obruchevella* are particularly abundant. Four species of *Obruchevella* have been detected: *O. parva* (Figs. 3.1–3.5, 7.1–7.7, 8.1, 8.2, 8.5, 8.6, 9.1–9.6), *O. parvissima* (Fig. 8.3, 8.4, 8.7, 8.8), *O. delicata*, and *O.* cf. *meishucunensis* (Fig. 3.6–3.10). As in genera of similarly helically coiled modern cyanobacteria (e.g., *Spirulina* and *Arthrospira*), such fossil trichomes typically exhibit little evidence of cell-defining transverse cell walls. Such septa, however, are preserved in some Chulaktau specimens of *O. parva*, showing their cells to be 5–10 μm in diameter. This species of *Obruchevella* is predominant in all Chulaktau samples here studied whereas other taxa of the genus—differentiated from *O. parva* by their filament diameters (viz., *O. parvissima*, 3–5 μm, *O. delicata*, 10–13 μm, and *O.* cf. *meishucunensis*, 20–22 μm)—are relatively uncommon.

Other filamentous Chulaktau cyanobacteria are here assigned to *Eomicrocoleus* (Fig. 11.9), *Siphonophycus*, *Oscillatoriopis* and *Palaeolyngbya*. *Siphonophycus*, most recently defined taxonomically by Butterfield et al. (1994) and Sergeev et al. (2012) and interpreted to be the extracellular trichome-enclosing tubular sheaths of oscillatoriacean cyanobacteria, is represented by three species differentiated by their breadths: *S. robustum* (2–4 μm; Fig. 11.11); *S. kestron* (8-16 μm); and *S. solidum* (16–32 μm; Figs. 3.21–3.24, 10.7, 10.8, 10.11, 10.12). These taxa, like those of *Obruchevella* spp., are of common occurrence in the Chulaktau cherts. The assemblage also includes three species of *Oscillatoriopsis*, each exhibiting well defined rounded terminal cells and disc- or cube-shaped medial cells and differentiated by their characteristic cell diameters: *Oscillatoriopsis* sp. (5–7 μm), *O. cuboides* (13–18.5 μm; Fig. 9.7–9.9), *O. longa* (22-30 μm; Figs. 10.5, 10.6, 11.7, 11.8). The Chulaktau cherts also contain two species of *Palaeolyngbya*, characterized by its sheath-enclosed uniseriate trichomes composed of discoidal to cylindrical cells: *P.* sp. (6–7 μm in diameter; Fig. 11.12, 11.13) and a much broader form, *P. catenata* (28–35 μm in diameter; Figs. 9.10, 9.11, 10.1–10.4, 10.9, 10.10, 11.1–11.6).

Given the phototaxis of the trichomes of oscillatoriaceans and their capability by gliding motility to vacate their encompassing tubular sheaths, it is possible that various of the taxa of trichomes and sheaths of *Siphonophycus*, *Oscillatoriopsis* and *Palaeolyngbya* co-occurring in the Chulaktau cherts represent differing parts of single biological entities. Thus, for example, the cell size–defined 13- to 18.5-μm broad taxon *Oscillatoriopsis cuboides* may have been a *Lyngbya*-like oscillatoriacean that was originally ensheathed by 16- to 32-μm diameter *Siphonophycus solidum* sheaths that might also have originally enclosed the 22- to 30-μm broad cellular trichomes of *O. longa*. Like their modern counterparts, these taxa were evidently mat-forming, in some instances preserved in the Chulaktau cherts in eroded and redeposited rounded or subrounded mat fragments.

Colonial and single-celled chroococcacean cyanobacteria.—Of the taxonomic families of coccoidal cyanobacteria identified in the Chulaktau microbiota, the mat-forming Entophysalidaceae is represented by *Eoentophysalis belcherensis* (Fig. 12.3, 12.6, 12.7–12.13), a taxon having spheroidal to ellipsoidal 3-to 10-μm diameter cells occuring in palmelloid colonies enclosed by multilayered envelopes. Of limited distribution in the assemblage, distinctive crustose pustular laminae like those formed by *E. belcherensis* in Proterozoic stromatolitic deposits (Hofmann, 1976; Sergeev et al., 1995, 2012) have not been observed in the Chulaktau cherts.

Among all types of fossil coccoidal cyanobacteria represented in the Chulaktau biota, colonial members of the Chroococcaceae are particularly abundant, their affinity to this family indicated typically by their occurrence in small clusters of 2, 4 or as many as 8 close-packed and commonly individually ensheathed cells produced by cell division in two mutually perpendicular planes and surrounded by a colony-enclosing originally mucilaginous envelope. Of these, *Tetraphycus acutus* (Figs. 3.11–3.20, 12.4, 12.5), having a cell size-range of 10-20 μm, is especially abundant, occurring in groups of small colonies spread laterally over hundreds of square microns. Although Chulaktau specimens of the morphologically similar colonial chroococcacean *Archaeophycus yunnanensis* (Fig. 12.1, 12.2), characterized by 8- to 15-μm-diameter cells, may represent apatite-replaced preservational variants of *Tetraphycus acutus*, the individual mineralized cells of such colonies are not sheath-enclosed and are typically somewhat smaller than those of *T. acutus*.

The colonial chroococcacean *Eoaphanocapsa molle* (Fig. 14.12) exhibits multilamellated spheroidal and ellipsoidal cells 12- to 17-μm in diameter that occur in loose clusters of a few to many tens of individuals embedded in a diffuse organic matrix and surrounded by a colony-defining envelope. *Eoaphanocapsa*, regarded as a fossil analogue of the modern chroococcacean *Aphanocapsa*, provides a useful form genus for colonies of multilamellated spheroidal cells that lack evidence of a cell division pattern like that known for such fossil chroococcaceans as *Gloeodiniopsis*. Like colonies of modern *Aphanocapsa*, those of fossil *Eoaphanocapsa* typically occur as benthic components of mat-building microbial communities dominated by filamentous cyanobacteria, not only in the Chulaktau cherts but also in those of the Proterozoic Min'yar and Sukhaya Tunguska formations (Nyberg and Schopf, 1984; Sergeev, 2006).

One additional coccoidal colonial Chulaktau taxon, *Synodophycus* sp. (Fig. 14.7–14.9), deserves mention. Fossils of

https://doi.org/10.1017/jpa.2015.56 Published online by Cambridge University Press

this genus occur as tightly packed spheroidal colonies of single-walled cells 10- to 15-µm in diameter that in some instances are enclosed by multilayered envelopes. Given their simple morphology and small cell size, these fossils are probably of cyanobacterial, chroococcacean affinity. Nevertheless, morphologically similar colonies occur also in other cyanobacterial families (e.g., the Pleurocapsaceae and Entophysalidaceae) as well as among microalgal eukaryotes. Described originally from the Neoproterozoic Draken Conglomerate of Spitsbergen (Knoll, 1982), species of *Synodophycus* have been reported less commonly from permineralized microbial communities than those of the other colonial Chulaktau taxa noted above. Similarly, unlike the benthic habit of the other colonial taxa, that of the Chulaktau *Synodophycus* specimens has yet to be established.

Planktonic acritarchs and other unicells.—Although the Berkuta and Chulaktau strata, unlike some Early Cambrian microbiotas, lack abundant spiny (acanthomorphic) acritarchs, the Chulaktau cherts contain the planktonic sphaeromorphs *Leiosphaeridia minutissima* (Fig. 13.10) and *L. tenuissima* (Fig. 13.9) as well as the problematic acanthomorphs *Vandalosphaeridium koksuikum* and *Cymatiosphaera* sp., all of probable of eukaryotic affinity. *Leiosphaeridia*, of broad stratigraphic range and the principal form genus of unornamented sphaeromorphic acritarch known from Proterozoic and Cambrian sediments, is commonly interpreted to be a unicellular prasinophycean (e.g., Tappan, 1980) or chlorophycean alga (Talyzina and Moczydłowska, 2000; Moczydłowska, 2010; Moczydłowska et al., 2010). Although for most specimens of *Leiosphaeridia* such affinities are likely correct, some leiosphaerids exhibit wall ultrastructure seemingly unlike that of eukaryotic green algae (e.g., Javaux et al., 2004). In addition to specimens permineralized in the Chulaktau cherts, carbonaceous compression-preserved vesicles assigned to *Leiosphaeridia* have been reported from interbedded shales of the formation (Korolev and Ogurtsova, 1981, 1982; Ogurtsova, 1985).

Of particular interest among the acritarchs of the Chulaktau assemblage is *Vandalosphaeridium koksuicum* (Fig. 14.3, 14.6), a form typified by its evidently single-layered more or less spheroidal vesicles, 40- to 45-µm in diameter, in which the vesicle-defining envelope appears to be sculptured by prominent semicrescent to transverse ramparts and short appendage-like possible processes. This characteristic sculpture pattern, exhibited also by specimens reported from the underlying Neoproterozoic Chichkan Formation (Schopf et al., 2010a; Sergeev and Schopf, 2010), coupled with the occurrence in Chulaktau and Chichkan specimens of a globular interior cyst-like body, suggests their probable chlorococcalean affinity (cf., Moczydłowska, 2010). A morphologically rather similar 55- to 65-µm-diameter acritarch co-occurring in the Berkuta and Chulaktau cherts is cf. *Cymatiosphaera* sp. (Fig. 14.1, 14.2, 14.4, 14.5). Because almost all previously described species of *Cymatiosphaera* have been defined on the basis of flattened compression-preserved specimens in shales, rather than three-dimensionally chert-permineralized specimens such as those studied here, we do not assign the Tamda Group specimens to a previously defined species.

Two species of the spheroidal-celled colonial or unicellular form genus *Myxococcoides*, *M. minor* and *M. inornata*, occur rather commonly in small colonies scattered among the benthic members of the Chulaktau assemblage, an irregular distribution suggesting that they may represent allocthonous plankton derived from overlying waters. The epithet *Myxococcoides* has been applied both to envelope-enclosed many-celled colonies of closely packed spherical cells such *M. minor* (Fig. 14.11), composed of 8.5- to 14-µm diameter cells, and to isolated cells and cell pairs like those of *M. inornata* (Fig. 14.10), 15–20 µm in diameter. Although all described species of *Myxococcoides* are plausibly chroococcacean (*Chroococcus*- or *Gloeocapsa*-like) cyanobacteria, as such forms were originally interpreted (Schopf, 1968), some bear resemblance also to extant small-celled eukaryotic chlorophycean algae (Knoll et al., 1991; Knoll, 1996; Schopf et al., 2010a; Sergeev and Schopf, 2010).

Filamentous microfossils of uncertain affinities.—This category includes only two of the 27 taxa here reported, *Botominella lineata* and *Berkutaphycus elongatus*. *Botominella lineata* (Fig. 13.1–13.5) exhibits a filamentous trichome-like body composed of cell-like segments 20- to 60-µm wide and 2- to 5-µm long. *Berkutaphycus elongates* (Figs. 4.1–4.20, 13.6–13.8, 13.11–13.16) is a previously unreported taxon here described from the Berkuta Member of the Kyrshabakta Formation where it is evidently represented by life cycle and preservational variants and is interpreted to include 11- to 34-µm broad filamentous tubes as well as spheroidal and cask-like structures 25- to 70-µm wide and 2- to 5-µm long. Like *Botominella lineata*, *Berkutaphycus elongatus* is of uncertain affinities, resembling large-diameter cyanobacteria and some filamentous eukaryotic algae.

Evolutionary and biostratigraphic significance of the Berkuta and Chulaktau microbiotas

The microbiotas of the Berkuta Member of the Kyrshabakta Formation and the overlying Chulaktau Formation are composed largely of morphologically simple filamentous and coccoidal microorganisms, mainly cyanobacteria, augmented by unornamented spheroidal planktonic acritarchs, presumably prasinophycean or chlorophycean algae. Thus, both resemble so-called 'typical Proterozoic microbiotas' (Mendelson and Schopf, 1982)—assemblages dominated by and in some instances composed entirely of filamentous and coccoidal, evolutionarily conservative (hypobradytelic) cyanobacteria (Schopf, 1994). Despite their 'Proterozoic-like' appearance, however, their Phanerozoic age is well established by the presence of lowermost Cambrian-defining small shelly fossils in the Kyrshabakta Formation Berkuta Member, specimens of which have also been reported to occur in the stratigraphically underlying tillite-overlying cap dolomite of the formation.

Both of the microbiotas studied here lack the richly diverse assemblage of morphologically relatively complex unicellular eukaryotes, including acanthomorphic acritarchs, of the underlying and much older Neoproterozoic (~750 Ma-old) Chichkan Formation (Schopf et al., 2010a; Sergeev and Schopf, 2010). Indeed, and although the Chulaktau assemblage includes sphaeromorphic acritarchs (viz., *Leiosphaeridia minutissima*

https://doi.org/10.1017/jpa.2015.56 Published online by Cambridge University Press

and *L. tenuissima*), acanthomorphs seem not to be represented (with the possible exception of rare specimens of the enigmatic taxa *Vandalosphaeridium koksuikum* and *Cymatiosphaera* sp.).

Why are acanthomorphic acritarchs, typical of Early Cambrian microbiotas in other locales, not abundant and perhaps not present in the Berkuta and Chulaktau assemblages? This absence may simply reflect the early Early Cambrian age of these assemblages, dating from the immediate aftermath of the phytoplankton extinction event of the latest Proterozoic (e.g., Vidal and Knoll, 1982; Schopf, 1992b; Knoll, 1994; Vidal and Moczydłowska-Vidal, 1997; Knoll et al., 2006), with available data indicating that the upsurge in diversity of acanthomorphs during the Early Ediacaran (Grey, 2005; Vorob'eva et al., 2009) was followed by a major decrease until the mid-Early Cambrian when there was a second sharp increase near the beginning of the Atdabanian (as evidenced, for example, in the Lükati [Talsy] Horizon of the East European Platform; Volkova et al., 1979; Sergeev, 1992).

A second possible explanation is environmental, a product of the fossil-preserving facies. In particular, it seems plausible that phytoplanktonic acanthomorphs may have been prevalent only in open marine settings and that their absence from the Berkuta microbiota is a result of its preservation in a shallow post-Baykonurian glacial basin of the Early Cambrian seas. Similarly, in consonance with the environmental model for deposition of the Karatau Member of the Chulaktau Formation proposed by Kholodov and Paul (1993a, 1993b; 1994), we envision the immediately underlying acanthomorph-lacking Aksai Chulaktau cherts to represent an extremely shallow environment of a restricted marine basin. Additional studies of distal offshore deposits of Berkuta- and Askai-age will be needed to establish the role that habitat may have played in excluding acanthomorphs from sediments in which they might otherwise have been expected.

The Berkuta microbiota is appreciably less diverse than that of the younger Chulaktau microbiota, lacking, for example, such taxa as *Leiosphaeridia minutissima*, *L. tenuissima*, *Myxococcoides minor*, *M. inornata*, *Archaeophycus yunnaensis*, *Siphonophycus kestron*, and *Oscillatoriopsis* sp. (of which the last two filamentous taxa are not illustrated in this paper). Although we interpret the relative lack of diversity of the Berkuta microbiota as most likely reflecting its preservation in a restricted shallow post-glacial basin, such differences may be due to vagaries of preservation: even in the comparatively better preserved and more diverse Chulaktau assemblage, *Siphonophycus kestron* and *Oscillatoriopsis* sp. are known only from sample 244 (outcrop K-32) whereas in the underlying Berkuta, *Berkutaphycus elongatus*, unknown from the Chulaktau, is present only in sample 115a (outcrop K-27).

By the facies-based interpretation suggested here, the compositions of the Berkuta assemblage and Chulaktau microbiota reflect their local environments, settings that are a product of the Early Cambrian global environment. The Neoproterozoic Ediacaran and Phanerozoic Cambrian Periods span a distinctive time in Earth history when the ecosystem changed radically with the rise of metazoans. During this time, huge accumulations of economically important phosphatic ores were deposited in basins worldwide—an event of particular paleontological significance because of the capability of such phosphate to permineralize microorganisms, as shown in Fig. 3, as well as soft animal tissues (e.g., Chen et al., 2007). Of the many such deposits known, that of the economically important Maly Karatau Range Lower Cambrian Chulaktau Formation has been investigated in particular detail.

Deposition of the Chulaktau phosphorites has typically been modeled as resulting from the upwelling of phosphate-saturated deep marine waters into shallow settings where phosphatic nodules, granules and oolitic sediments were precipitated (see Baturin, 1978, for additional references and discussion). This scenario and many variants have been suggested for the deposition of Karatau Member phosphorites (e.g., Cook and Shergold, 2005). Although a full discussion of such models is beyond the scope of this paper, because the mode of formation of the Chulaktau phosphorites bears on the fossilization, and, thus, the composition of the preserved microbiota, it merits consideration. Our favored model is that of Kholodov and Paul (1993a, 1993b, 1994) according to which the phosphorites were deposited in exceedingly shallow waters of a restricted basin that had a complicated shore geography composed of lagoons, inlets, evaporitic pools and diverse other near-shore facies. We envision this Early Cambrian restricted shallow basinal setting to have served as a trap for phosphate deposition that resulted in apatite permineralization of the Chulaktau microbiota (e.g., Fig. 3).

The diverse shallow near shore settings hypothesized by Kholodov and Paul (1993a, 1993b, 1994) and an influx of dissolved phosphate spurring the proliferation of cyanobacteria would have been ideal for the thriving "Proterozoic-like" community preserved in the Chulaktau cherts and might help to explain the apparent absence from the assemblage of more open ocean-inhabiting acanthomorphic acritarchs, while also suggesting that unornamented sphaeromorph leiosphaerids may have been relatively more abundant in near shore habitats. Similarly, this model is consistent with the Raman and fluorescence spectroscopic data presented here for the apatite-permineralization, -infilling and -encrustation of the Chulaktau fossils (Figs. 3 and 5).

Among the various taxa identified in the Chulaktau assemblage, entophysalidacean cyanobacteria occur today in extremely shallow intertidal or peritidal environments. That they also inhabited such settings in the Chulaktau basin is shown by the occurrence in the fossiliferous succession of such shallow-water indicators as desiccation cracks, intraclastic grainstones (flat-pebble conglomerates) and oolitic grainstones. To explain the oolitic texture of most of the Chulaktau phosphatic ores, the Kholodov and Paul (1993a, 1993b, 1994) model suggests that the shallow phosphate-depositing environment was highly energetic. This, in turn is consistent with our findings of the absence of coherent cyanobacterial mats in the Chulaktau cherts and the predominant occurrence of entophysalidaceans as loose clusters of gloeocapsoid cells and spheroidal aggregations rather than as lamina-defining crustose colonies such as those reported from Proterozoic cherts by Hofmann (1976) and Sergeev et al. (1995, 2012).

In sum, the Berkuta and Chulaktau strata were deposited in evidently very shallow waters, evidenced both by their sedimentological characteristics and by the compositions of their permineralized microbial assemblages. Subsequent to

https://doi.org/10.1017/jpa.2015.56 Published online by Cambridge University Press

their deposition, the late Atdabanian marine transgression established a more standard oceanic regime, a possible explanation for the absence of assured acanthomorphs from the Berkuta and Chulaktau assemblages and their abundance in basal horizons of the Chulaktau-overlying Shabakta Formation (Korolev and Ogurtsova, 1981, 1982; Ogurtsova, 1985; Sergeev, 1989, 1992).

Conclusions

The Berkuta and Chulaktau assemblages document the composition of a part of Earth's microbial biota during a key transition in evolutionary history when, with the rise of megascopic metazoans, the biosphere changed markedly. This biotic transition was no doubt gradual, rather than abrupt—occurring over tens of millions of years—with the two assemblages studied here providing insight into the adaptation of microbes to this global event. Because of their exceptional preservation, a result of environmental settings that promoted permineralization by both silica and phosphate, the microbiotas of the two units provide a clear view of Early Cambrian shallow-water microbial ecosystems.

In comparison with microbiotas permineralized in the underlying Neoproterozoic Chichkan Formation and the overlying Early Cambrian Shabakta Formation, those of the Berkuta and Chulaktau cherts and phosphorites are depauperate, most notably lacking assured acanthomorph acritarchs. Although the relatively low diversity of these two cyanobacterium-dominated "Proterozoic-like" communities in part reflects their occurrence in units deposited in the aftermath of the latest Proterozoic phytoplankton extinction event, paleoenvironmental considerations suggest that it may also have been a result of their preservation in shallow near-shore settings where the restricted basin served to inhibit an influx of acanthomorphs from distal open-marine environments.

In addition to documenting two previously undescribed microbial assemblages, this study demonstrates the use of new techniques to analyze permineralized microscopic fossils in situ at submicron spatial resolution. Thus, in addition to standard optical microscopy we have used three techniques recently introduced to paleobiology: confocal laser scanning microscopy, to document the three-dimensional organismal and cellular morphology of the microfossils; and both Raman and fluorescence spectroscopy and imagery, to document their carbonaceous composition, the geochemical maturity of the kerogen of which they are composed, and the composition of the fossil-enclosing matrix and of fossil-permineralizing, -infilling, and -encrusting minerals. For the first time, fluorescence spectroscopic data are provided here that suggest their use to infer the oxic or anoxic paleoenvironment of fossil-preserving apatite-formation.

This report of the Berkuta and Chulaktau microorganisms adds new information about the biological composition and evolutionary status of Early Cambrian (Nemakit-Daldynian and Tommotian, 542- to ~530-Ma-old) microbiotas preserved in restricted shallow-water chert- and phosphate-precipitating environments. The new approach to such studies documented here, the application of diverse newly applied techniques to analyze individual microscopic fossils, can provide useful insight into their biological affinities, paleoecology, taphonomy, and environment of preservation.

Systematic paleontology

Kingdom Eubacteria Woese and Fox, 1977
Phylum Cyanobacteria Stanier et al., 1978
Class Hormogoneae Thuret, 1875
Order Oscillatoriales Elenkin, 1949
Family Oscillatoriaceae (S.F. Gray) Kirchner, 1900
Genus *Eomicrocoleus* Horodyski and Donaldson, 1980

Type species.—*Eomicrocoleus crassus* Horodyski and Donaldson, 1980.

Eomicrocoleus crassus Horodyski and Donaldson, 1980
Figure 11.9

Eomicrocoleus crassus Horodyski and Donaldson, 1980, p. 154, figs 15A, 15B; Sergeev, 2001, p. 442, fig. 9.5; Sergeev, 2002, p. 559, pl. 2, fig. 6; Sergeev, 2006, p. 208, pl. 18, fig. 5, pl. 25, fig. 6; Sharma, 2006, p. 91, fig. 10d; Sergeev, Sharma and Shukla, 2012, p. 289, pl. 15, figs. 4–6, 9.

Description.—Bundles of tube-like trichomes having very rare cross-walls closely grouped within a common cylindrical sheath or without a surrounding sheath. Parallel or subparallel trichomes are 2–3 μm in diameter, mostly hollow, and have psilate walls ~0.5 μm thick; trichome-encompassing common sheaths, when present, are 25–30 μm in cross-sectional diameter, up to 80 μm long, ~1 μm thick, and are typically fine-to medium-grained.

Material examined.—Several well-preserved specimens.

Occurrence.—Widely distributed in Proterozoic and Lower Cambrian chert-permineralized organic-walled assemblages.

Remarks.—Trichomes and sheaths of the Chulaktau Formation are of slightly larger diameter than those of the type population and the bundles of trichomes commonly lack encompassing sheaths, an absence attributable to preservational alteration (Gerasimenko and Krylov, 1983, Sergeev et al., 1997).

Genus *Obruchevella* Reitlinger, 1948, emend.
Yakschin and Luchinina, 1981, emend. Kolosov, 1984,
emend. Yankauskas, 1989, emend. Burzin, 1995,
emend. Nagovitsin, 2000

Type species.—*Obruchevella delicata* Reitlinger, 1948.

Obruchevella parva Reitlinger, 1959, emend.
Golovenok and Belova, 1989, emend. Burzin, 1995
Figures 3.1–3.5, 7.1–7.7, 8.1, 8.2, 8.5, 8.6, 9.1–9.6

Obruchevella parva Reitlinger, 1959, p. 21, pl. 6, figs. 1, 2; Kolosov, 1977, p. 73,74, pl. 6, fig. 1; 1982, pl. 16, figs. 1a, 1б; Cloud, Awramik, Morrison and Hadley, 1979, p. 87-89, figs. 5J and 5K; Yakschin and Luchinina, 1981, p. 30, pl. 10, figs. 1–3; Golovenok and Belova, 1983, p. 1464, figs. 1B–1D;

https://doi.org/10.1017/jpa.2015.56 Published online by Cambridge University Press

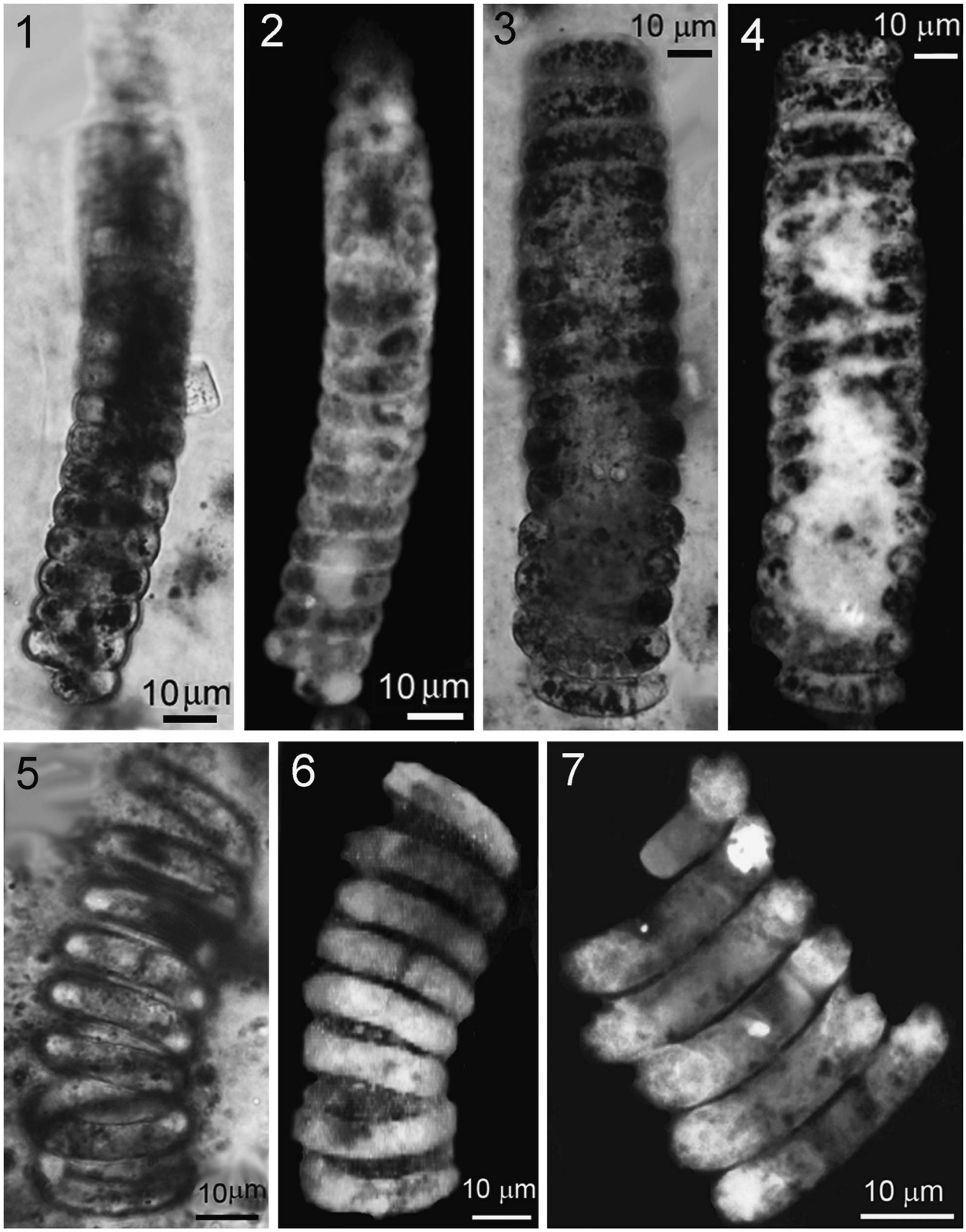

Figure 7. Optical photomicrographs (**1, 3, 5**) and confocal laser scanning micrographs (**2, 4, 6, 7**) of Chulaktau Formation quartz- and apatite-permineralized organic-walled specimens of *Obruchevella parva* Reitlinger, 1959: (**1, 2**) 4681-369 (102), specimen location point (p.) 19, England Finder Slide (EFS) Q40[3], GINPC 1250; (**3, 4**) 4681-365 (102), p. 2, EFS H35[3], GINPC 200; (**5, 6**) 4681-369 (102), p. 10, EFS N30[0], GINPC 1251; (**7**) 4681-369 (102), p. 13, EFS 044[2], GINPC 1252. Like many of the Chulaktau fossils, the kerogenous walls of these specimens were permineralized in quartz with their interior voids being infilled by apatite; if such apatite contains samarium and/or europium substituted for calcium (see text and Fig. 5), their presence can be evidenced in CLSM images by the occurrence of relatively bright, light gray to white fluorescent regions such as those evident in transverse sections of the spiral tubes in (**7**).

https://doi.org/10.1017/jpa.2015.56 Published online by Cambridge University Press

Song, 1984, p. 183, figs. 3.1–3.3, 3.8, 3.9; Sergeev, 1989, pl. 2, figs. 1–3, 5, 6, 8; Sergeev and Ogurtsova, 1989, pl. 1, figs. 1–3, 5–9, 12; Golovenok and Belova, 1989, p. 193, figs. 1d–1f; Sergeev, 1992, p. 89, pl. 24, figs. 5, 6, 11, pl. 25, figs. 1a, 1b, 2, 3, 5, 6a, 6b; Burzin, 1995, p. 10–11, 13, pl. 1, figs. 1–3, 4A, pl. 3, fig. 1; Prasad, Uniyal and Asher, 2005, p. 54, pl. 10, figs. 4, 12, Pl. 11, fig. 9; Prasad, 2007, pl. 1, figs. 3, 6, 15; Sergeev, Sharma and Shukla, 2012, p. 296, pl. 19, figs. 1–6, 14 (for additional synonymy, see Burzin, 1995, Golovenok and Belova, 1989, and Sergeev, Sharma, and Shukla, 2012).

Description.—Empty non-tapering cylindrical tubes, rarely exhibiting cell-defining septa, coiled into regular cylindrical spirals. Tube diameters range from 5 to 10 μm; coiled spirals are 20–35 μm in breadth and up to 155 μm long. Cross-walls, when present, define cellular segments 1.5–2.0 μm in length. Tube lateral- and cross-walls are fine-grained ~0.5 μm thick.

Material examined.—A few hundred well-preserved specimens.

Occurrence.—Widely distributed in Ediacaran (Vendian) and Lower Cambrian microfossil assemblages.

Remarks.—In the Chulacktau cherts, the permineralized spirals are commonly infilled by apatite. Golovenok and Belova (1983) described *O. parva* from units incorrectly assigned to the underlying Chichkan Formation, an error corrected in subsequent publications (Decision of Fifth All-union Colloquium on Precambrian Microfossils of the USSR, 1986; Ogurtsova and Sergeev, 1987; Sergeev and Ogurtsova, 1989; Sergeev, 1989, 1992).

Obruchevella parvissima Song, 1984
Figure 8.3, 8.4, 8.7, 8.8

Obruchevella parvissima Song, 1984, p. 183, figs. 3.14–3.16; Sergeev and Ogurtsova, 1989, pl. 1, fig. 11; Sergeev, 1992, p. 90, pl. 25, fig. 4; Prasad, Uniyal and Asher, 2005, p. 54, pl. 11, fig. 10; Prasad, 2007, pl. 1, fig. 16; Sergeev, Sharma and Shukla, 2012, p. 296, pl. 19, fig. 10.

Description.—Thin-walled empty cylindrical tubes, coiled into loose regular spirals in which the walls of adjacent tubes are not in contact. Tube diameters range from 3 to 5 μm; the outer diameter of the spiral coils ranges from 18 to 30 μm whereas their inner boundary ranges from 12 to 20 μm. Tube walls are medium-grained, opaque, and typically ≤ 1.0 μm thick.

Material examined.—A few well-preserved specimens.

Occurrence.—Ediacaran (Vendian): Nagod Limestone Formation, India; Lower Cambrian: Yuhucun Formation, China; Chulaktau Formation, South Kazakhstan.

Obruchevella cf. *O. meishucunensis* Song, 1984
Figure 3.6–3.10

Obruchevella cf. *O. meishucunensis* Song, 1984. Sergeev and Ogurtsova, 1989, pl. 1, fig. 11; Sergeev, 1992, p. 90, pl. 24, fig. 8; Sergeev, Sharma and Shukla, 2012, pl. 19, fig. 7.

Description.—Thin-walled empty cylindrical tubes, coiled into a loose regular spirals in which the walls of adjacent tubes are not in contact. Tube diameters range from 20 to 22 μm; the outer diameter of the spiral coils is ~120 μm whereas their inner boundary is ~80 μm. Tube walls are medium-grained, translucent, ~1.0 μm thick.

Material examined.—Several not very well-preserved trichomes.

Genus *Oscillatoriopsis* Schopf, 1968, emend.
Mendelson and Schopf, 1982, emend.
Butterfield, 1994 (in Butterfield, Knoll and Swett, 1994)

Type species.—*Oscillatoriopsis obtusa* Schopf, 1968.

Oscillatoriopsis cuboides Knoll, Strother and Rossi, 1988
Figure 9.7–9.9

Oscillatoriopsis cuboides Knoll, Strother, and Rossi, 1988, p. 275, 276, fig. 11c; Sergeev, Sharma, and Shukla, 2012, text-fig. 42D.

Description.—Solitary uniseriate unbranched cellular trichomes lacking encompassing sheaths. Terminal cells were not detected in the specimens studied; medial cells are quadrate, cask-shaped, translucent, 13.0–18.5 wide ($n = 6$, $\mu = 15$ μm, $\sigma = 2.3$, RSD = 15%) and 15–23 μm long ($n = 6$, $\mu = 18.6$ μm, $\sigma = 2.3$, RSD = 12%), and have a width-to-length ratio ranging from 1 to 1.5 occurring in trichomes up to 100 μm long. Cross walls are translucent, fine- to medium-grained, 0.5–1.0 μm thick.

Material examined.—Two well-preserved solitary trichomes.

Occurrence.—Lower Proterozoic: Duck Creek Formation, Australia; Lower Cambrian: Chulaktau Formation, South Kazakhstan.

Remarks.—*Oscillatoriopsis cuboides* is distinguished from other species of *Oscillatoriopsis* by its characteristic cell dimensions and cask-shaped, cuboidal, medial cells (Knoll et al., 1988; Sergeev et al., 2012). The Chulaktau specimens are broader than trichomes described from the Paleoproterozoic Duck Creek Formation (Knoll et al., 1988), having cell widths similar to those of *O. longa*. In assigning the Chulaktau specimens to *O. cuboides*, rather than to *O. longa*, we have followed the taxonomy of Sergeev et al. (2012) rather than that of Butterfield et al. (1994).

Oscillatoriopsis longa Timofeev and Hermann, 1979, emend. Butterfield, 1994

(in Butterfield, Knoll and Swett, 1994)
Figures 10.5, 10.6, 11.7, 11.8

Oscillatoriopsis longum Timofeev and Hermann, 1979, p. 139, pl. 29, figs. 3, 4.

https://doi.org/10.1017/jpa.2015.56 Published online by Cambridge University Press

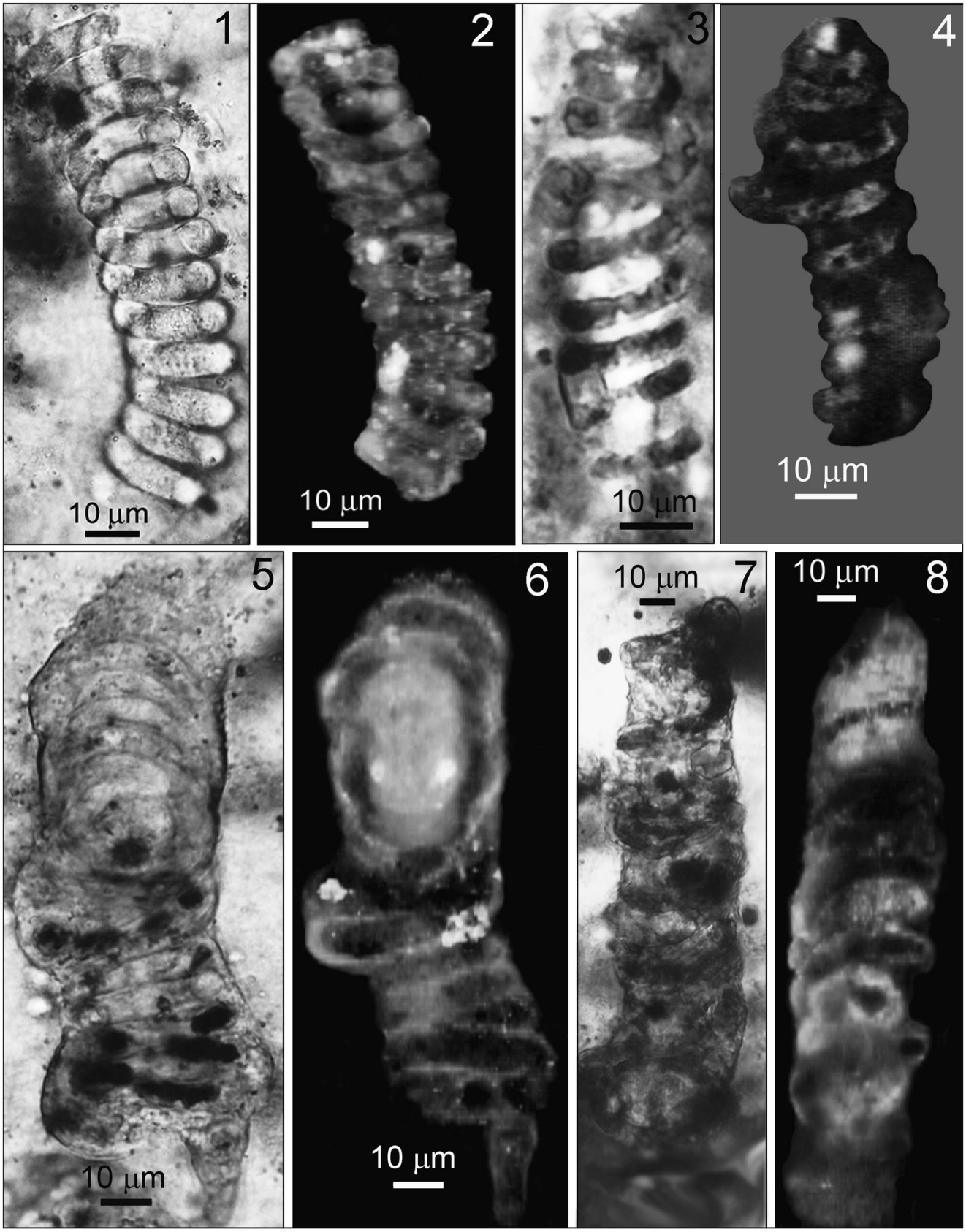

Figure 8. Optical photomicrographs (**1**, **3**, **5**, **7**) and confocal laser scanning micrographs (**2**, **4**, **6**, **8**) of Chulaktau quartz- and apatite-permineralized organic-walled specimens of *Obruchevella* spp. (**1**, **2**, **5**, **6**) *Obruchevella parva* Reitlinger, 1959: (**1**, **2**) 4681-366 (18), location point (p.) 7, England Finder Slide (EFS) H47[2], GINPC 201; (**5**, **6**) 4681-366 (18), p. 2, EFS E44[1], GINPC 1253. (**3**, **4**, **7**, **8**) *Obruchevella parvisima* Song, 1984: (**3**, **4**) 4681-370 (116), p. 2, EFS M26[2], GINPC 205; (**7**, **8**) 4681-1026 (273), p. 91, EFS V53[3], GINPC 1254.

https://doi.org/10.1017/jpa.2015.56 Published online by Cambridge University Press

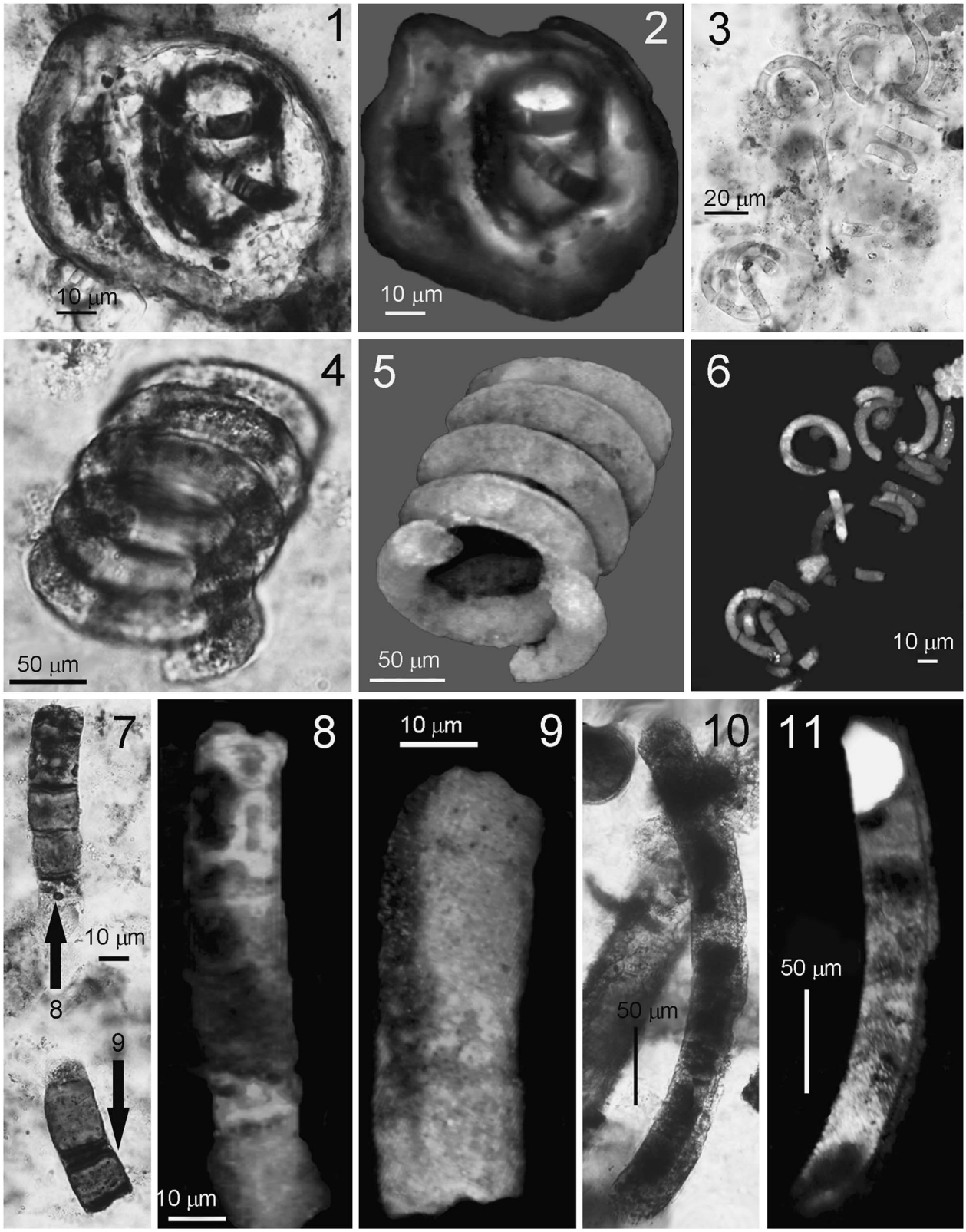

Figure 9. Optical photomicrographs (**1**, **3**, **4**, **7**, **10**) and confocal laser scanning micrographs (**2**, **5**, **6**, **8**, **9**, **11**) of filamentous quartz- and apatite-permineralized organic-walled microfossils from the Chulaktau Formation. Parts of the specimen in (**7**), indicated by the arrows, are shown at higher magnification in the CLSM images in (**8**) and (**9**), whereas the upper part of the filament in (**10**) is shown in the CLSM image in (**11**). (**1–6**) *Obruchevella parva* Reitlinger, 1959: (**1**, **2**) 4681-366 (18), specimen location point (p.) 10, England Finder Slide (EFS) H37[3], GINPC 1255; (**3**, **6**) 4681-399 (103), p. 26, EFS P31 [0], GINPC 1256; (**4**, **5**) 4681-391 (102), p. 34, EFS P28[0], GINPC 1300. (**7–9**), *Oscillatoriopsis cuboides* Knoll, Strother and Rossi, 1988, 4681-403 (241), p. 18, EFS Q42[3], GINPC 198. (**10**, **11**) *Palaeolyngbya catenata* Hermann, 1974, 4681-1026 (273), p. 50, EFS S31[1], GINPC 1257.

https://doi.org/10.1017/jpa.2015.56 Published online by Cambridge University Press

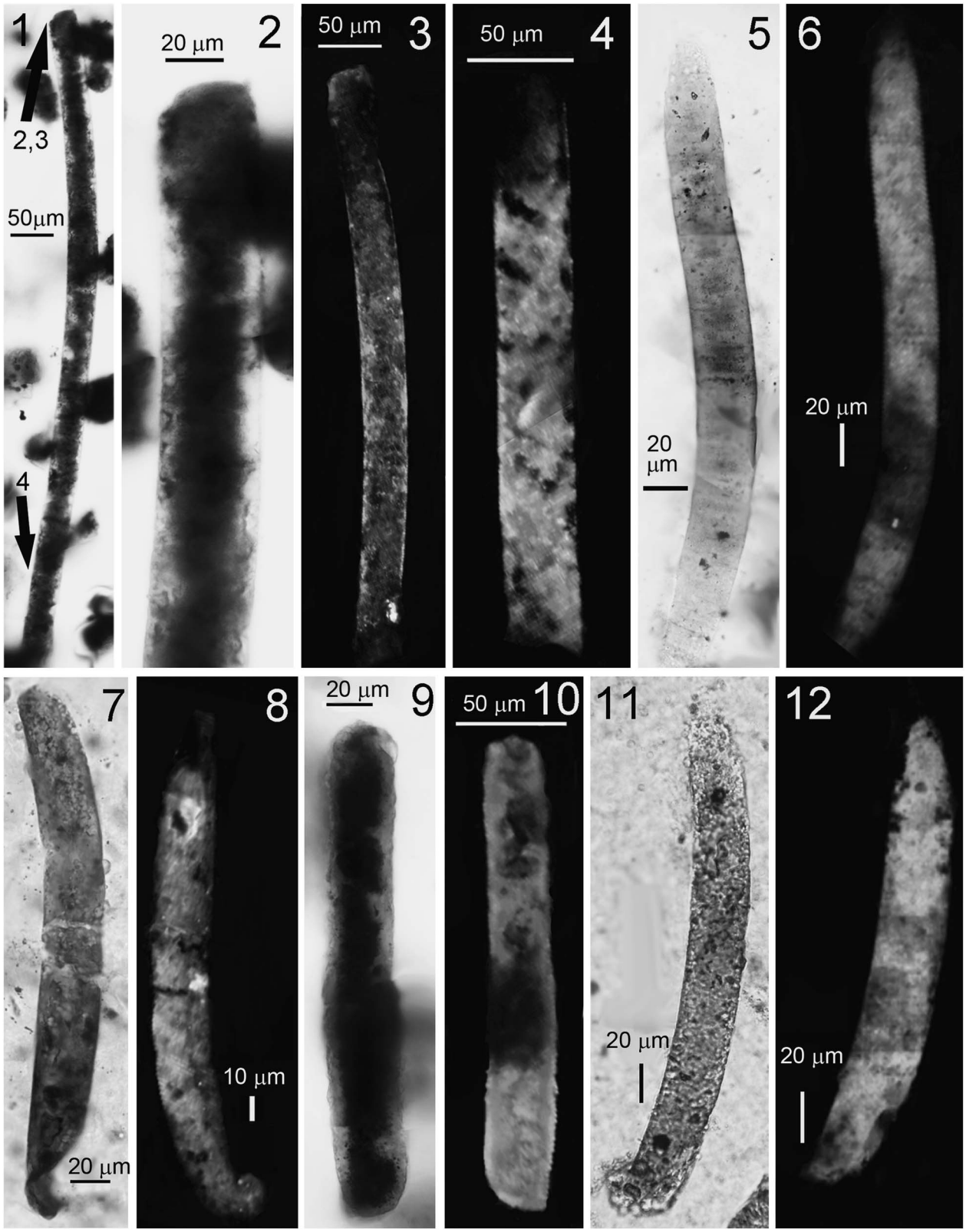

Figure 10. Optical photomicrographs (**1**, **2**, **5**, **7**, **9**, **11**) and confocal laser scanning micrographs (**3**, **4**, **6**, **8**, **10**, **12**) of filamentous quartz- and apatite-permineralized organic-walled microfossils from the Chulaktau Formation. Parts of the specimen in (**1**), indicated by arrows, are shown at higher magnification in optical (**2**) and CLSM images (**3**, **4**). (**1–4**, **9**, **10**) *Palaeolyngbya catenata* Hermann, 1974: (**1–4**) 4681-1026 (273), specimen location point (p.) 118, England Finder Slide (EFS) Z50[1], GINPC 1258; (**9**, **10**) 4681-1026 (273), p. 126, EFS Z40[0], GINPC 1259. (**5**, **6**) *Oscillatoriopsis longa* Timofeev and Hermann, 1979, 4681-391 (102), p. 33, EFS P42[0], GINPC 1260. (**7**, **8**, **11**, **12**) *Siphonophycus solidum* Golub, 1979: (**7**, **8**) 4681-391 (102), p. 21, EFS N31[0], GINPC 1261; (**11**, **12**) 4681-391 (102), p. 14, EFS H32[4], GINPC 1262.

https://doi.org/10.1017/jpa.2015.56 Published online by Cambridge University Press

Oscillatoriopsis longa Butterfield, Knoll and Swett, 1994, p. 60, figs. 24F–24G; Dong, Xiao, Shen, Zhou, Li and Yao, 2009, p. 39, figs. 6.10–6.11 (For additional synonymy see Butterfield et al., 1994 and Zhang et al., 1998).

Description.—Uniseriate straight to curved unbranched non-ensheathed trichomes that lack cell-defining constrictions and occur commonly as isolated individuals. Terminal cells are rounded to hemispheroidal, 12–21 μm wide (n = 5) and 4–6 μm long (n = 5); medial cells are disc-shaped, translucent, 23–30 μm wide (n = 48, μ = 26 μm, σ = 1.6, RSD = 6%), 4–9 μm long (n = 48, μ = 6 μm, σ = 1.0, RSD = 16%), and have a width to length ratio 4 to 8; trichome lengths range from 180 to 270 μm. Transverse cell walls are commonly indistinct whereas the trichome-defining lateral cell walls are typically distinct, translucent to opaque, fine- to medium grained, and 0.5–1.0 μm thick. Preserved remnants of degraded cytoplasm, a few micrometers wide and up to a few tens of micrometers long, occur commonly as thread-like inclusions inside the trichomes.

Material examined.—A few dozen well-preserved trichomes.

Occurrence.—Widely distributed in Proterozoic and Lower Cambrian microfossil assemblages.

Remarks.—*Oscillatoriopsis longa* is distinguished from other species of *Oscillatoriopsis* by its characteristic cell dimensions and its trichomic breadth. Although the diameter of trichomes of *O. longa* from the Chulaktau Formation is up to 35 μm—appreciably broader than the 25 μm upper size limit recognized by Butterfield et al. (1994) and Sergeev et al. (2012) for this taxon —similarly sized specimens of *O. longa* have been described from the Chulaktau-contemporaneous Yanjiahe and Yurtus formations of China (Dong et al., 2009). Only one other broader taxon of the genus has been reported, *O. majuscula*, described from a single incomplete specimen 63 μm in diameter from the Paleoproterozoic Duck Creek Formation (Knoll et al., 1988) and a species, however, that was not included in the Butterfield et al. (1994) taxonomic monograph of the genus.

Genus *Palaeolyngbya* Schopf, 1968, emend.
Butterfield, 1994 (in Butterfield, Knoll and Swett, 1994)

Type species.—*Palaeolyngbya barghoorniana* Schopf, 1968.

Palaeolyngbya catenata Hermann, 1974
Figures 9.10, 9.11, 10.1–10.4, 10.9, 10.10, 11.1–11.6

Palaeolyngbya catenata Hermann, 1974, p. 8 and 9, pl. 6, fig. 5; Butterfield, Knoll and Swett, 1994, p. 61, figs. 25F–25G; Sergeev and Lee Seong-Joo, 2001, p. 6, pl. 1, figs. 4–6; Sergeev and Lee Seong-Joo, 2004, p. 13, 15, pl. 2, figs. 1–3; Srivastava and Kumar, 2003, p. 30, 32, pl. 9, figs. 5, 7; Sergeev, 2006, p. 207, pl. 22, figs. 4–6, pl. 27, figs. 1–3; Sergeev, Sharma and Shukla, 2008, pl. 4, fig. 5, pl. 7, fig. 12, pl. 9, fig. 4; 2012, p. 300, 301, pl. 18, figs. 1–5, 8, text-fig. 43B.

Palaeolyngbya maxima Zhang, 1981, p. 495, pl. 2, figs. 4, 6, 7 (for additional synonymy, see Sergeev, Sharma, and Shukla, 2012).

Description.—Unbranched uniseriate trichomes having discoidal medial cells and rounded terminal cells that lack constrictions at septa and are encompassed by a prominent non-lamellated smooth sheath. Terminal cells are rounded to hemispheroidal, 22–26 μm wide and up to 7 μm long; medial cells are 28–35 μm wide (n = 60, μ = 32.5 μm, σ = 1.7, RSD = 5%) and 7–11 μm long (n = 60, μ = 8.5 μm, σ = 1.6, RSD = 18.5%), having a width-to-length ratio ranging from 3 to 5. Transverse cell walls are commonly indistinct; lateral, trichome-defining walls are translucent, fine-grained and 0.5–1.0 μm thick. Encompassing extracellular sheaths are translucent, 29–39 μm in diameter, 0.5–1.5 μm thick and up to 900 μm long.

Material examined.—More than one hundred well-preserved filaments.

Occurrence.—Widely distributed in Proterozoic microfossil assemblages.

Remarks.—The diameter of trichomes of *P. catenata* in the Chulaktau assemblage ranges up to 35 μm, broader than the upper size limit previously recognized for this species (Butterfield et al., 1994; Sergeev et al., 2012). In sheath diameter, the Chulaktau specimens span the range between *P. castenata* and *P. hebeiensis* (Zhang and Yan, 1984).

Palaeolyngbya sp.
Figure 11.12, 11.13

Description.—Unbranched uniseriate trichomes, up to 53 μm long, exhibiting discoidal medial cells and rounded terminal cells that lack constrictions at septa and are surrounded by a prominent unilayered smooth sheath. Medial cells are 6–7 μm wide and 1–2 μm long. Transverse walls are indistinct or missing; lateral cell walls are translucent, fine-grained, 0.5–1.0 μm thick. The encompassing sheath is translucent, single-layered, ~9 μm broad and ~0.5 μm thick.

Material examined.—One filament, not well preserved.

Genus *Siphonophycus* Schopf, 1968, emend.
Knoll and Golubic, 1979, emend.
Knoll, Swett and Mark, 1991

Type species.—*Siphonophycus kestron* Schopf, 1968.

Siphonophycus robustum (Schopf, 1968), emend.
Knoll and Golubic, 1979, comb. Knoll, Swett, and Mark, 1991
Figure 11.11

Eomycetopsis robusta Schopf, 1968, p. 685, pl. 82, figs. 2, 3; pl. 83, figs. 1–4; Knoll and Golubic, 1979, p. 149, figs. 4A, 4B; Mendelson and Schopf, 1982, p. 59, 60, 62, pl. 1, figs. 9, 10; Ogurtsova, 1985, p. 97 and 98, pl. 3, figs. 4, 6, pl. 10, figs. 1–6, pl. 11, figs. 2, 3, 5, 6; pl. 12, figs. 1, 3, 5, 7; Sergeev, 1992, p. 93 and 94, pl. 7, figs. 9, 10; pl. 16, figs. 3, 6, 7, 10; pl. 19, figs. 1, 5, 6, 7–10; pl. 24, fig. 7; Golovenok and Belova, 1993, pl. 2, fig. e.

https://doi.org/10.1017/jpa.2015.56 Published online by Cambridge University Press

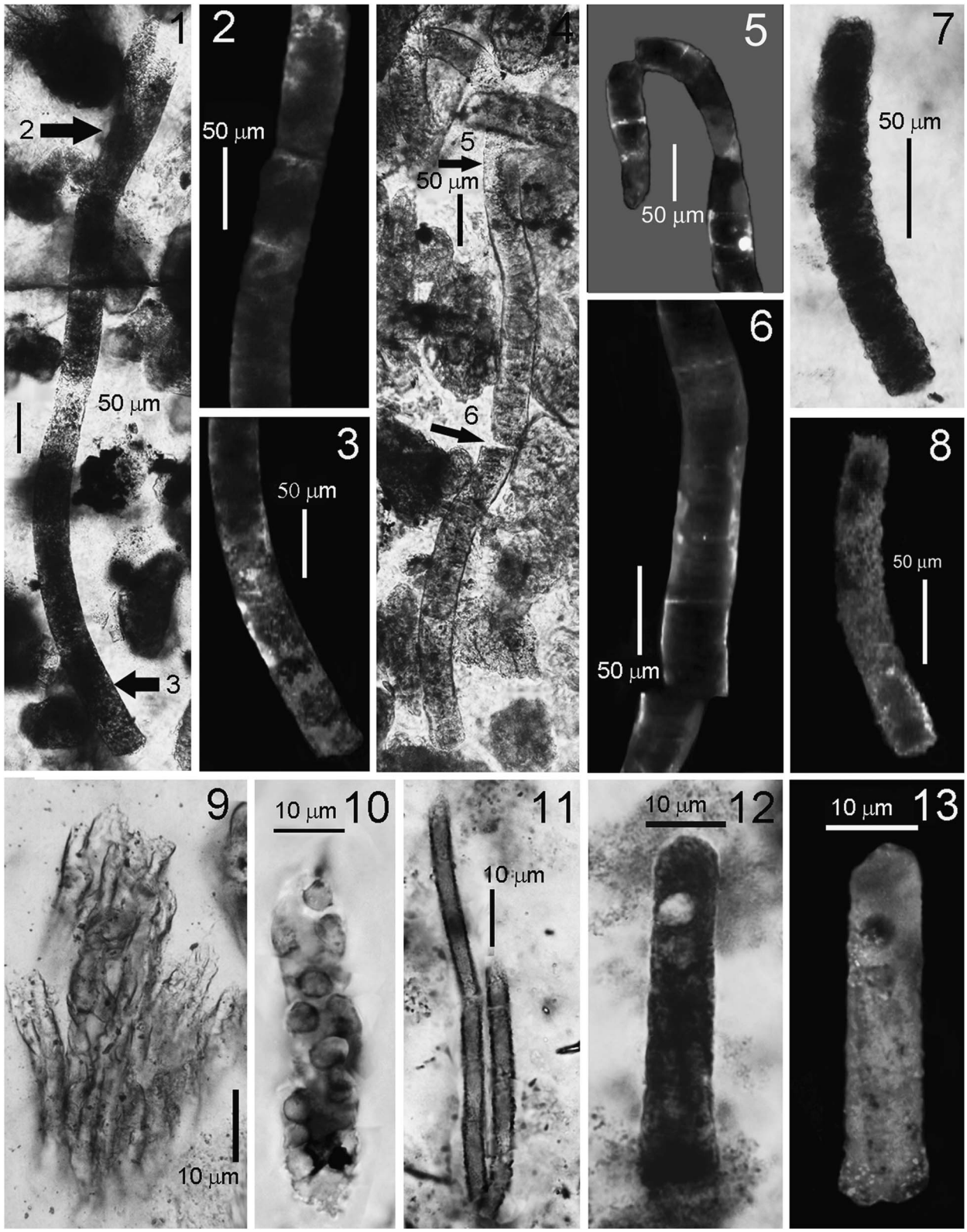

Figure 11. Optical photomicrographs (**1**, **4**, **7**, **9–12**) and confocal laser scanning micrographs (**2**, **3**, **5**, **6**, **8**, **13**) of filamentous quartz- and apatite-permineralized organic-walled microfossils from the Chulaktau Formation. Parts of the specimen in (**1**), indicated by the arrows, are shown at higher magnification in the CLSM images in (**2**) and (**3**), whereas parts of the specimen in (**4**), indicated by the arrows, are shown in the CLSM images in (**5**) and (**6**). (**1–6**) *Palaeolyngbya catenata* Hermann, 1974: (**1–3**) 4681-1026 (273), specimen location point (p.) 55, England Finder Slide (EFS) S39[4], GINPC 1263; (**4–6**) 4681-1026 (273), p. 28, EFS O60[4], GINPC 1264. (**7**, **8**) *Oscillatoriopsis longa* Timofeev and Hermann, 1979, 4681-1026 (273), p. 98, EFS V48[1], GINPC 1295. (**9**) *Eomicrocoleus crassus* Horodyski and Donaldson, 1980, 4681-1032 (273), p. 71, EFS Z28[1], GINPC 1265. (**10**) *Chlorogloeaopsis contexta* (Hermann, 1976), 4681-364 (102), p. 4a, EFS J48[2], GINPC 1266. (**11**) *Siphonophycus robustum* (Schopf, 1968), 4681-359 (15), p. 2, EFS G39[0], GINPC 1267. (**12**, **13**) *Palaeolyngbya* sp., 4681-363 (99), p. 2, EFS E45[3], GINPC 1268.

https://doi.org/10.1017/jpa.2015.56 Published online by Cambridge University Press

Eomycetopsis filiformis Schopf, 1968, p. 685 and 686, pl. 82, fig. 1, 4, pl. 83, figs. 5–8.

Siphonophycus robustum Knoll, Swett, and Mark, 1991, p. 565, figs. 10.3, 10.5; Butterfield, Knoll, and Swett, 1994, p. 64, 66, figs. 26A, 26G; Sergeev, Knoll, Kolosova, and Kolosov, 1994, pl. 3, fig. 6; Sergeev, Knoll, and Petrov, 1997, p. 230, fig. 14A; Sergeev and Lee Seong-Joo, 2001, p. 6, pl. 1, figs. 1, 2, 7, 11, 12; Sergeev, 2001, p. 442, figs. 7.8, 7.9; Sergeev, 2002, pl. 2, figs. 1, 3; Sergeev and Lee Seong-Joo, 2004, pl. 2, fig. 4; Sergeev, 2006, p. 213 and 214, pl. 6, figs. 9, 10, pl. 17, fig. 1, pl. 19, figs. 8, 9, pl. 22, figs. 1, 2, 7, 8, 11, 12, pl. 25, figs. 1, 3, pl. 27, figs. 4, 5, pl. 28, fig. 2, pl. 36, figs. 1, 2, pl. 44, figs. 1–7, 13, pl. 46, figs. 7–10, pl. 48, fig. 4; Sergeev and Schopf, 2010a, p. 387, fig. 6.4; Sergeev, Sharma and Shukla, 2012, p. 309, 310, pl. 21, figs. 2, 4, 8–10, text-figs. 8, 9, 16, 17 (for complete synonymy, see Butterfield, Knoll, and Swett, 1994 and Sergeev, Sharma, Shukla, 2012).

Description.—Unbranched nonseptate tubes, cylindrical to slightly compressed and 2–4 μm broad, that rarely contain degraded trichome-like fragments; tube walls, less than 0.5 μm thick, range from psilate to finely granulate. Specimens are solitary or entangled in masses of many individuals aligned subparallel to the bedding lamination.

Material examined.—A few dozen well-preserved specimens.

Occurrence.—Widely distributed both in chert-permineralized and compression-preserved organic-walled Proterozoic microfossil assemblages.

Remarks.—Like the other Chulaktau and Berkuta species of *Siphonophycus*, *S. robustum* is distinguished by its characteristic range of diameters.

Siphonophycus solidum (Golub, 1979), comb. Butterfield, 1994 (in Butterfield, Knoll and Swett, 1994)
Figures 3.21–3.24, 10.7, 10.8, 10.11, 10.12

Omalophyma solida Golub, 1979, p. 151, pl. 31, figs. 1–4, 7.

Siphonophycus solidum Butterfield in Butterfield, Knoll, and Swett, 1994, p. 67, figs. 25H, 25I, 27D; Sergeev, Knoll, and Petrov, 1997, p. 231, figs. 14I, 14K; Sergeev and Lee Seong-Joo, 2001, p. 8, pl. 1, figs. 1–3; Sergeev, 2001, p. 442 and 443, fig. 7.7; Sergeev, 2002, pl. 2, fig. 15; Sergeev and Lee Seong-Joo, 2004, pl. 2, fig. 8; Sergeev, 2006, p. 215, pl. 17, figs. 9, 10, pl. 19, fig. 7, pl. 22, figs. 1–3, pl. 25, fig. 15, pl. 28, figs. 4, 5, pl. 36, fig. 4, pl. 39, fig. 1, pl. 45, figs. 4, 7; Sergeev and Schopf, 2010, p. 387, figs. 7.6–7.8, 8.1, 8.2; Schopf, Kudryavtsev and Sergeev, 2010, figs. 2.5–2.15; Sergeev, Sharma and Shukla, 2012, p. 310, pl. 18, figs. 9–11, pl. 20, figs. 4–6, 8 (for complete synonymy, see Butterfield, Knoll, and Swett, 1994 and Sergeev, Sharma, Shukla, 2012).

Description.—Unbranched solitary nonseptate tubes, cylindrical to slightly compressed and 16–32 μm broad, that rarely contain degraded trichomic fragments; tube walls, 1–2 μm thick, range from smooth to fine- or medium-grained.

Material examined.—Approximately one hundred well-preserved specimens.

Occurrence.—Widely distributed both in chert-permineralized and compression-preserved Proterozoic assemblages.

Remarks.—The exterior surfaces of some Chulaktau specimens are encrusted by closely spaced small euhedral apatite crystals (Figs. 3.21–3.24, 5.2, 5.3).

Class Coccogoneae Thuret, 1875
Order Chroococcales Wettstein, 1924
Family Chroococcaceae Nägeli, 1849

Archaeophycus Wang, Zhang, and Guo, 1983

Type species.—*Archaeophycus yunnanensis* (Song *in* Luo et al., 1982) comb. Dong et al., 2009.

Archaeophycus yunnanensis (Song *in* Luo et al., 1982) comb. Dong et al., 2009
Figure 12.1, 12.2

Tetraphycus yunnanensis Song *in* Luo, Jiang, Wu, Song, and Ouyang, 1982, p. 216, pl. 31, figs. 3, 4; Luo, Jiang, Wu, Song, Ouyang, Xing, Liu, Zhang, and Tao, 1984, pl. 19, figs. 11, 12.

Archaeophycus venustus Wang, Zhang, and Guo, 1983, p. 153 and 154, figs. 5.10, 6.1, 8.3; Sergeev and Ogurtsova, 1989, pl. 2, fig. 11; Sergeev, 1992, pl. 26, fig. 5; Zhou, Yuan, Xiao, Chen, and Xue, 2004, p. 354, pl. 1, figs. 5–9.

?*Bigeminococcus grandis* Wang, Zhang, and Guo, 1983, p. 149–150, fig. 13.1–13.4.

Paratetraphycus giganteus Zhang Z., 1985, p. 166, pl. 1, figs. 1, 4, 6, 7; pl. 2, fig. 6; Zhang Y., Yin, Xiao, and Knoll, 1998, p. 46, fig. 20.4–20.8.

Tetraphycoides multa Cao, 1985, p. 189, pl. 1, figs. 1, 2.

Archaeophycus yunnanensis Dong, Xiao, Shen, Zhou, Li, and Yao, 2009, p. 37, figs. 6.1–6.6.

Description.—Spheroidal or polyhedral cells occurring in dyads, triads, tetrads and octets not surrounded by a common sheath that form colonial aggregates composed of a few to a few tens of individuals. Colony form varies from loose clusters of dyads and tetrads to more closely packed regularly cuboidal aggregations. Cell walls are 0.5–1.0 μm thick, transparent and medium-grained. Cell diameters range from 8 to 15 μm ($n = 80$, $\mu = 9$ μm, $\delta = 2$, RSD = 22%, DDI = 3). A single opaque inclusion 1–2 μm in diameter is commonly present within each cell.

Material examined.—Several hundred cells in tens of colonies.

Occurrence.—Ediacaran (Vendian): Doushantuo Formation, China. Lower Cambrian: Zhujiaqing, Yanjiahe and Yurtus Formations, China; Chulaktau formation, South Kazakhstan.

https://doi.org/10.1017/jpa.2015.56 Published online by Cambridge University Press

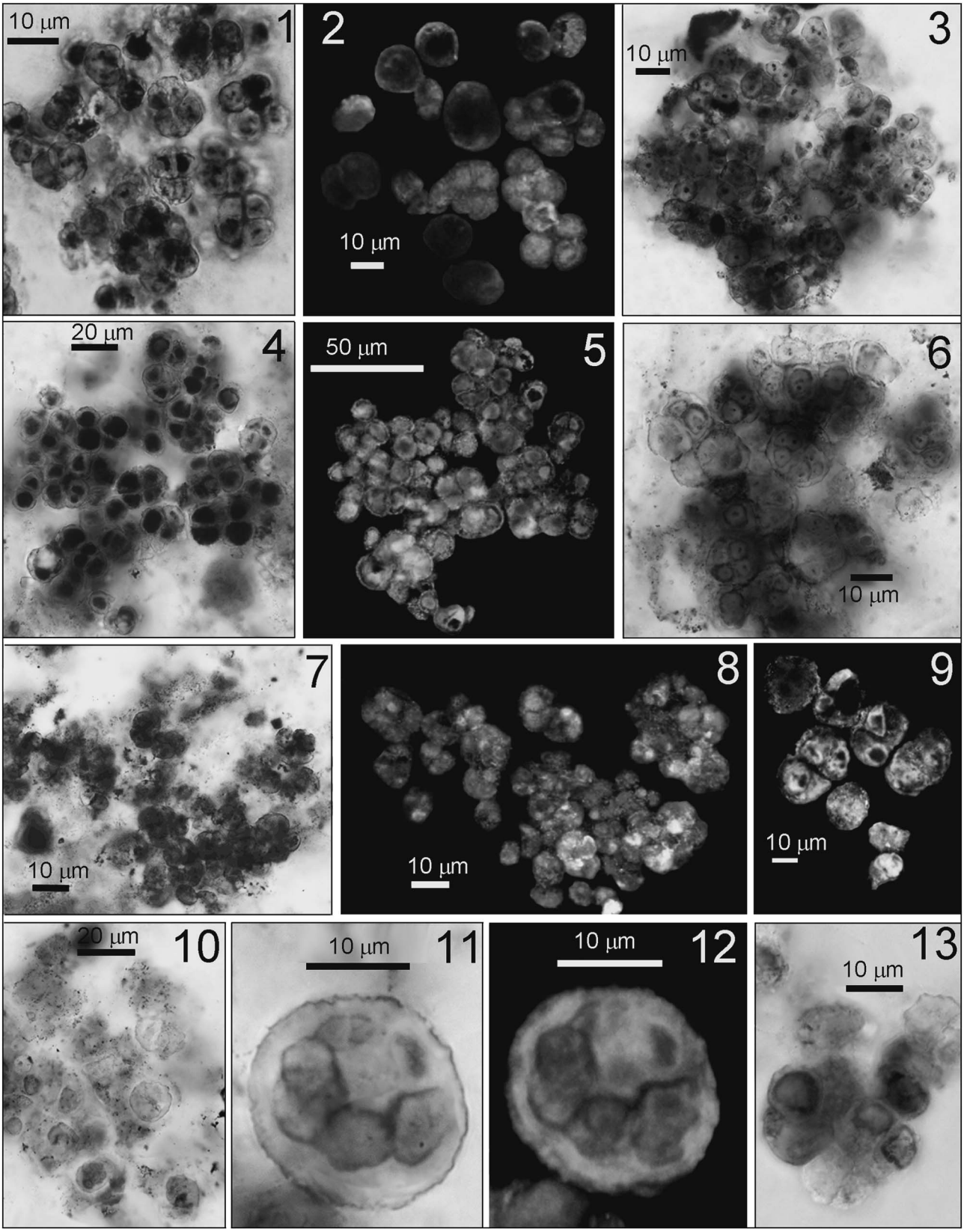

Figure 12. Optical photomicrographs (**1**, **3**, **4**, **6**, **7**, **10**, **11**, **13**) and confocal laser scanning micrographs (**2**, **5**, **8**, **9**, **12**) of coccoidal colonial chert- and apatite-permineralized organic-walled microfossils from the Chulaktau Formation. (**1**, **2**) *Archaeophycus yunnanensis* (Song *in* Luo et al., 1982), 4681-363 (99), location point (p.) 3, England Finder Slide (EFS) L44[1], GINPC 1271. (**4**, **5**) *Tetraphycus acutus* Sergeev, 1989, 4681-363 (99), p. 1, EFS O41[3], GINPC 207. (**3**, **6**, **7–13**) *Eoentophysalis belcherensis* Hofmann, 1976: *3*, 4681-399 (103), p. 24, EFS E38[1], GINPC 1272; *6*, 4681-399 (103), p. 26, EFS P31[0], GINPC 1296; (**7–9**, **13**) 4681-399 (103), p. 21, EFS M41[0], GINPC 1273; (**10**) 4681-399 (103), p. 26a, EFS P31[4], GINPC 1274; (**11**, **12**) 4681-399 (103), p. 26d, EFS P31[0], GINPC 1275.

https://doi.org/10.1017/jpa.2015.56 Published online by Cambridge University Press

Remarks.—In colonial organization and cell-shape and -size, *Archaeophycus yunnanensis* resembles *Tetraphycus acutus*, the distinction between the taxa being the absence in *A. yunnanensis* of distinct cell- and colony-encompassing sheaths. Although the two taxa may represent preservational variants of a single species (which would demote *Tetraphycus acutus* to the status of a junior synonym of *Archaeophycus yunnanensis*), the lack of cell- and cell tetrad-encompassing sheaths is a diagnostic character of the genus *Archaeophycus* (Dong et al., 2009). Because of the absence of transitional forms between these species in the Chulaktau Formation, we elected to maintain the taxa as separate entities.

Genus *Eoaphanocapsa* Nyberg and Schopf, 1984

Type species.—*Eoaphanocapsa oparinii* Nyberg and Schopf, 1984.

Eoaphanocapsa molle Sergeev, 1989 (in Sergeev and Ogurtsova, 1989)
Figure 14.12

Eoaphanocapsa molle Sergeev *in* Sergeev and Ogurtsova 1989, p. 65, pl. 2, fig. 9; Sergeev, 1992, p. 78 and 79, pl. 26, fig. 3; Sergeev, Sharma and Shukla, 2012, p. 240, pl. 4, fig. 7.

Description.—Individual colonial cells, 12–17 μm in diameter, surrounded by single-layered envelopes, occurring in loose colonies commonly about 60 μm broad that are composed of tens of individuals. Cell-enclosing envelopes and cell walls are translucent, fine-grained, 0.5–1.0 μm thick. Some cells include a spot-like inclusion 1–2 μm in diameter.

Material examined.—A few well-preserved colonies comprising dozens of vesicles.

Occurrence.—Lower Cambrian, Chulaktau Formation, South Kazakhstan.

Genus *Tetraphycus* Oehler, 1978

Type species.—*T. gregalis* D. Oehler, 1978.

Tetraphycus acutus Sergeev, 1989 (in Sergeev and Ogurtsova, 1989), emend.
Figures 3.11–3.20, 12.4, 12.5

Tetraphycus acutus Sergeev *in* Sergeev and Ogurtsova, 1989, p. 64, pl. 2, fig. 8; Sergeev, 1992, p. 80, 81, pl. 26, fig. 4.

In part: *Tetraphycus amplus* Golovenok and Belova, 1984. Sergeev and Ogurtsova, 1989, pl. 2, figs. 6, 12; Sergeev, 1992, pl. 26, figs. 1, 2.

Diagnosis (emended).—Spheroidal and polyhedral single-walled cells 10–20 μm in diameter that occur in dyads, triads and planar tetrads surrounded by a common sheath. Ensheathed tetrads may occur in closely associated groups.

Description.—Spheroidal or polyhedral cells enclosed by single-layered sheaths occurring in dyads, triads and tetrads that comprise larger colonial aggregates of a few to a few tens of cell-groups. Colony morphology varies from loose clusters of tetrads to more regular cuboidal aggregations in which the tetrads commonly occur in closely packed groups encompassed in a surrounding originally mucilaginous organic matrix. Cell walls are 1 2 μm thick, translucent and course-grained; transparent outer sheaths, $\geq$0.5 μm thick, are fine-grained. Cell diameters range from 10 to 20 μm (n = 28, μ = 15 μm, δ = 2.6, RSD = 17%, DDI = 3); sheath diameters range from 12 to 22 μm. A single opaque inclusion 1 to 2 μm in diameter is commonly present within individual cells.

Material examined.—A few hundred vesicles in tens of colonies.

Occurrence.—Lower Cambrian: Chulaktau Formation, South Kazakhstan.

Remarks.—Modern counterparts exhibiting cell shapes and sizes similar to those of *Tetraphycus acutus* occur among chroococcacean and entophysalidacean cyanobacteria as well as chlorococcacean green algae, and planar tetrads like those of *Tetraphycus* are particularly common among coccoical colonial cyanobacteria. Two species of the genus, *T. acutus* and *T. amplus*, have previously been described from the Chulaktau Formation (Sergeev and Ogurtsova, 1989). *T. amplus* was originally described by from the Proterozoic Billyakh Group of the Anabar Uplift (Golovenok and Belova, 1984) but was later regarded to be a junior synonym of *Myxococcoides grandis* (Sergeev et al., 1995). We have therefore amended *T. acutus* to include this and other forms previously described as *T. amplus*.

Family Entophysalidaceae Geitler, 1932

Genus *Eoentophysalis* Hofmann, 1976 emend. Mendelson and Schopf, 1982

Type species.—*Eoentophysalis belcherensis* Hofmann, 1976.

Eoentophysalis belcherensis Hofmann, 1976
Figure 12.3, 12.6–12.13

Eoentophysalis belcherensis Hofmann, 1976, p. 1070, 1072, pl. 4, figs. 1–5, pl. 5, figs. 3–6, pl. 6, figs. 1–14; Hofmann and Schopf, 1983, p. 347, pl. 14-2, figs. G-J, pl. 14-6, figs. L-M, pl. 14-8, fig. C, Pl. 14-9, figs. O-Q; Sergeev, 1992, p. 81 and 82, pl. 9, figs. 1–3; Sergeev, Knoll and Grotzinger, 1995, p. 27 and 28, figs. 12.1–12.4, 12.6, 12.12–12.14, 17.1–17.10; Sergeev, 2006, p. 196 and 197, pl. 5, figs. 1–4, 6, 12–14, pl. 8, figs. 1–10; pl. 34, figs. 1, 2, pl. 41, figs. 11–15; Sergeev, Sharma and Shukla, 2012, p. 263, pl. 10, figs. 1–10 (for complete synonymy see Sergeev, Sharma, and Shukla, 2012).

Eoentophysalis sp. Sergeev, 1992, pl. 26, fig. 6.

Description.—Spheroidal or polyhedral cells enclosed by multilamellated envelopes and occurring in dyads, tetrads, octets that comprise colonies of a few tens of cell groups. The colonies typically are enclosed within a translucent envelope and vary

https://doi.org/10.1017/jpa.2015.56 Published online by Cambridge University Press

from loose clusters of gloeocapsoid cells to more regular spheroidal aggregations. Outermost envelopes enclosing individual cells are fine-grained and ~0.5 μm thick; inner envelopes are medium- to coarse-grained, ~1.0 μm thick; cell diameters range from 3 to 10 μm (n = 80, μ = 6 μm, σ = 1.5, RSD = 26%, DDI = 5). A single opaque inclusion 0.5–1.0 μm in diameter is commonly present within individual cells.

Material examined.—Approximately 200 cells in several colonies.

Occurrence.—Widely distributed in Paleo-, Meso-, Neoproterozoic, Ediacaran, and Lower Cambrian chert-permineralized organic-walled assemblages.

Remarks.—A taxon particularly common in Paleo-Mesoproterozoic microbial assemblages, *Eoentophysalis* is morphologically highly variable, the several stages of its complex life cycle being subject to varying degrees of preservational alteration (Hofmann, 1976; Golubic and Hofmann, 1976; Hofmann and Schopf, 1983; Knoll et al., 1991; Sergeev at al., 1995, 2012; Sergeev, 2006). In many Proterozoic deposits, colonies of *E. belcherensis* comprise crustose stratiform laminae. However, those of the Chulaktau population occur only as isolated gloeocapsoid palmelloid colonies, presumably as a result of the dynamic, highly energetic environment evidenced by the Chulaktau phosphoites (Kholodov and Paul, 1993a, 1993b, 1994)

Family Xenococcaceae Ercegović, 1932

Genus *Synodophycus* Knoll, 1982, emend.
Knoll, Swett and Mark, 1991

Synodophycus sp.
Figure 14.7–14.9

Synodophycus sp. Sergeev and Ogurtsova, 1989, pl. 2, fig. 7; Sergeev, 1992, pl. 26, fig. 8.

Description.—Aggregates of equidimensional 10- to 15-μm diameter cells, commonly surrounded by single or multilayered envelopes and clustered in irregular spheroidal colonies 40–50 μm across composed of 16–64 individuals. Cell walls are <0.5 μm thick, translucent and fine-grained; when present, surrounding sheaths are single- or multilayered, transparent, fine-grained and up to 2 μm thick.

Material examined.—A few colonies comprising tens of individuals.

Remarks.—*Synodophycus* has been assigned to the cyanobacterial pleurocapsalean family Xenococcaceae (Knoll et al., 1991). Although not a widely reported genus, many colonial fossils assigned to other cyanobacterial genera may actually be taxa of this genus.

Incertae Sedis

Genus *Berkutaphycus* new genus

Type species.—*Berkutaphycus elongatus* gen. sp. nov. by monotype.

Diagnosis.—Single-walled unbranched cylindrical filaments separated by cross walls into cell-like segments having lengths greater than widths. Filaments can be broken into short cylindrical bodies, cask-like fragments having rounded ends, or spheroidal vesicles. The filaments occur singly or in groups of tangled subparallel-oriented individuals.

Etymology.—From the name of Berkuta settlement, situated near the source of the Kyrshabakta Formation Berkuta Member (Lower Dolomite) holotype-containing fossiliferous chert and with reference to cyanobacterial/algal affinity.

Berkutaphycus elongatus new species
Figures 4.1–4.20, 13.6–13.8, 13.11–13.16

Siphonophycus sp., Sergeev and Ogurtsova, 1989, pl. 2, figs. 2, 3.

Palaeosiphonella sp., Sergeev and Ogurtsova, 1989, pl. 2, fig. 1; Sergeev, 1992, pl. 24, fig. 3.

Siphonophycus sp_4., Sergeev, 1992, pl. 24, figs. 1, 2, 4, 10.

Diagnosis.—Single-walled cylindrical filaments, 11–70 μm broad, commonly separated by cross- or end-walls into segments 70–80 μm long. Filaments can be broken into short cylindrical bodies 25–70 × 40–205 μm having rounded ends, or into 25- to 60-μm diameter spheroidal vesicles.

Description.—Single-walled unbranched cylindrical filaments separated by cross walls into cell-like segments having lengths larger than widths. Filaments can be broken into short cylindrical bodies, cask-like fragments having rounded ends, or spheroidal vesicles. The filaments occur singly or in entangled groups of subparallel-oriented individuals. Filaments are 11–34 μm in diameter (n = 80, μ = 23 μm, σ = 5.1, RSD = 22%) and up to 500 μm long (incomplete specimen). Filament fragments, equant to more elongate cylindrical bodies, range from 25 to 70 μm in width and 40 to 205 μm in length, whereas the diameters of isolated vesicles range from 25 to 60 μm; diameters of the entire population range from 11 to 70 μm (n = 85, μ = 24 μm, σ = 9.2, RSD = 38%). Filament walls are translucent, medium-grained, and 1 to 2 μm thick. In the Berkuta cherts, the interiors of *Berkutaphycus elongatus* filaments commonly contain elongate or actinomorphic anthraxolite-like degraded cytoplasmic remnants.

Etymology.—From the Latin *elongatus* referring to the elongate to the distinctive cylindrical elongate shape of the cell-like segments.

Holotype.—Figure 13.11, 13.12, GINPC 192; Lower Cambrian, Nemakit-Daldynian Stage; Kyrshabakta Formation, Lower Dolomite, locality 27, the Koksu River basin.

Material examined.—More than 500 well-preserved specimens.

https://doi.org/10.1017/jpa.2015.56 Published online by Cambridge University Press

Occurrence.—Lower Cambrian: Kyrshabakta Formation (Berkuta Member), South Kazakhstan.

Remarks.—The distinctive features of *Berkutaphycus elongatus*, such as the breakage of its filaments into elongate segments and the presence of isolated akinete-like cylindrical and spherical bodies, suggest affinity to hormogonian cyanobacteria (or, perhaps, to eukaryotic green or chrysophyte algae). The anthraxolite-like contents of the Berkuta filaments are not uncommon in metamorphosed Proterozoic deposits but are relatively rare in Cambrian and younger strata. Though this new taxon is somewhat similar to *Cyanonema majus* described from the Lower Cambrian of Tarim Platform of China (Dong et al., 2009), in the absence of a comparative study of the Chinese population it would be premature to propose a formal synonymy.

Genus *Botominella* Reitlinger, 1959

Type species.—*Botominella lineata* Reitlinger, 1959.

Botominella lineata Reitlinger, 1959
Figure 13.1–13.5

Botominella lineata Reitlinger, 1959, p. 25, pl. 10, figs. 1–7.

(non) *Botominella lineata* Reitlinger, 1959. Sergeev, 1989, pl. 1, figs. 11.

Description.—Solitary, unbranched, unsheathed, nontapering filaments up to 130 μm long (complete specimen) that consist of separated short-discoidal opaque cell-like bodies that range from 2 to 5 μm in width and 20 to 60 μm in length that are separated by 1.5- to 3.5-μm gaps.

Material examined.—Three well-preserved specimens.

Occurrence.—Widely distributed in Lower Cambrian formations.

Remarks.—*Botominella lineata*, first described by Reitlinger (1959) from the Lower Cambrian Pestrocvetnaya Formation of Siberia, is known from numerous Lower Cambrian carbonate units. Similar structures, initially referred to *Botominella lineata* and reported from the Chulaktau-underlying Neoproterozoic Chichkan Formation (Sergeev, 1989), have been interpreted to be inorganic and of nonbiological origin (Sergeev, 1992, pl. 23, figs. 1–3). However, the Chulaktau specimens described here differ morphologically from these earlier reported pseudofossils and their biological origin is confirmed by Raman spectroscopy that shows them to be composed of apatite-permineralized kerogen. The morphology of the Chulaktau specimens suggests them to be either relatively broad cyanobacterial oscillatoriacean filaments or, less likely, eukaryotic (chlorophycean?) algae.

Genus *Chlorogloeaopsis* Maithy, 1975, emend. Hofmann and Jackson, 1994

Type species.—*Chlorogloeaopsis zairensis* Maithy, 1975.

Chlorogloeaopsis contexta Hermann, 1976 (in Timofeev, Hermann and Mikhailova, 1976), comb. Hofmann and Jackson, 1994
Figure 11.10

Polysphaeroides contextus Hermann, 1976 in Timofeev, Hermann and Mikhailova, 1976, p. 42 and 43, pl. 14, figs. 3, 4; Yankauskas, 1989, p. 119, pl. 27, figs. 10a, 10б; Hermann, 1990, pl. 7, fig. 8; Schopf, 1992c, pl. 24, figs. B_1, B_2; Sergeev, 2001, p. 443, fig. 9.1–9.3; Sergeev, 2006, p. 230 and 231, pl. 18, figs. 1–3.

Chlorogloeaopsis contexta Hofmann and Jackson, 1994, p. 19, figs. 12.13–12.15; Prasad, Uniyal and Asher, 2005, pl. 7, fig. 9, pl. 11, fig. 14; Sergeev, Sharma and Shukla, 2012, pl. 14, figs. 7–9 (see Hofmann and Jackson, 1994, p. 19 for additional synonymy).

Description.—Solitary unbranched non-ensheathed nontapering filaments composed of irregularly oriented spheroidal compressed cells. Cell walls are single-layered, translucent, fine-grained, and <0.5 μm thick. Cell diameters vary from 3.5 to 4.5 μm; filament diameters range from 7.5 to 12.5 μm, having a maximum length of 50 μm.

Material examined.—Three specimens, none well preserved.

Occurrence.—Mesoproterozoic: Bylot Supergroup, Baffin Island, Canada. Neoproterozoic: Burovaya and Miroedikha formations, Turukhansk Uplift; Nelkan, Kumakhtinskaya, Kandykskaya and Ust'-Kirba formations, Uchur-Maya Region; Daskinskaya Formation, Yenisey Ridge, Siberia. Lower Cambrian, Chulaktau Formation, South Kazakhstan.

Remarks.—The Chulaktau *C. contexta* specimens are probably compessed remnants of chroococcalean cyanobacterial colonies or, less likely, of stigonematalean cyanobacterial filaments or filamentous green algae.

Figure 13. Optical photomicrographs (**1**, **5**, **6**, **9–11**, **13**), confocal laser scanning micrographs (**2**, **7**, **12**, **14**, **16**), two-dimensional Raman images showing the spatial distribution of kerogen (**3**; blue, acquired at its ~1605 cm^{-1} major band) and apatite (**4**; red, acquired at its major band at ~965 cm^{-1}), and optical images superimposed by kerogen 2-D Raman images (**8**, **15**; blue) of quartz- and apatite-permineralized organic-walled microfossils from the Chulaktau Formation (**1–5**, **9**, **10**) and chert-permineralized specimens from the Berkuta Member of the Kyrshabakta Formation (**6–8**, **11–16**). A part of the specimen in (**1**), indicated by the arrow, is shown in the Raman images in (**3**) and (**4**), whereas the part of a specimen denoted by the arrow in (**13**) is shown in the combined optical-Raman kerogen image in (**15**). (**1–5**) *Botominella lineata* Reitlinger, 1959: (**1–4**), 4681-365 (102), specimen location point (p.) 1, England Finder Slide (EFS) P47[3], GINPC 1282; *5*, 4681-371 (117), p. 1, EFS F42[0], GINPC 1283. (**6–8**, **11–16**) *Berkutaphycus elongatus* new genus and new species: (**6–8**) 4681-372 (115a), p. 25, EFS Q40[3], GINPC 1284; (**11**, **12**) 4681-372 (115a), p. 1, EFS H38[0], GINPC 192; (**13–15**) 4681-372 (115a), p. 24, EFS H38[0], GINPC 1285; (**16**) 4681-382 (115a), p. 3, EFS Q42[0], GINPC 1286. (**9**) *Leosphaeridia tenuissima* Eisenack, 1958, 4681-371 (117), p. 7, EFS G39[2], GINPC 1287. (**10**) *Leiosphaeridia minutissima* (Naumova, 1949), 4681-364 (102), p. 4, J48[1], GINPC 1288.

https://doi.org/10.1017/jpa.2015.56 Published online by Cambridge University Press

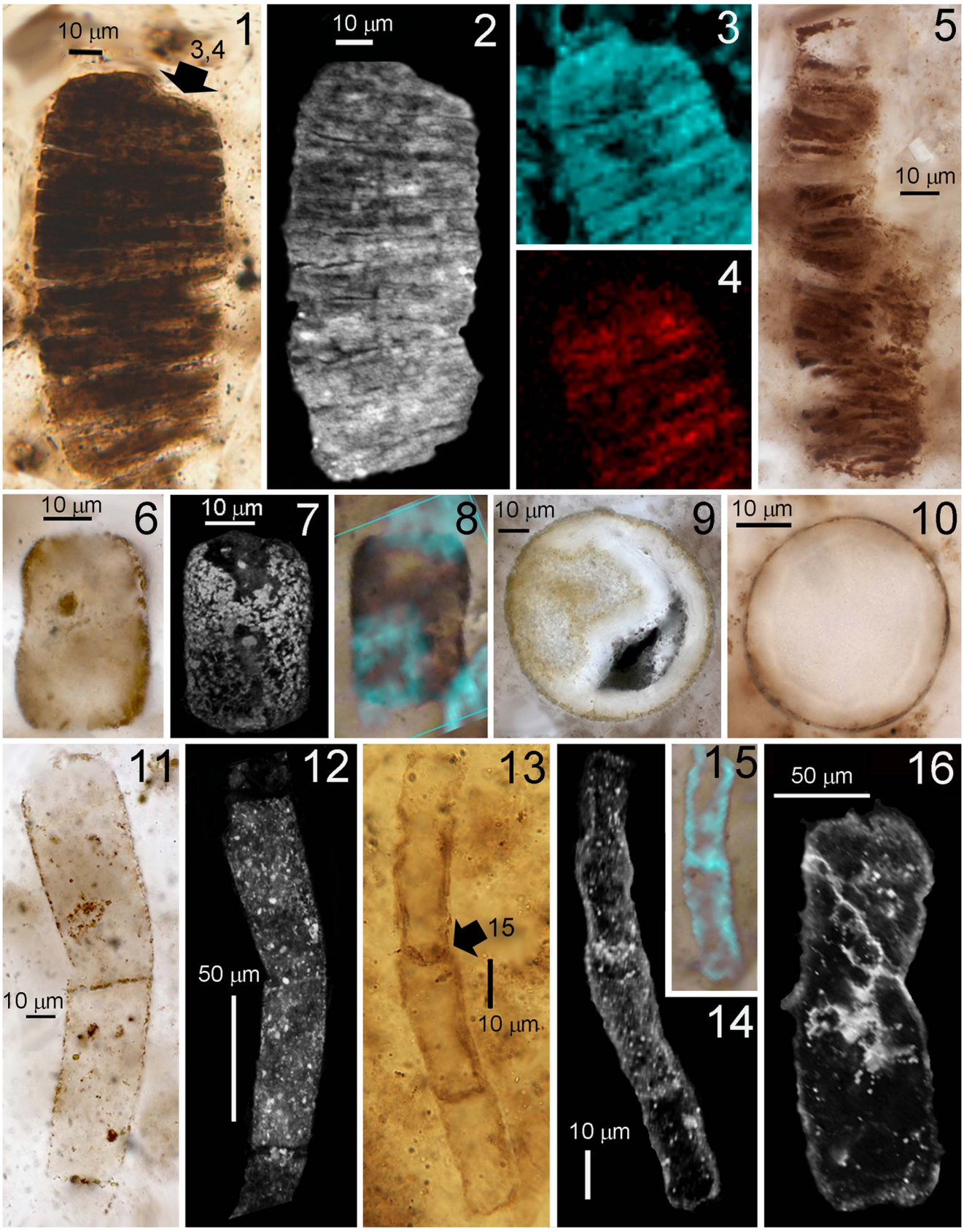

https://doi.org/10.1017/jpa.2015.56 Published online by Cambridge University Press

Genus *Cymatiosphaera* Wetzel, 1933, emend. Deflandre, 1954

cf. *Cymatiosphaera* sp.

Figure 14.1, 14.2, 14.4, 14.5

Description.—Spheroidal vesicles, subcircular in cross-section and 55 to 65 μm in diameter, having medium-grained 1- to 2-μm thick walls the surface of which is folded into distinctive polygonal fields 5–7 μm broad and 12–17 μm long.

Material examined.—Two well-preserved specimens.

Remarks.—Some six species of this widely occurring planktonic taxon have been reported from Lower Cambrian microfossil assemblages. However, because most such taxa have described on the basis of compression-preserved rather than permineralized specimens, it is difficult to compare them with the Chulaktau specimens recorded here to which we therefore do not assign a specific epithet.

Genus *Leiosphaeridia* Eisenack, 1958, emend.
Downie and Sarjeant, 1963, emend.
Turner, 1984, emend. Yankauskas, 1989

Type species.—*Leiosphaeridia baltica* Eisenack, 1958.

Leiosphaeridia minutissima (Naumova, 1949), emend.
Yankauskas, 1989 (in Yankauskas, 1989)
Figure 13.10

Leiotriletes minutissimus Naumova, 1949, pl. 3, fig. 4. For complete synonymy, see Yankauskas, 1989.

Leiosphaeridia minutissima Yankauskas *in* Yankauskas, 1989, p. 79 and 80, pl. 9, figs. 1–4, 11; Grey, 2005, p. 185, fig. 68D; Vorob'eva, Sergeev, and Knoll, 2009, p. 185, fig. 14.9; Sergeev, Sharma and Shukla, 2012, p. 332 and 333, pl. 26, fig. 9.

Description.—Spheroidal, solitary, single-walled vesicles 35–40 μm in diameter; walls are translucent, hyaline to fine-grained, <1 μm thick and have a smooth surface texture.

Material examined.—Nine well-preserved specimens.

Occurrence.—Widely distributed in Proterozoic and Paleozoic rocks.

Leiosphaeridia tenuissima Eisenack, 1958
Figure 13.9

Leiosphaeridia tenuissima Eisenack, 1958, pl. 1, fig. 2; Yankauskas, 1989, p. 81, pl. 9, figs. 12, 13; Butterfield *in* Butterfield, Knoll and Swett, 1994, p. 42, fig. 16I (for complete synonymy, see Yankauskas, 1989).

Description.—Spheroidal, solitary, single-walled vesicles 70–80 μm in diameter; walls are translucent, hyaline to fine-grained, about 2-μm thick, and have a smooth surface texture.

Material examined.—Four well-preserved specimens.

Occurrence.—Widely distributed in Proterozoic and Paleozoic sedimentary rocks.

Remarks.—Species of *Leiosphaeridia* are identified following a formal scheme based on envelope diameter and wall thickness (see Yankauskas, 1989, p. 24 and 25). Although some specimens of *Leiosphaeridia* may be empty envelopes that originally enclosed cyanobacterial colonies, the great majority are remains of eukaryotic unicellular phytoplankton.

Genus *Myxococcoides* Schopf, 1968

Type species.—*Myxococcoides minor* Schopf, 1968.

Myxococcoides inornata Schopf, 1968
Figure 14.10

Myxococcoides inornata Schopf, 1968, p. 676 and 677, pl. 84, fig. 7; Sergeev, Knoll, and Petrov, 1997, p. 234, figs. 18B, 18G; Sergeev, 2001, p. 444, fig. 10.11; Sergeev and Lee Seong-Joo, 2004, p. 17, pl. 3, fig. 12; Sergeev, 2006, p. 226, pl. 15, figs. 6, 7, pl. 21, fig. 1, pl. 29, fig. 18; Sergeev and Schopf, 2010, p. 393, fig. 12.3, 12.4; Schopf, Kydryavtsev and Sergeev, 2010a, fig. 5.1–5.4; Sergeev, Sharma, and Shukla, 2012, pl. 5, fig. 8, pl. 6, fig. 9.

Description.—Spheroidal cells, solitary or occurring in colonies composed of few to tens of individuals embedded in a diffuse commonly well-defined organic matrix. Cell diameters range from 15 to 20 μm; colony size is 50–70 × 100–120 μm. The single-layered cell walls are typically translucent, fine- or medium-grained, 0.5–1.0 μm thick. Some cells contain an opaque spheroidal inclusion 1–2 μm in diameter that appears to be attached to the inner surface of the cell wall.

Material examined.—Tens of well-preserved cells in several colonies.

Figure 14. Optical photomicrographs (**1**, **3**, **4**, **7**, **9–12**) and confocal laser scanning micrographs (**2**, **5**, **6**, **8**) of Chulaktau Formation coccoidal colonial and unicellular chert- and apatite-permineralized organic-walled microfossils. (**1**, **2**, **4**, **5**) *Cymatiosphaera* sp.: (**1**, **2**) 4681-1026 (273), specimen location point (p.) 17, England Finder Slide (EFS) F60[3], GINPC 1289. Although here referred to *Cymatiosphaera*, the numerous hemispherical cuspate structures situated on the inner wall of this specimen may be sites of apatite nucleation (cf. Fig. 3.16 and 3.17), an interpretation consistent with the resemblance of the elongate linear arcuate band that extends across the upper part of the spheroid interior to mineralic structures that are a result of void-filling crystallization. If not *Cymatiosphaera*, this specimen is probably an apatite-infilled leiosphaerid. (**4**, **5**) 4681-367 (100), p. 5b, EFS P50[3], GINPC 1290. The upper hemisphere of this specimen of *Cymatiosphaera* was ground away during preparation of the fossil-bearing petrographic thin section resulting in exposure of the ring-like circularity of the medial plane of the specimen at the upper surface of the section. (**3**, **6**) *Vandalosphaeridium koksuicum* Sergeev and Schopf, 2010, 4681-1026 (273), p. 130, EFS Q27[0], GINPC 1291. (**7–9**) *Synodophycus* sp.: (**7**, **8**) 4681-367 (100), p. 5a, EFS P50[3], GINPC 1292; *9*, 4681-413 (238), p. 10, U40[1], GINPC 214. (**10**) *Myxococcoides inornata* Schopf, 1968, 4681-364 (192), p. 10a, EFS P48[1], GINPC 1293. (**11**) *Myxococcoides minor* Schopf, 1968, 4681-359 (15), p. 3, EFS G31[0], GINPC 1294. (**12**) *Eoaphanocapsa molle* Sergeev, 1989, 4681-368 (98), p. 7, EFS INPC 209.

https://doi.org/10.1017/jpa.2015.56 Published online by Cambridge University Press

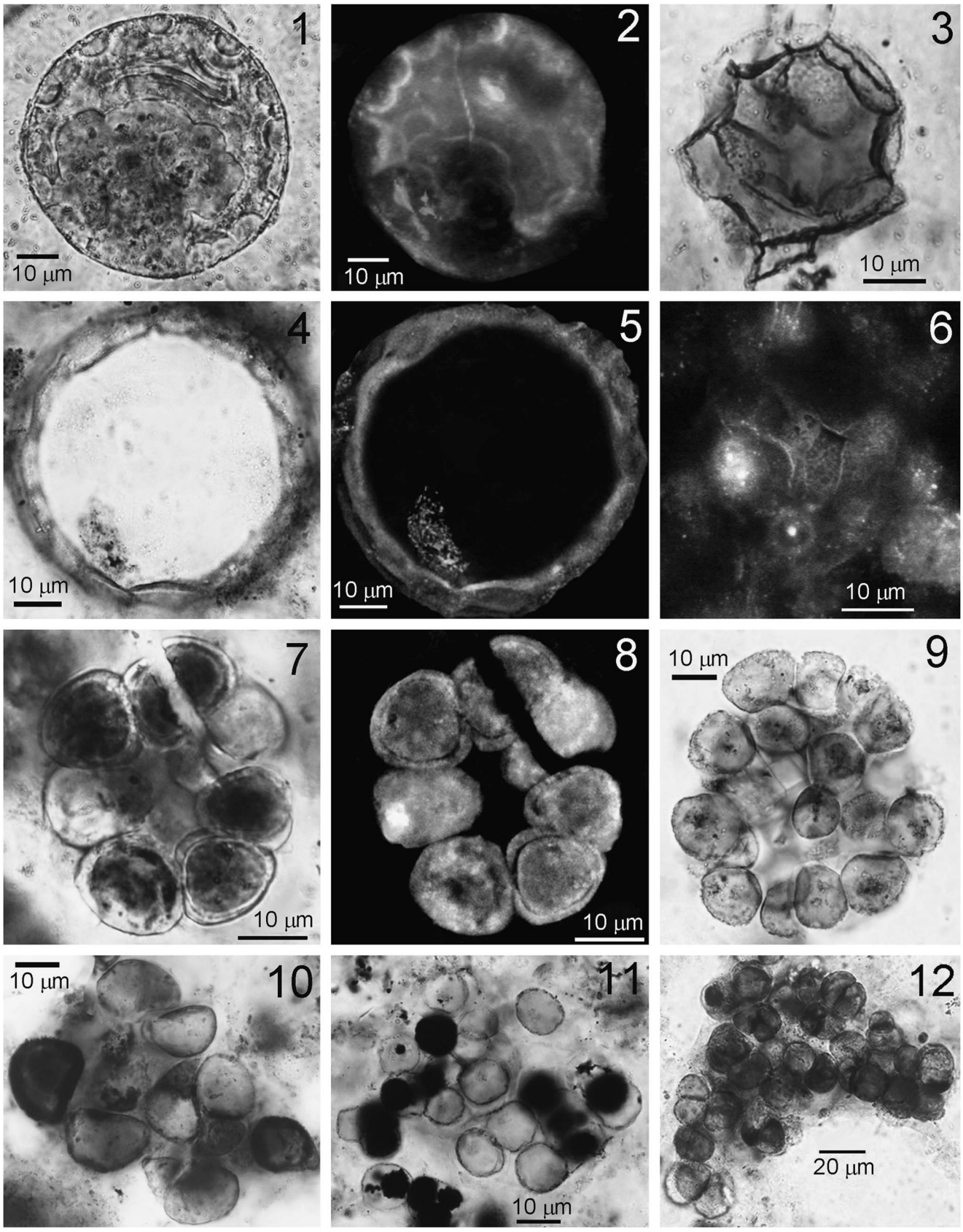

https://doi.org/10.1017/jpa.2015.56 Published online by Cambridge University Press

Occurrence.—Widely distributed in Proterozoic chert-permineralized microfossil assemblages.

Remarks.—Although *Myxococcoides* was established in 1968 to include colonies of simple spheroidal microfossils interpreted to be chroococcacean cyanobacteria (Schopf, 1968), this genus name has since been used to encompass diverse microfossils of heterogeneous origin (Green et al., 1989; Knoll et al., 1991; Butterfield et al., 1994; Sergeev et al., 1995, 2012). Some such species are no doubt chroococcaceans (though this may be uncertain for the type population of *M. minor*; Knoll, 1981) whereas others also resemble small-celled chlorococcalean green algae (Green et al., 1989; Knoll et al., 1991; Sergeev and Schopf, 2010). Still others have been suggested to have different affinities; for example, specimens of the relatively large-diameter taxon *M. grandis* have been suggested to represent the empty originally colony-enclosing envelopes of colonial prokaryotes (Fairchild, 1985; Sergeev, 1992, 2006) or the akinetes of nostocalean cyanobacteria (Sergeev et al., 1995; 2012). Because of such uncertainty regarding the affinities of *Myxococcoides* taxa, *M. inornata* and *M. minor* are classified here as *Incertae Sedis*. To date, more than 30 species of this genus have been described.

Myxococcoides minor Schopf, 1968
Figure 14.11

Myxococcoides minor Schopf, 1968, p. 676, pl. 81, fig. 1, pl. 83, fig. 10; Schopf, 1992b, pl. 32, figs. H, I; Sergeev, Knoll, and Petrov, 1997, p. 234, figs. 18C, 18D; Sergeev, 2001, p. 443, fig. 8.11; Sergeev, 2006, p. 225 and 226, pl. 15, figs. 2, 5; pl. 20, fig. 11; pl. 48, fig. 5; Sergeev, Sharma, and Shukla, 2008, pl. 5, fig. 8, pl. 6, fig. 9; Sergeev and Schopf, 2010, p. 393, figs 12.3, 12.4; Schopf, Kydryavtsev and Sergeev, 2010a, figs 5.5, 5.6; Sergeev, Sharma, and Shukla, 2012, pl. 5, fig. 8, pl. 6, fig. 9.

Description.—Spheroidal closely packed cells 8.5–14.0 μm in diameter, occurring in organic matrix-embedded colonies of a few to tens of individuals, defined by single-layered fine-grained walls ~ 0.5 μm thick. Some cells contain spheroidal to irregularly shaped opaque bodies, evidently condensed cytoplasmic remnants, that partially or nearly completely infill cell lumina.

Material examined.—Tens of well-preserved colonies and hundreds of individuals.

Occurrence.—Widely distributed in Proterozoic chert-permineralized microfossil assemblages.

Genus *Vandalosphaeridium* Vidal, 1981

Type species.—*Vandalosphaeridium reticulatum* (Vidal), 1981.

Vandalosphaeridium koksuicum Sergeev and Schopf, 2010
Figure 14.3, 14.6

Vandalosphaeridium koksuicum Sergeev and Schopf, 2010, p. 397, figs. 13.1, 13.2a, 13.2b, 13.3, 13.4a, 13.4b.

Description.—Spheroidal vesicles, subcircular in cross-section, having a surface folded into numerous polygonal fields from the walls of which protrude unbranched broadly conical processes that are more or less evenly distributed across the surface. Vesicle diameters range from 40 to 45 μm (n = 3, x = 43); processes are commonly indistinct, evidently 5 to 7 μm long and taper from being 2–5 μm broad at their base to 1–2 μm wide in their distal parts. A globular opaque polygonal (pyrite-like) inclusion, 4–5 μm broad, is present within some vesicles.

Material examined.—Three well-preserved specimens.

Occurrence.—Neoproterozoic: Chichkan Formation, South Kazakhstan; Lower Cambrian, Chulaktau Formation, South Kazakhstan.

Remarks.—The taxonomic status of this genus is uncertain. Described initially from the Late Neoproterozoic Visingsö Group of Sweden as a morphologically distinctive acanthomorphic acritarch (Vidal, 1981), *Vandalosphaeridium* has been reported from numerous other Neoproterozoic units including the Chulaktau-underlying Chichkan Formation (Sergeev and Schopf, 2010) and Ediacaran-age strata of Australia (Grey, 2005). The Chulaktau taxon, *Vandalosphaeridium koksuicum*, exhibits distinctive broadly conical processes and differs in size and morphology from such other described species as *V. reticulatum* and *V. varangeri*. Although at least one species of the genus (*V. walcottii*, described from the Neoproterozoic Chuar Group of Arizona; Vidal and Ford, 1985) was defined on the basis of what appear to be rather poorly preserved specimens of *Trachyhystrichosphaera aimika*, the distinctive morphology of *V. koksuicum* and the occurrence in many Chichkan specimens of a vesicle-enclosed globular organic body (Sergeev and Schopf, 2010) that is similar to that of the (pyrite-replaced?) inclusions of the Chulaktau specimens, suggests that *V. koksuicum* is a legitimate taxon, most probably allied to planktonic chlorophycean green algae.

Acknowledgments

We thank two anonymous reviewers for constructive reviews of the manuscript and M. A. Semikhatov, M. A. Fedonkin, T. A. Litvinova, P. Yu. Petrov, N. G. Vorob'eva, N. M. Chumakov, and the late V. V. Missarzhevskii for helpful discussions. The four-week visit in 2012 of V.N.S. to the University of California, Los Angeles, where parts of this study were carried out, was supported by the UCLA Center for the Study of Evolution and the Origin of Life (CSEOL). Fieldwork involved in the collection of the fossiliferous samples studied and the research carried out by V.N.S. at GIN, the Geological Institute RAS in Moscow, were supported by RFBR Grants #13-05-00127, #14-05-00323, and the Program of the Presidium of Russian Academy of Sciences #28. The participation of A.B.K. is this study was supported by CSEOL and the PennState Astrobiology Research Center (PSARC).

References

Ankinovich, S.G., 1961, Lower Paleozoic of Northern Tian-Shan and Western Margin of Central Kazakhstan Vanadium Bearing Basin, Part I: Alma-Ata, AN Kazakhskoi SSR, 272 p. [in Russian]

Baturin, G.L., 1978, Phosphorites on the bottom of oceans: Moscow, Nauka, 231 p. [in Russian]

Bezrukov, P.L., 1941, The results of Karatau phosphorite basin research, *in* Developments in Kazakhstan Geological Research for 20 Years: Alma-Ata. AN Kazakhskoi SSR, p. 137–149. [in Russian]

Burzin, M.B., 1995, Late Vendian helicoid filamentous microfossils: Paleontological Journal, v. 29(1A), p. 1–34.

Butterfield, N.J., Knoll, A.H., and Swett, K., 1994, Paleobiology of the Neoproterozoic Svanbergfjellet Formation, Spitsbergen: Fossils and Strata, v. 34, 84 p.

Cao, F., 1985, The new data of algal microfossils from the Sinian Doushantuo Formation: Bulletin, Tianjin Institute of Geology and Mineral Resources, v. 12, p. 183–193. [in Chinese]

Chen, J.-Y., Schopf, J.W., Bottjer, D.J., Zhang, C.-Y., Kudryavtsev, A.B., Wang, X.-Q., Yang, Y.H., and Gao, X., 2007, Raman spectra of a Lower Cambrian ctenophore embryo from SW Shaanxi, China: Proceedings of the National Academy of Sciences USA, v. 104, p. 6289–6292.

Chumakov, N.M., 2009, The Baykonurian glaciohorizon of the Late Vendian: Stratigraphy and Geological Correlation, v. 17, p. 373–381.

Chumakov, N.M., 2010, Precambrian glaciations and associated biospheric events: Stratigraphy and Geological Correlation, v. 18, p. 467–479.

Chumakov, N.M., 2011, Late Proterozoic African Glacial Era: Stratigraphy and Geological Correlation, v. 19, p. 1–20.

Claxton, N.S., Fellers, T.J., and Davidson, M.W., 2005, Laser scanning confocal microscopy: http://www.olympusfluoview.com/theory/LSCMIntro.pdf (accessed January 2016).

Cloud, P., Awramik, S.M., Morrison, K., and Hadley, D.G., 1979, Earliest Phanerozoic or latest Proterozoic fossils from Arabian shield: Precambrian Research, v. 10, p. 73–93.

Cohen, P.A., Schopf, J.W., Butterfield, N.J., Kudryavtsev, A.B., and Macdonald, F.A., 2011, Phosphate biomineralization in mid-Neoproterozoic protists: Geology, v. 39, p. 539–542.

Cook, P.J., and Shergold, J.H., eds., 2005, Phosphate deposits of the World, volume 1: Proterozoic and Cambrian phosphorites: Cambridge-London-New York-New Rochelle-Melbourne-Sydney, Cambridge University Press, 408 p.

Decision of fifth all-union colloquium on precambrian microfossils of the USSR, 1986, Leningrad, Academy of Sciences of the USSR, 18 p. [in Russian]

Deflandre, G., 1954, Systematique des hystrichosphaeridiès: sur I'acception de genre *Cymatiosphaera* O. Wetzel. Comptes Rendu: Geological Society of France, v. 12, p. 257–259.

Dong, L., Xiao, S., Shen, B., Zhou, C., Li, G., and Yao, J., 2009, Basal Cambrian microfossils from the Yangtze Gorges area (South China) and the Aksu area (Tarim Block, Northwestern China): Journal of Paleontology, v. 83, p. 30–44.

Downie, C., and Sarjeant, W.A.S., 1963, On the interpretation and status of some *Hystrichosphaera* genera: Palaeontology, v. 6, p. 83–96.

Eganov, E.A., 1988, Origin of phosphorites and stromatolites: Novosibirsk, Institute of Geology and Geophysics of the Siberian Branch of AN SSSR, 90 p.

Eganov, E.A., and Sovietov, Yu.K., 1979, Karatau – A Model for Phosphorite Deposition: Novosibirsk, Nauka, 192 p. [in Russian]

Eganov, E.A., Sovietov, Yu.K., and Yanshin, A.L., 1986, Proterozoic and Cambrian phosphorites deposits: Karatau, southern Kazakhstan, USSR, *in* Cook, P.J., and Shergold, J.H., eds., Phosphate Deposits of the World: volume 1 Proterozoic and Cambrian Phosphorites: Cambridge, UK, Cambridge University Press, p. 175–189.

Eisenack, A., 1958, Microfossilien aus dem Ordovizium des Baltikums, 1, Markasitschicht, Dictyonema-Scheifer, Glaukonitsand, Glaukonitkalk: Senckenbergian Lethaea, v. 39, p. 389–404.

Elenkin, A.A., 1949, Monographie algarum Cyanophycearum aquidulcium et terrestrium infinibus URSS inventarum: Moscow, Izdatelstvo AN SSSR, Pars specialis (Systematica), Fascicie II, p. 985–1908. [in Russian]

Ercegović, A., 1932, Studes écologique et sociologique des Cyanophycées lithophytes de la côte Yugoslave de l'Adriatique: Bulletin International de l'Académie Yougoslave de la Sciences des Arts, Classe Mathematic et Naturelles, v. 26, p. 33–56.

Ergaliev, G. Kh., and Pokrovskaya, N.A., 1977, Lower Cambrian Trilobites of the Malay Karatau Range (South Kazakhstan): Alma-Ata, Nauka. [in Russian]

Fairchild, T.R., 1985, Size as criterion for distinguishing probable eukaryotic unicells in silicified Precambrian microfloras, *in* Campos, D.A., Ferreira, C.S., Brito, I.M., and Viana, C.F., eds., Coletânea de Trabalhos Paleontológicos, Brasil, Departamento Nacional de Produção Mineral, Série Geologia no. 27, Brasília, Seção Paleontologia e Estratigrafia no. 2, p. 315–320.

Gaft, M., Reisfeld, R., Panczer, G., Boulon, G., Shoval, S., and Champagnon, B., 1997a, Accommodation of rare-earths and manganese by apatite: Optical Materials, v. 8, p. 149–156.

Gaft, M., Reisfeld, R., Panczer, G., Shoval, S., Champagnon, B., and Boulon, G., 1997b, Eu^{+3} luminescence in high-symmetry sites of natural apatite: Journal of Luminescence, v. 72–74, p. 572–774.

Gaft, M., Reisfeld, R., and Panczer, G., 2005, Modern Luminescence Spectroscopy of Minerals and Materials: Berlin, Springer-Verlag, 356 p.

Geitler, L., 1932, Cyanophyceae, *in* Rabenhorst, L., ed., Kryptogamen-Flora von Deutschland, Österreich und der Schweiz, Band 14: Leipzig, Akademische Verlagsgesellschaft, pp. 673–1196.

Gerasimenko, L.M., and Krylov, I.N., 1983, Post-mortem alteration of cyanobacteria in the algal-bacterial mats from the Kamchatka Peninsula thermal springs: Doklady AN SSSR, v. 272(1), p. 201–203. [in Russian]

Gerasimenko, L.M., Goncharova, I.V., Zhegallo, E.A., Zavarzin, G.A., Zaitseva, L.V., Orleanskii, V.K., Rozanov, A.Yu., and Ushatinskaya, G.T., 1996, The mineralization (phosphatization) of filamentous cyanobacteria: Lithology and Mineral Resources, v. 2, p. 185–191.

Gerasimenko, L.M., Zavarzin, G.A., Rozanov, A.Yu., and Ushatinskaya, G.T., 1999, The role of cyanobacteria in the formation of phosphorite deposits: Journal of General Biology, v. 64, p. 415–430.

Golovenok, V. K., and Belova, M.Yu., 1983, *Obruchevella* from the Riphean of the Patom Highland and the Vendian of southern Kazakhstan: Doklady AN SSSR, v. 272, p. 1462–1465. [in Russian]

Golovenok, V.K., and Belova, M.Yu., 1984, Riphean microbiotas in cherts of the Billyakh Group on the Anabar Uplift: Paleontologicheskii Zhurnal, v. 4, p. 20–30. [English version]

Golovenok, V.K., and Belova, M.Yu., 1989, Microfossils of *Obruchevella parva* Reitlinger from Vendian deposits of Lena River basin: Doklady AN SSSR, v. 306, p. 190–193. [in Russian]

Golovenok, V.K., and Belova, M.Yu., 1993, The microfossils in the cherts from the Riphean deposits of the Turukhansk Uplift: Stratigraphy and Geological Correlation, v. 1(3), p. 51–61. [English version]

Golub, I.N., 1979, A new group of problematic microfossils from Vendian deposits of the Orshan depression (Russian Platform), *in* Sokolov, B.S., ed., Paleontology of Precambrian and Early Cambrian: Leningrad, Nauka, p. 147–155. [in Russian]

Golubic, S., and Hofmann, H.J., 1976, Comparison of Holocene and mid-Precambrian Entophysalidaceae (Cyanophyta) in stromatolitic algal mats: cell division and degradation: Journal of Paleontology, v. 50, p. 1074–1082.

Green, J., Knoll, A.H., and Swett, K., 1989, Microfossils from silicified stromatolitic carbonates of the Upper Proterozoic Limestones - Dolomite 'Series,' Central East Greenland: Tectonics, v. 119, p. 567–585.

Grey, K., 2005, Ediacaran palynology of Australia: Association of Australasian Palaeontologists: Memoir, v. 31, 439 p.

Hermann, T.N., 1974, Finds of massive accumulations of trichomes in the Riphean, *in* Timofeev, B.V., ed., Microfossils of the Proterozoic and Early Paleozoic of the USSR: Leningrad, Nauka, p. 6–10. [in Russian]

Hermann, T.N., 1990, The Organic World a Billion Years Ago: Leningrad, Nauka, 50 p. [in Russian, with English summary]

Hofmann, H.J., 1976, Precambrian microflora, Belcher Island, Canada: significance and systematics: Journal of Paleontology, v. 50, p. 1040–1073.

Hofmann, H.J., and Schopf, J.W., 1983, Early Proterozoic microfossils, *in* Schopf, J.W., ed., Earth's Earliest Biosphere: Its Origin and Evolution: Princeton, New Jersey, Princeton University Press, p. 321–360.

Hofmann, H.J., and Jackson, C.D., 1994, Shale-facies microfossils from the Proterozoic Bylot Supergroup, Baffin Island, Canada: Palaeontological Society: Memoir, v. 37, p. 1–39.

Horodyski, R. J., and Donaldson, J.A., 1980, Microfossils from the Middle Proterozoic Dismal Lakes Group, Arctic Canada: Precambrian Research, v. 11, p. 125–159.

Javaux, E.J., Knoll, A.H., and Walter, M.R., 2004, TEM evidence for eukaryotic diversity in mid-Proterozoic oceans: Geobiology, v. 2, p. 121–132.

Jehlička, J., Urban, A., and Pokorny, J., 2003, Raman spectroscopy of carbon and solid bitumens in sedimentary and metamorphic rocks: Spectrochimica Acta, v. A59, p. 2341–2352.

Keller, B.M., Korolev, V.G., and Krylov, I.N., 1965, Subdivision of the Upper Proterozoic in Tian Shan: Izvestiya AN SSSR: Seria Geologicheskaya, v. 4, p. 101–115. [in Russian]

Kholodov, V.N., and Paul, R.K., 1993a, Biota and problems of ancient phosphorite formation, *in* Ecosysteme Restructures and the Evolution of the Biosphere: Moscow, Nedra, p. 333–339. [in Russian]

Kholodov, V.N., and Paul, R.K., 1993b, Problem of phosphorites origin: Lithology and Mineral Resources, v. 3, p. 110–115. [in Russian]

Kholodov, V.N., and Paul, R.K., 1994, Morphogenetic peculiarities of the Karatau phosphorites (Kazakhstan) and the problem of the ancient biogenetic phosphorous formation, *in* Ecosystem Restructures and the Evolution of the Biosphere: Moscow, Nedra, p. 339–347. [in Russian]

Kirchner, O., 1900, Shizophyceae, *in* Engler, A., and Prantl, K., eds., Die Natürlichen Pflanzenfamilien: Leipzig, I Teil, Abteilung Ia, p. 115–121.

Knoll, A.H., 1981, Paleoecology of Late Precambrian microbial assemblages, *in* Niklas, K., ed., Paleobotany, Paleoecology and Evolution: New York, Praeger, p. 17–54.

https://doi.org/10.1017/jpa.2015.56 Published online by Cambridge University Press

Knoll, A.H., 1982, Microfossils from the Late Precambrian Draken Conglomerate, Ny Friesland, Svalbard: Journal of Paleontology, v. 56, p. 577–790.
Knoll, A.H., 1994, Proterozoic and Early Cambrian protists: evidence for accelerating evolutionary tempo: Proceedings of the National Academy of Sciences, USA, v. 91, p. 6743–6750.
Knoll, A.H., 1996, Archean and Proterozoic Paleontology, *in* Jansonius, J., and McGregor, D.C., eds., Palynology: Principles and Applications: American Association of Stratigraphic Palynologists Foundation, v. 1, p. 51–80.
Knoll, A.H., and Golubic, S., 1979, Anatomy and taphonomy of a Precambrian algal stromatolite: Precambrian Research, v. 10, p. 115–151.
Knoll, A.H., Strother, P.K., and Rossi, S., 1988, Distribution and diagenesis of microfossils from the Lower Proterozoic Duck Creek Dolomite, Western Australia: Precambrian Research, v. 38, p. 257–279.
Knoll, A.H., Swett, K., and Mark, J., 1991, Paleobiology of a Neoproterozoic tidal flat/lagoonal complex: the Draken Conglomerate Formation, Spitsbergen: Journal of Paleontology, v. 65, p. 531–570.
Knoll, A.H., Javaux, E.J., Hewitt, D., and Cohen, P., 2006, Eukaryotic organisms in Proterozoic oceans: Philosophical Transactions of the Royal Society of London B, v. 361, p. 1023–1038.
Kolosov, P.N., 1977, Ancient Oil and Gas-bearing Deposits from the Southeast Siberian Platform: Novosibirsk, Nauka, 90 p.
Kolosov, P.N., 1984, Late Precambrian microorganisms from the eastern Siberian Platform: Yakutsk, Yakutian Filial of Siberian Branch of Academy of Sciences of the USSR, 84 p. [in Russian]
Korolev, V.G., 1961, Schema of Tian-Shan and adjacent areas tectonic zones: Izvestiya Kyzgyzskogo Filiala VGO, v. 3, p. 81–102. [in Russian]
Korolev, V.G., 1971, Upper Precambrian stratigraphy of Tian-Shan Mountains and Karatau, *in* Precambrian Stratigraphy of Kazakhstan and Tian-Shan: Moscow, MGU, p. 117–118. [in Russian]
Korolev, V.G., and Ogurtsova, R.N., 1981, Acritarchs of the upper part of Lower Cambrian deposits from the Talas-Karatau zone (Maly Karatau Range): Doklady AN SSSR, v. 261(1), p. 162–164. [in Russian]
Korolev, V.G., and Ogurtsova, R.N., 1982, Correlation of the Vendian-Lower Cambrian boundary deposits of the Talas-Karatau zone (Maly Karatau Range) with the reference sections of the East European and Siberian Platforms: Izvestiya AN SSSR, Seria Geologicheskaya v. 6, p. 27–36. [in Russian]
Krylov, I.N., 1967, Riphean and Lower Cambrian Stromatolites of Tian-Shan Mountains and Karatau: Moscow, Nauka, 76 p. [in Russian]
Levashova, N.M., Meert, J.G., Gibsher, A.S., Grice, W.C., and Bazhenov, M.L., 2011, The origin of microcontinents in the Central Asian Orogenic Belt: constraints from paleomagnetism and geochronology: Precambrian Research, v. 185, p. 37–54.
Luo, H., Jian, Z., Wu, X., Song, X., and Ouyang, L., 1982, The Sinian-Cambrian Boundary in Eastern Yunnan, China: People's Publishing House of Yunnan, Kunming, 265 p. [in Chinese]
Luo, H., Jian, Z., Wu, X., Song, X., Ouyang, L., Xing, Y., Liu, G., Zhang, S., and Tao, Y., 1984, Sinian-Cambrian Boundary Stratotype Section at Meishucun, Jinning, Yunnan, China: People's Publishing House of Yunnan, Kunming, 154 p. [in Chinese]
Maithy, P. K., 1975, Microorganisms from the Bushimay System (Late Precambrian) of Kanshi, Zaire: Palaeobotanist, v. 22, p. 133–149.
Mambetov, A.M., 1993, The earliest skeletonized fossils and zonal stratigraphy of the upper Precambrian–Lower Cambrian of North Tian Shan, *in* Mambetov, M., ed., Novyye Dannyye po Biostratigrafii Dokembriya i Paleozoya Kyrgyzstana: Ilim, Bishkek, p. 15–23. [in Russian]
Mendelson, C.V., and Schopf, J.W., 1982, Proterozoic microfossils from the Sukhaya Tunguska, Shorikha and Yudoma Formations of the Siberian Platform: U.S.S.R. Journal of Paleontology, v. 56, p. 42–83.
McMillan, P.F., and Hofmeister, A.M., 1988, Infrared and Raman spectroscopy: Review of Mineralogy, v. 18, p. 99–159.
Meert, J.G., Gibsher, A.S., Levashova, N.M., Grice, W.C., Kamenov, G.D., and Ryabinin, A.B., 2011, Glaciation and ~770 Ma Ediacara [?] fossils from the Lesser Karatau Microcontinent, Kazakhstan: Gondwana Research, v. 19, p. 867–880.
Missarzhevskii, V.V., 1989, The oldest shelly fossils and the stratigraphy of the Precambrian-Cambrian boundary deposits: Moscow, Nauka, 237 p. [in Russian]
Missarzhevskii, V.V., and Mambetov, A.M., 1981, Stratigraphy and Fauna of the Maly Karatau Precambrian-Cambrian Boundary Deposits: Moscow, Nauka, 92 p. [in Russian]
Moczydłowska, M., 2010, Life cycle of Early Cambrian microalgae from the *Skiagia*-plexus acritarchs: Journal of Paleontology, v. 84, p. 216–230.
Moczydłowska, M., Schopf, J.W., and William, S., 2010, Micro- and nano-scale ultrastructure of cell walls in Cryogenian microfossils: revealing their biological affinity: Lethaia, v. 43, p. 129–136.
Nägeli, C., 1849, Gattungen einzelliger Algen, physiologisch und under systematisch bearbeitet, Neue Denkschriften der Allgemeinen schweizerischen Gesellschaft für die gesamten: Naturwissenschaften, v. 8, p. 44–60.
Nagovitsin, K.E., 2000, Silicified microbiotas of the Upper Riphean of the Yenisei Ridge: news in paleontology and stratigraphy: Geologia i Geofizika, v. 41(2/3), p. 7–31. [English version]
Naumova, S.N., 1949, Spores of the Lower Cambrian: Izvestiya Akademiya Nauk SSSR: Seriya Geologicheskaya, v. 4, p. 49–56. [in Russian]
Nyberg, A.V., and Schopf, J.W., 1984, Microfossils in stromatolitic cherts from the Upper Proterozoic Min'yar Formation, southern Ural Mountains, USSR: Journal of Paleontology, v. 58, p. 738–772.
Oehler, D.Z., 1978, Microflora of the Middle Proterozoic Balbirini Dolomite [McArthur Group] of Australia: Alcheringa, v. 2, p. 269–309.
Ogurtsova, R.N., 1985, Plant Microfossils of the Vendian-Lower Cambrian Maly Karatau Reference Section: Ilim, Frunze, 136 p. [in Russian]
Ogurtsova, R.N., and Sergeev, V.N., 1987, The microbiota of the Upper Precambrian Chichkanskaya Formation in the Lesser Karatau Region (southern Kazakhstan): Paleontologicheskii Zhurnal, v. 2, p. 101–112. [English version]
Ogurtsova, R.N., and Sergeev, V.N., 1989, Megasphaeromorphids from the Upper Precambrian Chichkan Formation, southern Kazakhstan: Paleontologicheskii Zhurnal, v. 2, p. 119–122. [in Russian]
Pasteris, J.D., and Wopenka, B., 1991, Raman spectra of graphite as indicators of degree of metamorphism: Canadian Mineralogist, v. 29, p. 1–9.
Popov, L.E., Bassett, M.G., Zhemchuzhnikov, V.G., Holmer, L.E., and Klishevich, I.A., 2009, Gondwanan faunal signatures from early Paleozoic terranes of Kazakhstan and Central Asia: evidence and tectonic implications, *in* Bassett, M.G., ed., Early Paleozoic Peri-Gondwana Terranes: New Insights from Tectonics and Biogeography: Geological Society of London, Special Publications, v. 325, p. 23–64.
Prasad, B., 2007, *Obruchevella* and other terminal Proterozoic (Vendian) organic-walled microfossils from the Bhander Group (Vendian Supergroup), Madhya Pradesh: Journal of the Geological Society of India, v. 69, p. 295–310.
Prasad, B., Uniyal, S.N., and Asher, R., 2005, Organic walled microfossils from the Proterozoic Vindhyan Supergroup of Son Valley, Madhya Pradesh, India: Palaeobotanist, v. 54, p. 13–60.
Reisfeld, R., Gaft, M., Boulon, G., Panczer, C., and Jorgensen, C.K., 1996, Laser-induced luminescence of rare-earth elements in natural fluor-apatites: Journal of Luminescence, v. 69, p. 343–353.
Reitlinger, E.A., 1948, Cambrian foraminifera of Yakutia: Bulletin of Moscow Nature Investigators Society: Geological Section, v. 23, p. 77–81. [in Russian]
Reitlinger, E.A., 1959, Atlas of Microscopic Organic Remains and Problematica of Ancient Deposits of Siberia: Moscow, Academiya Nauk SSSR, 62 p. [in Russian]
Schopf, J.W., 1968, Microflora of the Bitter Springs Formation, Late Precambrian, central Australia: Journal of Paleontology, v. 42, p. 651–688.
Schopf, J.W., 1976, Are the oldest "fossils," fossils?: Origins of Life, v. 7, p. 19–31.
Schopf, J.W., 1992a, Informal revised classification of Proterozoic microfossils, *in* Schopf, J.W., and Klein, C., eds., The Proterozoic Biosphere: A Multidisciplinary Study: New York, Cambridge University Press, p. 1119–1166.
Schopf, J.W., 1992b, Evolution of the Proterozoic biosphere: benchmarks, tempo, and mode, *in* Schopf, J.W., and Klein, C., eds., The Proterozoic Biosphere: A Multidisciplinary Study: New York, Cambridge University Press, p. 584–600.
Schopf, J.W., 1992c, Atlas of representative Proterozoic microfossils, *in* Schopf, J.W., and Klein, C., eds., The Proterozoic Biosphere: A Multidisciplinary Study: New York, Cambridge University Press, p. 1055–1118.
Schopf, J.W., 1994, Disparate rates, differing fates: the rules of evolution changed from the Precambrian to the Phanerozoic: Proceedings of the National Academy of Sciences, USA, v. 91, p. 6735–6742.
Schopf, J.W., and Kudryavtsev, A.B., 2005, Three-dimensional imagery of Precambrian microscopic organisms: Geobiology, v. 3, p. 1–12.
Schopf, J.W., and Kudryavtsev, A.B., 2010, A renaissance in studies of ancient life: Geology Today, v. 26, p. 141–146.
Schopf, J.W., and Kudryavtsev, A.B., 2012, Biogenicity of Earth's earliest fossils: a resolution of the controversy: Gondwana Research, v. 39, p. 761–771.
Schopf, J.W., Kudryavtsev, A.B., Agresti, D.G., Wdowiak, T.J., and Czaja, A.D., 2002, Laser-Raman imagery of Earth's earliest fossils: Nature, v. 416, p. 73–76.
Schopf, J.W., Kudryavtsev, A.B., Agresti, D.G., Czaja, A.D., and Wdowiak., T.J., 2005, Raman imagery: a new approach to assess the geochemical maturity and biogenicity of permineralized Precambrian fossils: Astrobiology, v. 5, p. 333–371.
Schopf, J.W., Tripathi, A., and Kudryavtsev, A.B., 2006, Three-dimensional confocal optical microscopy of Precambrian microscopic organisms. Astrobiology, v. 6, p. 1–16.

Schopf, J.W., Kudryavtsev, A.B., and Sergeev, V.N., 2010a, Confocal laser scanning microscopy and Raman imagery of the late Neoproterozoic Chichkan microbiota of South Kazakhstan: Journal of Paleontology, v. 84, p. 402–416.
Schopf, J.W., Kudryavtsev, A.B., Tripathi, A.B., and Czaja, A.D., 2010b, Three-dimensional morphological (CLSM) and chemical (Raman) imagery of cellularly mineralized fossils, *in* Allison, P.A., and Bottjer, D.J., eds., Taphonomy: Process and Bias through Time: Amsterdam, the Netherlands, Springer-Verlag, p. 457–486.
Schopf, J.W., Farmer, J.D., Foster, I.S., Kudryavtsev, A.B., Gallardo, V.A., and Espinoza, C., 2012, Gypsum-permineralized microfossils and their relevance to the search for life on Mars: Astrobiology, v. 12, p. 619–633.
Sergeev, V.N., 1989, Microfossils from transitional Precambrian-Phanerozoic strata of Central Asia: Himalayan Geology, v. 13, p. 269–278.
Sergeev, V.N., 1992, Silicified microfossils from the Precambrian and Cambrian deposits of the southern Ural Mountains and Middle Asia: Moscow, Nauka, 134 p. [in Russian]
Sergeev, V.N., 2001, Paleobiology of the Neoproterozoic (Upper Riphean) Shorikha and Burovaya silicified microbiotas, Turukhansk Uplift, Siberia: Journal of Paleontology, v. 75, p. 427–448.
Sergeev, V.N., 2002, Silicified microfossils from the Vendian Yudoma Group, the Uchur-Maya Region of Siberia: facies dependence and biostratigraphic potential: Stratigraphy and Geological Correlation, v. 10(6), p. 547–564. [English version]
Sergeev, V.N., 2006, Precambrian Microfossils in Mherts: Their Paleobiology, Classification and Biostratigraphic Usefulness: Moscow, GEOS, 280 p. [in Russian]
Sergeev, V.N., and Seong-Joo, L., 2001, Microfossils from cherts of the Middle Riphean Svetlyi Formation, the Uchur-Maya Region of Siberia and their stratigraphic significance: Stratigraphy and Geological Correlation, v. 9(1), p. 1–10. [English version]
Sergeev, V.N., and Seong-Joo., L., 2004, New data on silicified microfossils from the Satka Formation of the Lower Riphean stratotype, the Urals: Stratigraphy and Geological Correlation, v. 12(1), p. 1–21. [English version]
Sergeev, V.N., and Ogurtsova, R.N., 1989, Microbiota from the Lower Cambrian phosphatic deposits of the Maly Karatau (South Kazakhstan): Izvestiya Akademiya Nauk SSSR, Seriya Geologicheskaya, v. 3, p. 58–66. [In Russian]
Sergeev, V.N., and Schopf, J.W., 2010, Taxonomy, paleoecology and biostratigraphy of the Late Neoproterozoic Chichkan microbiota of South Kazakhstan: the marine biosphere on the eve of metazoan radiation: Journal of Paleontology, v. 84, p. 363–401.
Sergeev, V.N., Knoll, A.H., and Grotzinger, J.P., 1995, Paleobiology of the Mesoproterozoic Billyakh Group, Anabar Uplift, Northeastern Siberia: Paleontological Society Memoir, v. 39, 37 p.
Sergeev, V.N., Knoll, A.H., Kolosova, S.P., and Kolosov, P.N., 1994, Microfossils in cherts from the Mesoproterozoic Debengda Formation, the Olenek Uplift, northeastern Siberia: Stratigraphy and Geological Correlation, v. 2(1), p. 23–38. [English version]
Sergeev, V.N., Knoll, A.H., and Petrov, P.Yu., 1997, Paleobiology of the Mesoproterozoic-Neoproterozoic transition: the Sukhaya Tunguska Formation, Turukhansk Uplift, Siberia: Precambrian Research, v. 85, p. 201–239.
Sergeev, V.N., Sharma, M., and Shukla, Y., 2008, Mesoproterozoic silicified microbiotas of Russia and India-characteristics and contrasts: Palaeobotanist, v. 57, p. 323–358.
Sergeev, V.N., Sharma, M., and Shukla, Y., 2012, Proterozoic fossil cyanobacteria: Palaeobotanist, v. 61, p. 189–358.
Sharma, M., 2006, Palaeobiology of Mesoproterozoic Salkhan Limestone Semri Group, Rohtas, Bihar, India: systematics and significance: Journal of Earth System Sciences, v. 115, p. 67–78.
Song, X., 1984, *Obruchevella* from the Early Cambrian Meishucunian Stage of the Meishucun section, Jinning, Yunnan, China: Geological Magazine, v. 121, p. 179–183.
Sovietov, Yu.K., 2008, Neoproterozoic rifting and sedimentary basins evolution located on the Tarim-type microcontinents: Maly Karatau, southern Kazakhstan, *in* Sedimentogenesis and Lithogenesis Types and their Evolution through Earth's History, Transactions of 5th All-Russian Lithological Conference. Russian Academy of Science, Yekaterinburg. p. 143–146. [in Russian]
Srivastava, P., and Kumar, S., 2003, New microfossils from the Meso–Neoproterozoic Deoban Limestone, Garhwal, Lesser Himalaya, India: Palaeobotanist, v. 52, p. 13–47.
Stanier, R.Y., Sistrom, Y.R., Hansen, T.A., Whitton, B.A., Castenholz, R.W., Pfennig, N., Gorlenko, V.M., Kondratieva, E.N., Eimhjellen, K.E., Whittenbury, R., Gherna, R.L., and Trüper, , H.G., 1978, Proposal to place nomenclature of the Cyanobacteria [blue-green algae] under the rules of the International Code of Nomenclature of bacteria: International Journal of Systematic Bacteriology, v. 28, p. 335–336.
Talyzina, N., and Moczydłowska, M., 2000, Morphological and ultrastructural studies of some acritarchs from the Lower Cambrian Lukati Formation, Estonia: Review of Palaeobotany and Palynology, v. 112, p. 1–21.
Tappan, H., 1980, The Paleobiology of Plant Protists: San Francisco, Freeman, 1028 p.
Thuret, G., 1875, Essai de classification des nostocines: Annales des Sciences Naturelles: Paris (Botanique), v. 6, p. 372–382.
Timofeev, B.V., and Hermann, T.N., 1979, The Precambrian microbiota of the Lakhanda Formation, *in* Sokolov, B.S., ed., Paleontology of Precambrian and Early Cambrian: Leningrad, Nauka, p. 137–147. [in Russian]
Timofeev, B.V., Hermann, T.N., and Mikhailova, N.S., 1976, Microphytofossils from the Precambrian, Cambrian and Ordovician: Leningrad, Nauka, 106 p. [in Russian]
Turner, R.E., 1984, Acritarch from type area of the Ordovician Caradoc Series, Shropshire, England: Palaeontographica Abteilung B, v. 190(4-6), p. 87–157.
Vidal, G., 1981, Micropalaeontology and biostratigraphy of the Upper Proterozoic and Lower Cambrian Sequence in East Finnmark, northern Norway: Norges Geologiske Underssogelse Bulletin, v. 362, p. 1–53.
Vidal, G., and Ford, T.D., 1985, Microbiotas from the Late Proterozoic Chuar Group (Northern Arizona) and Uinta Group (Utah) and their chronostratigraphic implications: Precambrian Research, v. 28, p. 344–389.
Vidal, G., and Knoll, A.H., 1982, Radiations and extinctions of plankton in the late Proterozoic and early Cambrian: Nature, v. 296, p. 57–60.
Vidal, G., and Moczydłowska-Vidal, M., 1997, Biodiversity, speciation and extinction trends of Proterozoic and Cambrian phytoplankton: Paleobiology, v. 23, p. 230–246.
Volkova, N.A., Kirjanov, V.V., Piskun, L.V., Paskeviciene, L.T., and Yankauskas, T.V., 1979, Plant microfossils, *in* Upper Precambrian and Cambrian Palaeontology of the East European Platform: Moscow, Nauka, p. 5–46. [English version, 1983, p. 7–46]
Vorob'eva, N.G., Sergeev, V.N., and Knoll, A.H., 2009, Neoproterozoic microfossils from the northeastern margin of the East European Platform: Journal of Paleontology, v. 83, p. 161–196.
Wang, F., Zhang, X., and Guo, R., 1983, The Sinian microfossils from Jinning, Yunnan, Southwest China: Precambrian Research, v. 23, p. 133–175.
Wettstein, F.V., 1924, Handbuch der Systematischer Botanik, 3rd ed., Leipzig, Franz Deutike, Band 1, 1017 p.
Wetzel, W., 1933, Die in organischer Substanz erhaltenen Mikrofossillien des baltischen Kreide-Feuersteins mit einem sediment-petrographischen und stratigraphischen Anhang: Palaeontographica Abteiling A, v. 77, p. 141–186.
Williams, K.P.J., Nelson, J., and Dyer, S., 1997, The Renishaw Raman Database of Gemological and Mineralogical Materials: Gloucestershire, England, Renishaw Transducers Systems Division, 298 p.
Woese, C., and Fox, G., 1977, Phylogenetic structure of the prokaryotic domain: Proceedings of the National Academy of Sciences USA, v. 74, p. 5088–5090.
Wopenka, B., and Pasteris, J.D., 1993, Structural characterization of kerogens to granulite–facies graphite, p. applicability of Raman microprobe spectroscopy: American Mineralogist, v. 78, p. 533–557.
Yankauskas, T.V., ed., 1989, Precambrian Microfossils of the USSR: Leningrad, Nauka, 188 p. [in Russian]
Yakschin, M.S., and Luchinina, V.A., 1981, New data on fossilized algae of the family Oscillatoriaceae (Kirchn.) Elenkin, *in* Precambrian-Cambrian Boundary Deposits of the Siberian Platform: Novosibirsk, Nauka, p. 28–34. [in Russian]
Zhang, Y., 1981, Proterozoic stromatolite microfloras of the Gaoyuzhuang Formation (Early Sinian: Riphean), Hebei, China: Journal of Paleontology, v. 55, p. 485–506.
Zhang, Z., 1985, Coccoid microfossils from the Doushantuo Formation (Late Sinian) of South China: Precambrian Research, v. 28, p. 163–173.
Zhang, Y., and Yan, X., 1984, Microfossils from the Gaoyuzhuang Formation in Laishui County, Hebei, China: Acta Geologica Sinica, v. 3, p. 196–204.
Zhang, Y., Yin, L., Xiao, S., and Knoll, A.H., 1998, Permineralized fossils from the Terminal Proterozoic Doushantuo Formation, China: Paleontological Society Memoir, v. 50, 56 p.
Zhegallo, E.A., Rozanov, A.Yu., Ushatinskaya, G.T., Hoover, R.B., Gerasimenko, L.M., and Ragozina, L.M., 2000, The Atlas of Microorganisms from the Ancient Khubsugul Phosphorites (Mongolia): Huntsville, Alabama, USA, 168 p.
Zhou, C., Yuan, X., Xiao, S., Chen, Z., and Xue, Y., 2004, Phosphatized fossil assemblage from the Doushantuo Formation in Baokang, Hebei Province: Acta Micropalaeontologica Sinica, v. 21, p. 349–366.

Accepted 4 March 2015*

*This acceptance date has been corrected since original publication. An addendum detailing this change was also published (DOI 10.1017/jpa.2016.79).